Atomic Spectroscopy

January/February 2004 Volume 25, No. 1

In This Issue:

ASPND7 25(1) 01–52 (2004)
ISSN 0195-5373

Issues also available electronically.

(see inside back cover)

Atomic Absorption

Just touch and go.

There, that's all the training you need.

Walk up to the AAnalyst 200 and let the touch screen guide you through everything from setup to analysis. It practically tells you what to do—and in your own language. All instrument controls are right there on the screen, available at your fingertips. Even troubleshooting and repairs are easier, with quick-change parts you simply snap out and snap in. No service visit, no down time. As rugged and reliable as ever, our newest AAnalyst is a better way to do AA. Experience it for yourself. Talk to a PerkinElmer inorganic analysis specialist today.

PerkinElmer®
precisely.

ISO 9001 CERTIFIED

U.S. 800-762-4000 (+1) 203-925-4600

www.perkinelmer.com

Multielement Determination Using On-line Emulsion Formation and ICP-MS/FAAS for the Characterization of Virgin Olive Oils by Principal Component Analysis

***María S. Jiménez, Rosario Velarte, María T. Gomez, and Juan R. Castillo**
Analytical Spectroscopy and Sensors Group, Department of Analytical Chemistry
University of Zaragoza, Pedro Cerbuna, 12, Zaragoza-50009, Spain

ABSTRACT

Several virgin olive oil samples from different Spanish origin denominations were analyzed for the multielement determination of Al, Ba, Bi, Ca, Cu, Mg, Mn, Na, Pb, and Sn with on-line emulsion formation by flow injection analysis and determination by ICP-MS and flame atomic spectroscopy. The data obtained from the automated multielement determination were treated with Principal Components Analysis to assess the feasibility of using the concentration of the different elements in the olive oil for classifying the oils according to geographical origin and the type of olive used. The statistical analysis carried out showed that Al, Ba, and Mn have a differentiating ability which permits separation of the olive oils analyzed according to their geographical origin and the type of olive employed, whereas Bi, Cu, Sn, and Pb are related to contamination and do not display differentiating capacity.

INTRODUCTION

The interest shown by consumers in the geographical origin and/or variety of foodstuffs has increased in recent years because these factors are generally thought to be a better guarantee of quality and authenticity.

The European Economic Council (EEC) regulations 2881/91 and 2082/91 are both of a general nature and pertain to every origin denomination (O.D) of virgin olive oils. These regulations take into account consumer expectations and, in particular, the expectations of producers with regard to better protection of virgin olive oils which, coming from areas especially suitable for olive growing, have peculiar characteristics from an organoleptic or compositional point of view. Some of the compounds present in olive oil, like fatty acids and un-saponifiable compounds (n-alkanes), depend on the type of olive used because genetics is a determining factor in the biosynthetic reaction which leads to the lipidic synthesis. Factors such as climate and altitude, storage conditions of the olives, transport, and the oil extraction procedure may modify the chemical composition of the oils. As an example, olive oils from areas with warm climates are richer in fatty acids than those from colder areas.

It is well known that the presence of certain trace elements (Cu and Fe in particular) in edible oils accelerates oxidation processes which negatively affects oil quality, while other elements such as Cd, Pb, As, and Hg are subject to legal restrictions due to their toxicity (1,2). Na, K, Ca, Mg, Mn, Fe, Zn,Cu, and P are found at different concentrations in the mesocorp (pulp) of olives. The metallic content of oils and the different forms in which metals are present in edible oils depend on several factors: the presence of metals in the ground itself, their introduction during the production process, or by contamination of the processing material used and/or storage.

The determination of metals in organic samples has always been a challenge in analytical chemistry. There is much literature available on the analysis of lubricating oils but considerably less concerning the analysis of edible oils. Analysis of edible oils for different elements at sub-ppm levels has been performed using different techniques, most of which require sample pretreatment to destroy organic material. These techniques are time-consuming and subject to contamination problems due to the low concentration of metals in olive oil, especially in the best quality virgin olive oil.

A simple and advantageous alternative method used by our research group (3,4) for determining metals in olive oil by inductively coupled plasma mass spectrometry (ICP-MS) (given the low metallic content of this type of oil) and by other authors (5) using inductively coupled plasma optical emission spectrometry (ICP-OES) in spiked sunflower oil is the use of oil-in-water emulsions with an emulsifying agent. One of the main advantages of emulsions is that aqueous solutions can be used for the preparation of calibration standards. If, however, on-line emulsion formation by flow injection analysis (FIA) is used (4), more concentrated emulsions can be introduced and the detection limits are thereby improved. Owing to the transitory nature of FIA, the sample volume introduced is much smaller than in the continuous mode and more concentrated emulsions can therefore be introduced without reducing sensitivity. The analyst hardly takes part in the emulsion preparation and thus the risk of contamination is avoided. The analysis time is significantly reduced (each sample takes about 4 min), resulting in increased sample throughput and improved reproducibility.

**Corresponding author.*
e-mail: jimenezm@unizar.es

In spite of the numerous factors affecting the chemical composition of the oils and their organoleptic properties, studies were performed with the view of classifying oils according to their geographical origin. Up to now, classifications have always been based on the measurement of the different organoleptic characteristics or the analysis of different organic compounds. Rodríguez-Méndez et al. (6) succeeded in differentiating oils with different organoleptic characteristics from different areas in Spain using the sensorial data provided by an electronic nose. Moreno and co-workers (7) used methods based on an electronic nose and pattern recognition treatments to classify vegetable oils and possible adulterants. The analysis of triglycerides by high performance liquid chromatography (HPLC) has made it possible to differentiate oils geographically from two different types of olives at different stages of maturity (8). The analysis of triacylglycerol by reverse-phase liquid chromatography and chemometric techniques has also been used to detect adulterants in oil (9). Alberghina et al. (10) classified oils from three areas of Sicily using the results obtained from the analysis of fatty acids and sterols by gas chromatography. Lee et al. (11) characterized different types of vegetable oils, including primary evaluation of category similarity, detection of adulterants, and quality control. Measurement of hydrocarbon concentration and composition by gas chromatography (12) and isotopic analysis of ^{13}C, ^{18}O, and D of the organic material (13) with the application of statistical procedures have also permitted the characterization and authentication of olive oil samples.

Generally speaking, the research works found in the literature on the characterization of olive oils by origin and/or the variety of olives showed that chemometrics was used to obtain the analytical results from the determination of organic compounds in oils by HPLC or gas chromatography (in many cases after liquid-liquid extraction or solid phase extraction). This process is time-consuming and involves considerable reagent consumption.

In this paper, we propose the possibility of characterizing olive oils from different Spanish origin denominations by performing multielement determination by ICP-MS with an automated FIA system that permits on-line preparation of oil-in-water emulsions (4). The automated FIA system was coupled to a flame atomic absorption spectrometer for the determination of Na, K, and Mg because these elements are more difficult to determine by ICP-MS due to numerous spectroscopic interferences. There are a limited number of references available that report on the possibility of classifying foodstuffs (different types and from different areas) according to their mineral content [e.g., potatoes (14), honey (15), wine (16), and vinegar (17, 18)].

In our study and in order to differentiate between the different virgin olive oils, Principal Components Analysis (PCA) was applied to the analytical results obtained from the multielement analysis of the virgin olive oil samples from different origin denominations and different parts of Spain with differing climates. In addition, an attempt was made to classify the metals according to the area of their origin, identifying those coming from the soil, those depending on the climatic conditions or type of olive cultivated, and those due to contamination or the type of process involved.

EXPERIMENTAL

Instrumentation

A PerkinElmer SCIEX ELAN® 6000 ICP Mass Spectrometer (PerkinElmer SCIEX, Concord, Ontario, Canada) was used for the multielement determination of Al, Ba, Bi, Cu, Mn, Pb, and Sn. Nickel cones were used.

A PerkinElmer® Model 2380 Flame Atomic Absorption Spectrometer (PerkinElmer Life and Analytical Sciences, Shelton, CT, USA) was used for the determination of Na, Ca, and Mg. Na was determined by emission and Ca and Mg by absorption. Ca and Mg hollow cathode lamps (PerkinElmer) were used.

The different olive oil samples were introduced into the ICP-MS or FAAS in the form of oil-in-water emulsions previously formed on-line using a FIA system with merging zones.

The instrumental setup, described in greater detail in a previous paper (4), can be seen in Figure 1. The setup consisted of two peristaltic pumps (P1 and P2, Gilson Minipuls™-3, Villiers le Bel, France), three 6-way automatic injection valves (V1, V2 and V3, from Eurosas, Zaragoza, Spain) with V1 and V2 being used as the sample injection valve and emulsifier injection valve (with and without standards), respectively, and V3 as the by-pass valve of the emulsion formed to the ICP-MS. The injection loops, consisting of a PTFE tube with an internal diameter (i.d.) of 0.8 mm, had an injection volume of 0.4 mL for V1 and V2. The two valves were connected to Y (Omnifit) by means of two PTFE tubes (C1 and C2). Connected to Y was the emulsion formation reactor R consisting of a PTFE tube (1 m length, i.d. 1.6 mm). The reactor and Y were both submerged in an ultrasonic bath (J.P. Selecta,

Atomic Spectroscopy
Vol. 25(1), Jan./Feb. 2004

TABLE I A
Instrumental Operating Conditions and Measurement Parameters for Quantitative FIA-ICP-MS Analysis

Forward Power	1150 W
Sample Uptake Rrate	3 mL min^{-1}
Coolant Argon Flow	14 L min^{-1}
Sweeps/Reading	1
Readings/Replicate	280
Replicates	1
Dwell Time	50 ms
Scan Mode	Peak Hopping

Carretera Nacional II, Km 585.1, Barcelona, Spain), 250 W power and 40 KHz frequency. A PTFE tube with an internal diameter of 0.8 mm, connectors (Omnifit) and different peristaltic pump tubes consisting of Teflon® tubes with an internal diameter of 1.42 mm (to propel the V1 carrier solution) and 2.79 mm (for the V2 carrier) were also used. The whole system was computer-controlled.

Details of the instrumental operating conditions and measurement parameters for the quantitative analysis by ICP-MS and FAAS are given in Tables IA and IB. Prior to all experiments, the ICP-MS instrument was optimized for routine multielement analysis following the manufacturer's instructions. Nebulizer gas flow rate, oxides, lens voltage, and the daily performance of the instrument were optimized by aspirating a solution containing Rh, Mg, Pb, Ba, and Ce (10 µg L^{-1} of each); the autolens calibration was optimized by aspirating a solution of Be, Co, In, and U (10 µg L^{-1} of each).

The computer program UNSCRAMBLER (Version 7.5, CAMO ASA, Oslo, Norway) was used for the statistical treatment of the data obtained.

TABLE I B
Instrumental Parameters for Quantitative FIA-FAAS Analysis

	Na	Ca	Mg
Wavelength (nm)	589	422.7	289
Bandwith (nm)	0.2	0.7	0.7
Observation Height (cm)	8	8	8
Air Flow Rate (L min^{-1})	12.5	12.5	12.5
Acetylene Flow Rate (L min^{-1})	2	2	2

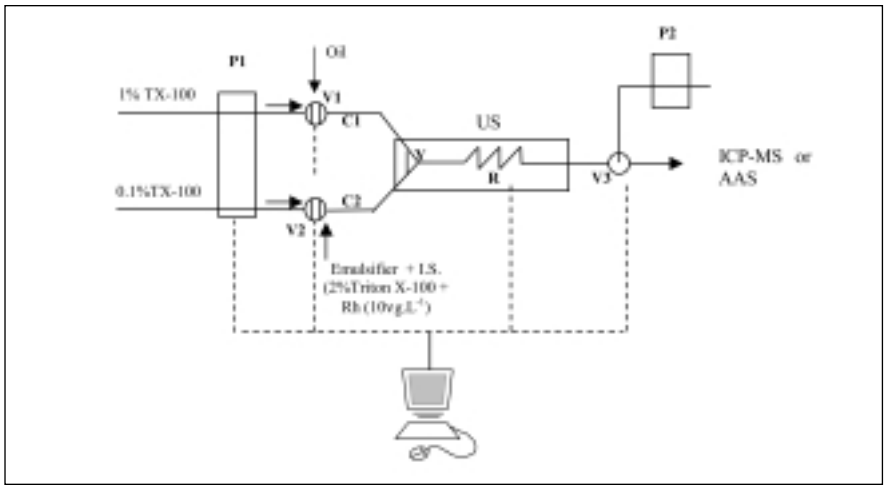

Fig. 1. Schematic diagram of the FIA system for on-line emulsion formation: P1 and P2: Peristaltic pumps; V1: oil valve (injection volume: 0.4 mL); V2: emulsifier valve (injection valve: 0.4 mL), the emulsifier solution contains the internal standard and the calibration standards or spikes for the recovery studies; C1: Connection between V1 and Y (Length=1 m, i.d.=0.8 mm); C2: Connection between V2 and Y (Length=0.5 m, i.d.=2.4 mm); US: ultrasonic bath; R: Emulsion formation reactor (Length= 1 m, i.d.=1.6 mm); V3: By-pass valve. Emulsion formation flow rate: 3 mL.min^{-1}.

Reagents, Standards, and Sample Preparation

Nitric acid (Baker Instra-analyzed, J.T. Baker B.V., Deventer, Holland) and Triton® X-100 (pro analysis, Merck, Darmstadt, Germany) were used. A 5% (v/v) HNO_3 solution was prepared and introduced continuously into the ICP-MS when the emulsion was not being introduced. 0.1%, 1%, and 2% (m/v) solutions of Triton X-100 were prepared by dilution of a more concentrated 10% (m/v) solution of Triton X-100.

Two different aqueous stock solutions with different concentrations of different metals were used:

Standard 1 (500 mg L^{-1} Al; 100 mg L^{-1} As, Be, Cr, Co, Cu, Fe, Pb, Mn, Ni, and Zn; 250 mg L^{-1} V; 25 mg L^{-1} Cd; and 5 mg L^{-1} Hg) (Baker Instra-analyzed, J.T. Baker, Phillipsburg, NJ, USA);

Standard 2 (500 mg L^{-1} Ba, Ca, Mo, and Na; 100 mg L^{-1} Mg; 100 mg L^{-1} K) (Baker Instra-analyzed, J.T. Baker, Phillipsburg, NJ, USA).

A monoelement solution of Sn (1000 mg L^{-1}, Atomic Absorption Standard, Fluka AG, Buchs, Switzerland) was also used. 1 mg L^{-1} intermediate solutions were prepared from the Sn standard and Standards 1 and 2.

The different multielement solutions used in the study were prepared with these intermediate solutions. A multielement solution prepared by dilution of the 1-mg L^{-1} intermediate solution containing 10 µg L^{-1} of Ba, Bi, Cu, Mn, Pb, Sn and 50 µg L^{-1} of Al in 2% Triton X-100 was used to optimize the FIA system employed for the on-line formation of emulsions and Rh (10 µg L^{-1}) as the internal standard.

A monoelement solution of Rh (1000 mg L^{-1}) was prepared from $(NH_4)_3RhCl_6$ (Puriss, Fluka AG, Buchs, Switzerland) and used as the internal standard. A 1-mg L^{-1} intermediate solution was prepared from this standard solution of Rh.

Several standard solutions were prepared for the quantitative analysis with increasing concentrations of Al, Ba, Bi, Cu, Mn, Pb, and Sn in 2% Triton X-100. Rh (10 µg L^{-1}) was added as the internal standard for the calibration.

Several types of virgin olive oil from different regions of Spain were analyzed. These oils are listed in Table II together with their geographical origins (see "Code" column in Table II and Figure 2), origin denominations (O.D), and the type of olive used for the oil. Most of the oils analyzed were not processed from a single type of olive, but the main variety in each oil was around 80%.

The different areas from which the oils studied chemometrically came from are given in Figure 2 (A, B, C, D, and E refer to the geographical origin of oils in Table II). It should be noted that areas A, B, and C are in close proximity, D and E come from areas with very similar climates, and A and B come from the same type of olive (Empeltre).

TABLE II
Different Virgin Olive Oil Samples

Area of Origin	Product Name	Main Type of Olive Used	Bottling Material	Code[b]
Campo de Borja	Oliambel	Empeltre	Glass	1A
	Sigmun Naturalis		Glass	2A
Bajo Aragón[a]	Arboleda[a]	Empeltre	Glass	3B
	Arboleda [a]		PVC	4B
	Reales Almazaras[a]		Glass	5B
	Vadueña[a]		Glass	6B
	Alcober[a]		Glass	7B
Cataluña	Sensat	Arbequina	Glass	8C
	Oleastrunverd[a]		Glass	9C
Baena[a]	Germán Baena[a]	Picudo	Glass	10D
	Nª Sra. De Guadalupe[a]		Glass	11D
	Valle de las Flores[a]		Glass	12D
Plasencia	La Chinata	Manzanilla	Tin Plate	13E

[a]With origin denomination.
[b]Code: Letters refer to area of origin (see Figure 2).

Fig. 2. Map of Spain showing the different areas of origin of the virgin olive oil samples.

Recovery studies were carried out by adding spikes to the oils containing 10 µg L^{-1} of Ba, Bi, Cu, Mn, Pb, and Sn; and 50 µg L^{-1} of Al. Rh (10 µg L^{-1}) was used as the internal standard for the analysis of the different spiked and unspiked samples.

The salts used for determining Na, Ca and Mg by FAAS were as follows: LiCl (Pro Analysis, Merck, Darmstadt, Germany), NaCl, $MgCl_2$,

TABLE III
FIA Program for On-line Emulsion Formation and ICP-MS or FAAS Determination

Step	Time (s)	Vo	Ve	Vp	Ub	P	Flow Rate (mL min^{-1})	Trg	Comments
1	0–8	1	1	1	0	1	28.2	0	Reactor cleaning
2	8–20	0	0	1	0	1	6[a], 22.2[b]	0	Oil and emuls. injection
3	20–210	0	0	0	1	1	3	1	ICP-MS or FAAS measurement
4	210–220	1	1	1	0	1	28.2	0	Cleaning reactor
5	220–221	1	1	1	0	0	28.2	0	Stand-by

Vo, Ve = Injection Valves for Oil and Emulsifier: 1= Loading, 0= Injection.
Vp= By-pass Valve, 1= Waste, 0= ICP-MS.
Ub= Ultrasonic Bath, 1= ON, 0= OFF.
P= Peristaltic Pump, 1= ON, 0= OFF.
Trg= Trigger sends measuring order to ICP-MS.

[a]Oil Flow Rate; [b]Emulsifier Flow Rate.

and $CaCl_2$ (Suprapur®, Merck, Darmstadt, Germany). Individual solutions containing 1000 mg L^{-1} of Na, Ca, and Mg, and 2000 mg L^{-1} of Li were prepared. Intermediate solutions of 50 mg L^{-1} were prepared for each metal from the solutions of 1000 mg L^{-1} of Na, Ca, and Mg. Several standard solutions were prepared with increasing concentrations of Na, Ca, and Mg in 2% Triton X-100 (0.1-5 mg L^{-1}) for the quantitative analysis. Li (400 mg L^{-1}) was added as the spectral buffer to the blank, standard solutions, and spiked and unspiked samples for the determination of Na by atomic emission spectrometry. Recovery studies were also carried out by adding spikes to the oils containing 0.5 mg L^{-1} of Na, 1 mg L^{-1} of Ca, and 0.5 mg L^{-1} of Mg.

Aqueous solutions were prepared using ultrapure water, with a resistivity of 18.2 MΩ obtained from a Milli-Q™ water purification system (Millipore, Saint Quentis Yvelines, France). All polyethylene material was decontaminated with nitric acid (10% v/v) for at least 72 h, rinsed with ultrapure water, and dried.

Procedure

The on-line emulsion formation process by FIA-merging zones is completely computer–controlled and has been described previously (4). The program used is listed in Table III. The emulsion formation process was as follows: a quantity of the olive oil sample (0.38 g) was introduced through valve V1 using a 1% Triton X-100 solution as the carrier. The emulsifier solution, a 2% Triton X-100 solution needed for emulsion formation, was introduced by V2. This solution contains the internal standard (Rh, 10 µg L^{-1}) for the analysis of the olive oil samples or internal standard and standards for the calibration or recovery studies. A 0.1% Triton X-100 solution was used as the carrier in V2. In step 2 of the program, injection from the two valves was simultaneous so that mixing of the olive oil sample (or blank solution) and 2% Triton X-100 emulsifier (with or without standards) was synchronized in Y. Formation of the emulsion in the reactor R takes place during step 4 in which the ultrasonic agitator is connected automatically. The emulsion formed is then introduced into the ICP-MS or FAAS through V3 for multi-element determination. The final step of the program is cleaning of the reactor.

RESULTS AND DISCUSSION

The previously described procedure with on-line emulsion formation by flow injection was used for the multielement determination in different oil samples. As stated previously, Al, Ba, Bi, Cu, Mn, Pb, and Sn were determined simultaneously using an ICP-MS. Na was determined by FAES (Flame Atomic Emission Spectrometry) and Ca and Mg by FAAS, although these two elements could not be determined in some samples because their concentration was below the detection limits. Three different analyses were carried out for all samples on different days with four replicates of each sample per day. As can be seen in Table II, there were 13 samples, and the results obtained for the determination of the different metals in the samples are gathered in Table IV. The detection limits (DL) (based on three times the standard deviation of the blank signals, n=10) and the recovery values for the different olive oils from a single analysis are also given in Table IV. It can be observed that the recoveries were quite satisfactory, in most cases around 100%. Moreover, the concentrations found for most of the elements are in agreement with those in the literature for olive oil samples (19–21).

TABLE IV
Mean Metal Concentration of Triplicate Analyses (ng g^{-1}) in Olive Oil Samples, Recoveries (%), and Detection Limits (ng g^{-1}), Together With Descriptive Statistics: Mean, Standard Deviation (SD), Minimum and Maximum Value

	Al	Mn	Cu	Pb	Sn	Bi	Ba	Na[a]	Ca[a]	Mg[a]
1A	21.08 ± 1.70	14.39 ± 0.17	1.47 ± 0.61	1.22 ± 0.03	0.57± 0.07	0.25 ± 0.10	1.76 ± 0.02			
[b]	81.6	121	100.3	125	80.1	98	107.1			
2A	19.09 ± 1.43	8.10 ± 0.04	5.48 ± 0.40	9.35 ± 0.23	< DL	< DL	1.44 ± 0.47			
[b]	90.5	97.7	101.9	119.1	108	141	98.8			
3B	25.21 ± 1.02	3.77 ± 0.10	2.31 ± 0.11	0.90 ± 0.22	0.53 ± 0.20	0.16 ± 0.08	0.50 ± 0.09			
[b]	99.3	113.4	108.3	120.2	108.7	104.6	100.4			
4B	30.37 ± 1.66	6.40 ± 0.42	2.50 ± 0.27	1.79 ± 0.26	< DL	0.14 ± 0.07	0.43 ± 0.19			
[b]	93	98.7	108	119.2	98.1	102.7	94.6			
5B	21.23 ± 0.86	3.54 ± 0.62	1.39 ± 0.27	1.03 ± 0.46	0.13 ± 0.07	< DL	0.37 ± 0.12			
[b]	114	120	127	109	92.5	125	82.8			
6B	23.91 ± 2.85	3.33 ± 0.50	2.26 ± 0.29	2.12 ± 0.32	0.20 ± 0.10	0.39 ± 0.15	0.57 ± 0.004			
[b]	95.7	82.4	106.8	113.1	90.3	113	93.8			
7B	18.10 ± 1.71	3.96 ± 1.12	2.45 ± 1.33	0.23 ± 0.036	< DL	< DL	0.28 ± 0.07			
[b]	114	120	127	109	92.5	125	82.8			
8C	22.38 ± 1.25	19.98 ± 0.27	1.80 ± 0.10	1.71 ± 0.12	0.67 ± 0.03	< DL	5.82 ± 0.14	910 ± 32	560 ± 8	120 ± 16
[b]	72.5	70.9	89.1	116.3	71.3	89	107	62.5	91.3	104.5
9C	9.75 ± 0.70	1.97 ± 0.07	1.79 ± 0.02	0.64 ± 0.02	0.53 ± 0.03	0.45 ± 0.20	0.61 ± 0.16			
[b]	88.7	101.4	105.0	105.1	76.8	86.3	102			
10D	39.56 ± 2.46	50.25 ± 1.36	5.59 ± 0.12	6.22 ± 0.25	0.85 ± 0.06	0.48 ± 0.20	27.16 ± 0.49	1750 ± 99	2970 ± 276	350 ± 23
[b]	107.3	116	108.2	118	97.7	139	157	88.4	89	91.6
11D	43.61 ± 4.73	16.24 ± 1.13	1.83 ± 0.15	0.83 ± 0.13	0.34 ± 0.038	0.45 ± 0.14	5.55 ± 0.13			
[b]	117	106	118	98	74.3	130	87			
12D	54.34 ± 0.21	25.93 ± 0.01	3.28 ± 0.26	1.64 ± 0.062	< DL	1.48 ± 0.50	9.85 ± 0.24	470 ± 31	1500 ± 71	295 ± 23
[b]	124	129	114	72.1	85	119	83.1	97.5	83.3	73.5
13E	47.40 ± 3.19	38.63 ± 1.41	4.66 ± 1.50	0.66 ± 0.21	4.66 ± 0.22	< DL	4.99 ± 0.41		841 ± 79	173 ± 9
[b]	108	161	122	99.1	80.8	127	83.8		117	90.3
DL	5.31	0.98	1.09	0.33	0.44	0.02	0.15			
Median	29.05	16.73	2.83	2.16	0.71	0.3	4.56	299	573	78
S.D.	13.14	19.65	1.47	2.64	1.19	0.4	7.42	501	822	120
Minimum Value	9.75	1.97	1.39	0.23	0.22	0.01	0.28	75	175	9.5
Maximum Value	54.34	71.25	5.59	9.35	4.6	1.48	27.16	1750	2972	349

[a]If there is no value for Na, Ca, and Mg, it is because the metal content in the sample is below the detection limit.
[b]Recoveries (%) obtained for each virgin olive sample.
DL: Detection limits (ng g^{-1}).

The results for all the metals vary considerably, indicating significant differences in the mineral composition of the different oil samples. Al and Mn and, in particular, Na, Ca, and Mg have much higher standard deviations than the other metals. Preprocessing (autoscaling) of the original matrix data was carried out for the subsequent statistical treatment so that all the analytes would have the same variance.

Correlation Study

The correlation matrix (see Table V) shows the correlation between pairs of variables (metals). The elements of the matrix are the Statistic named as Correlation Pearson coefficient (22,23). The matrix elements, which are close to the unit, show a correlation between pairs of variables. The correlated variables are due to the same cause or source of variance, that is, the same fundamental variable. Variables that display similarities (as their Pearson coefficients are close to 1) are shown in bold type. A close relationship can be seen between the alkaline earth metals (Ba, Ca, and Mg) and those with Mn. Na (alkaline) differs significantly from the other metals.

The mean values for Mn and Ba for olive oils from the Campo de Borja, Bajo Aragón, Catalonia, and Baena areas are plotted in Figure 3 in order to determine whether these elements have a differentiating capacity. It should be noted that the greater the differentiating capacity, the farther apart the points representing each type of oil should be. The oils of the Baena origin denomination clearly differ from the rest. The Mn and Ba variables are therefore suitable for differentiating oils from the north vs. those from the south, the differences being basically the climatic conditions, the soil, and the different types of olive used.

Principal Components Analysis

Principal Component Analysis (PCA) (24) was used to find groupings of variables, that is, to find out which manifest variables (metals) are interrelated and related to a specific principal component (latent variable) which is associated with a fundamental variable (for instance, climate, type of soil, etc.). Each principal component provides information about fundamental variables, which causes the buildup of one metal or another. Another objective was to determine whether the metallic content can be used to establish differences between the oils studied.

PCA (24) transforms the original data matrix $X_{n \times m}$ (Table IV) into a product of two matrices, one of which contains information about the samples (Scores matrix $S_{n \times m}$), and the other about manifest variables (metals) (Loadings matrix $L_{m \times m}$); "n" is the number of samples and "m" is the number of variables.

TABLE V
Correlation Matrix (Pearson Coefficients)

	Al	Mn	Cu	Pb	Sn	Bi	Ba	Na	Ca	Mg
Al	1.00									
Mn	0.64	1.00								
Cu	0.46	0.67	1.00							
Pb	0.04	0.36	0.76	1.00						
Sn	0.42	0.46	0.41	-0.13	1.00					
Bi	0.59	0.29	0.16	0.02	-0.17	1.00				
Ba	0.55	**0.94**	0.60	0.42	0.15	0.41	1.00			
Na	0.31	**0.83**	0.47	0.41	0.02	0.26	**0.92**	1.00		
Ca	0.58	**0.93**	0.63	0.39	0.22	0.47	**0.97**	**0.89**	1.00	
Mg	0.70	**0.89**	0.61	0.27	0.33	0.58	**0.88**	**0.80**	**0.95**	1.00

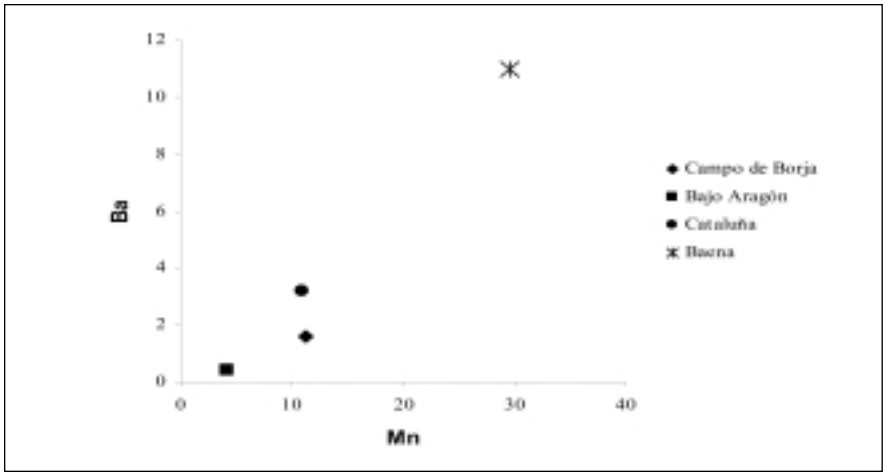

Fig. 3. Correlation plot between Mn and Ba.

The PCA results are graphically displayed using two plots. The Score plot shows the relationships between the samples (olive oil samples). Each point whose coordinates are the scores on the principal components (axes on the plot) corresponds to a sample. Groups or clusters of similar samples can be detected visually. The Loading plot shows the similarities (correlations) between the variables. Each point, whose coordinates are the loadings on the principal components, corresponds to a variable (metal). The variables with small factor loadings on a specific principal component have little influence. The most important variables on a principal component have high factor loadings. Two variables are strongly correlated when their factor loadings are similar to each other, that is, when there is a small distance between them on the Loading plot. The score and loading plots are complementary and give the most valuable information about both the samples and the variables when studied together. When a sample has a position in the score plot that is corresponding to the position of the variable in the loading plot, it means that the sample has a high value for the variable.

The maximum amount of variance contained in the data is concentrated in the first component (PC1). The second principal component, orthogonal to the first, contains the next largest possible variation (PC2).

As previously mentioned, the matrix data required preprocessing by hole filling for unknown data when the concentrations were below the detection limits. It is assumed that the values of the holes are half the detection limit (22). Scaling of the original data was also carried out; this will make the result independent on the scale of the original variables. PCA was subsequently applied to the autoscaled data using the UNSCRAMBLER program.

The first component accounts for 58% of the total variability and the second one represents 16% of the total variance. PC1 and PC2 explain the largest possible variation in the data and therefore PC1 and PC2 account for most of the information.

When outliers are found in a PC plot, one should first identify and then eliminate the outliers and carry out the PCA again. It was assumed that there were no anomalous samples as the validity of the method has been previously shown (4), the recovery values were quite satisfactory, and anomalous metallic concentration was due to randomized sources of contamination. The criterion used was selection of the minimum number of variables needed for a correct classification. The variables that do not provide sufficient information (they have small factor loadings in any principal component) were excluded from the chemometric study.

The factor loadings for all the variables in both components are given in Table VI. Ba, Mn, Ca, Mg,

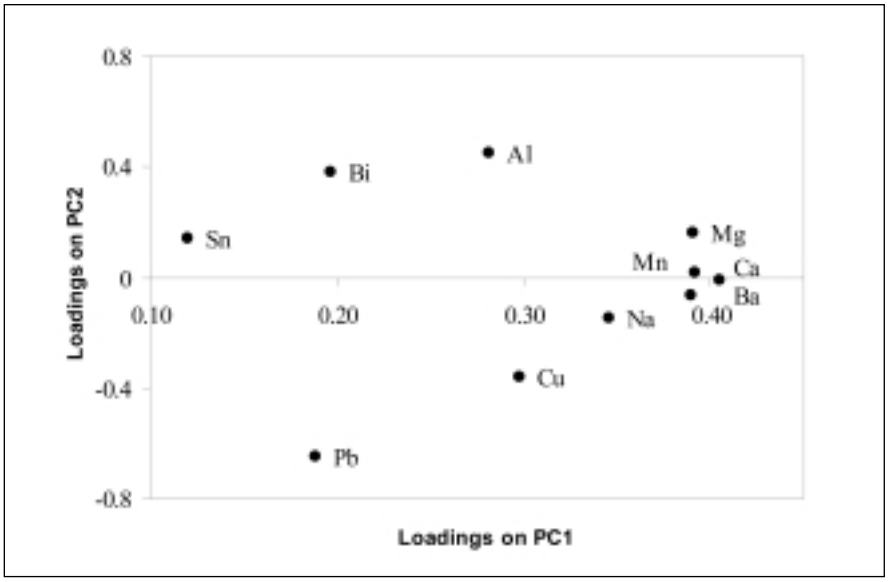

Fig. 4. Loadings plot (10 variables).

TABLE VI
Factor Loadings of Principal Components

Principal Component	Variable									
	Al	Mn	Cu	Pb	Sn	Bi	Ba	Na	Ca	Mg
1	0.282	0.392	0.298	0.189	0.120	0.197	0.39	0.346	0.405	0.391
2	0.449	0.017	–0.363	–0.647	0.139	0.381	–0.068	–0.147	–0.008	0.164

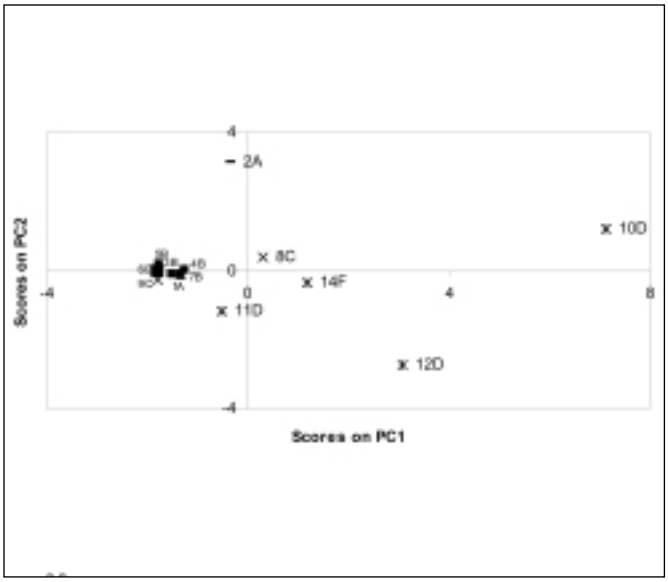

Fig. 5a. Scores plot (9 variables).

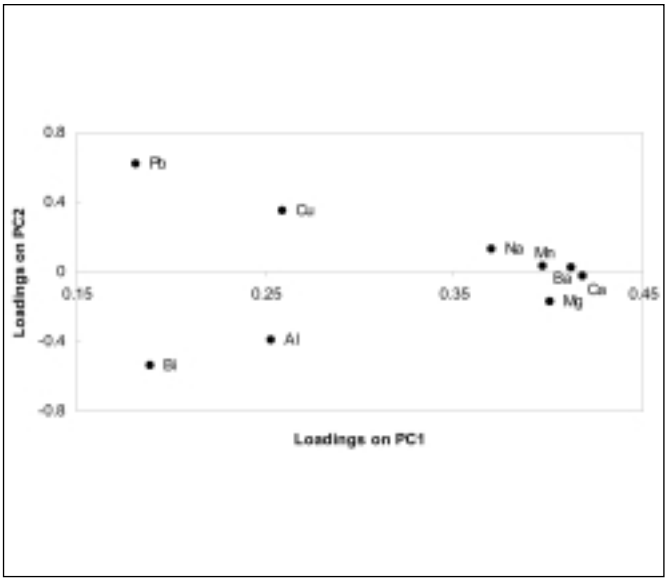

Fig. 5b. Loadings plot (9 variables).

and Na are the predominant elements in the first component as they have the highest factor loadings. Moreover, they are correlated to each other because they have similar factor loadings. Sn does not seem to be important in any principal component as this element is the closest to the origin in the loading plot (see Figure 4) and it has no influence on any other component. It was therefore excluded on account of its poor differentiating capacity with all the variables. When the scores and loadings were plotted for the remaining variables (Figures 5a and 5b), no clearly defined clusters were observed in the scores plot. When comparing the two plots (Figures 5a and 5b), it can be seen that Pb (high loading value in the second component, small value in the first) coincides with sample 2A (high score value in the second component, small value in the first). This sample (2A) is Sigmun Naturalis, and it can be seen in Table IV that it has an abnormally high Pb concentration which could be due to atmospheric contamination, fertilizers, or herbicides used. The origin of Pb is randomized and hence avoids the clusters between samples.

A comparison of the scores and loadings plots after repetition of the PCA without Pb shows that Bi coincides with sample 12D (Valle de las Flores). As occurred with Pb, the buildup of Bi in the sample is abnormal (see Table IV) and has an adverse effect on cluster formation. Bi was therefore excluded as a variable. The scores and loadings plots after exclusion of Sn, Pb, and Bi can be seen in Figures 6a and 6b, respectively.

It can be observed in the loadings plot that Al is the principal element in component 2. PC2 depends on Al as this element has a high loading value in this principal component, while Mg, Mn, Ca, and Ba are correlated because the distance between them is very small. Moreover, these elements predominate in component 1 as the loading values are very high. Cu does not contribute in either compound since its factor loadings in PC1 and PC2 are the smallest. Na, however, has a significant contribution in both.

Judging from the initial data (Table IV), Na, Mg, and Ca are present at very high concentrations in the oils from the south but are below detection limits in the others. These elements were therefore excluded as they provide very little information about the oils from the other areas studied. When the study was repeated with the remaining variables (Al, Mn, Ba, and Cu), two clusters or groupings disappeared. It was observed that Cu coincides with sample 2A (*Sigmun Naturalis*) which has a much higher Cu concentration than the other samples from similar geographical origins. Elements were therefore excluded not only because of the type of soil, type of olive or climate, but above all on sources of contamination which possibly caused the abnormal accumulation of these elements in certain samples.

The scores and loadings graphs (Figures 7a and 7b) were plotted with three variables, after exclusion of the variables that provided little information. Three clearly defined clusters can be observed.

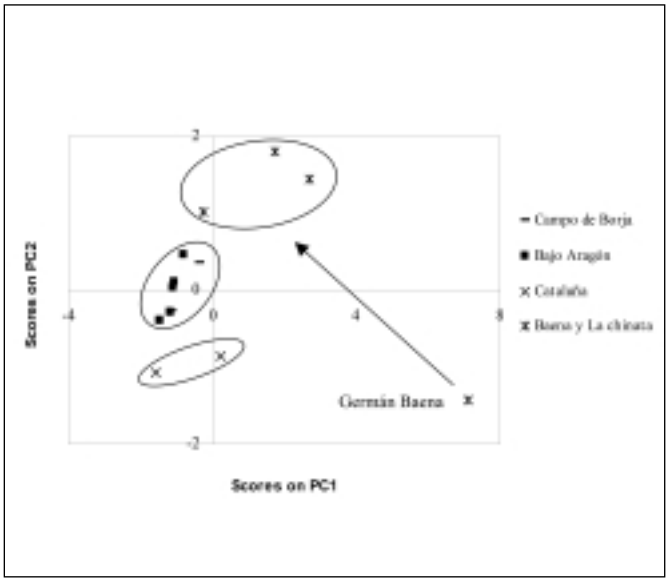

Fig. 6a. Scores plot (7 variables).

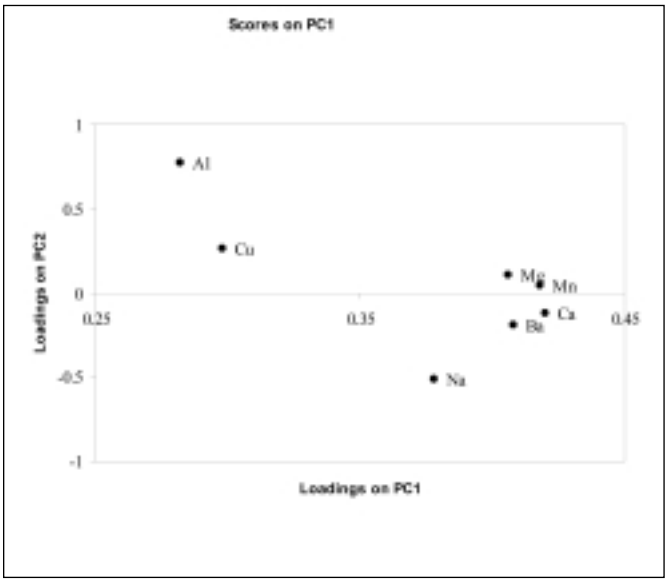

Fig. 6b. Loadings plot (7 variables).

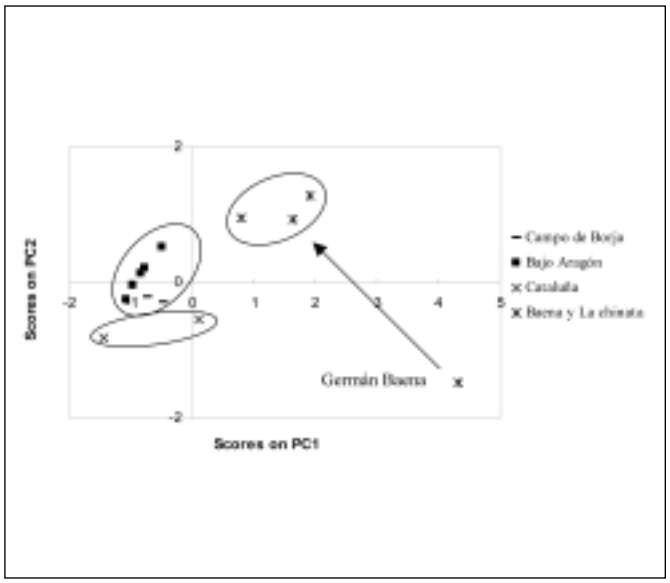

Fig. 7a. Scores plot (3 variables).

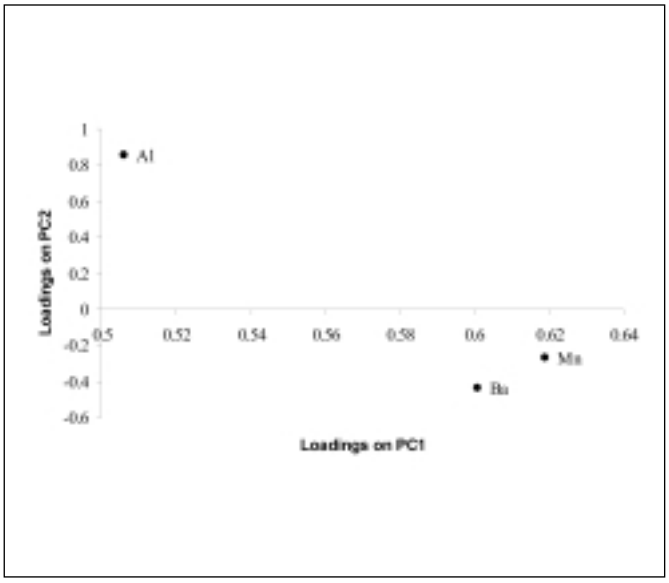

Fig. 7b. Loadings plot (3 variables).

The group including the Baena and La Chinata oils are farther apart from the rest after exclusion of Cu and are located in the positive quadrant. As occurred previously with the oils from Bajo Aragón and Campo de Borja, they cannot be differentiated, which could be due to their geographical proximity and because the olive variety is the same (Empeltre). These oils differ from the oils from Catalonia because, if not geographically far apart, the olive variety cultivated is different. The La Chinata oil from Plasencia (Cáceres) is in the group of oils belonging to the Baena origin denomination and, although the olive used is different, the climate and soil are very similar. The Germán Baena oil, on the other hand, is located at a distance from the other samples. When compared with the other samples, Germán Baena has very high Mn and Ba concentrations. However, it was not considered an anomalous

sample as its exclusion had a negative effect on the appearance of clusters.

The loadings from the PCA showed that Al is the principal element in the second component, while Mn and Ba predominate in the first, although Al is also present. Mn and Ba are interrelated and their presence in the oil is for the same reason. In comparing the scores and loadings plots (Figures 7a and 7b), it can be concluded that the oils from Bajo Aragón and Campo de Borja can only really be differentiated from those from Catalonia on account of Al, which predominates in the second component. The Baena and La Chinata groups differ from most of the oils from the north not only with regard to Al, but Mn and Ba as well. The oils from the north (Bajo Aragón, Campo de Borja, and Catalonia) come from areas in close proximity and it can, therefore, be assumed that the type of soil has little influence. Consequently, it is impossible to differentiate between Bajo Aragón and Campo de Borja on the basis of their geographical proximity, climate, and type of olive (Empeltre in both cases). The Catalonian oils can be differentiated, but given the geographical proximity, this probably has nothing to do with the type of soil. As far as climatic conditions are concerned, temperature and rainfall may have an influence on the mineral composition of the olives. However, the controlling bodies of the origin denominations studied define their respective climates as warm continental, with cold winters and hot summers and a similar annual rainfall. The main difference lies in the type of olive used: Empeltre in Bajo Aragón and Arbequina in Catalonia.

The Baena oils differ from those from the north of Spain on account of the two principal components and, consequently, the Al, Mn, and Ba variables. The olive variety is not the same as those predominantly used in the north, which marks the first principal component (Al) as the difference. Moreover, the Baena oils differ in the second principal component where Mn and Ba predominate. Unlike the oils from the north, the second component in the Baena olive oil is related to the type of soil. In other studies carried out with different foodstuffs, Herrero et al. (14) showed that Mn, Ca, Mg, Rb, and Li are related to the type of soil and make it possible to differentiate between potatoes from Galicia (Spain) and potatoes from other countries. According to M.J. Latorre (15), Mn is a geographical indicator for differentiating between honeys and wines from Galicia and products from other geographical origins. It should be noted that although the Germán Baena sample is different from the samples from the north, it cannot be included in the Baena group as the concentrations of Mn and Ba are significantly higher, possibly because the process leads to an accumulation of Mn and Ba in the sample.

CONCLUSION

The determination of metals in different virgin olive oil samples from different areas and origin denominations was carried out using ICP-MS by on-line emulsion formation with a view to their possible classification. The statistical treatment of the data was performed applying Principal Component Analysis, and the metals with a differentiating capacity (Al, Mn, and Ba) were identified. The fact that some metals (Sn, Pb, Bi, and Cu) do not permit classification or produce anomalous samples could be due to contamination or the type of process involved.

Al, Mn, and Ba permitted differentiation between samples from Bajo Aragón and Catalonia and those from Baena, but were not sufficiently accurate to differentiate them from the Campo de Borja samples owing to the geographical proximity and the fact that the same olive was used. The Al content appears to depend, above all, on the olive variety. This theory, however, has not been proven; there is no mention in the literature about how the genetics of the olive tree influences the Al concentration in the olive. In fact, the Mn and Ba concentrations depend basically on the type of soil and permit differentiation between oils from the north (Campo de Borja, Catalonia, and Bajo Aragón) and oils from the south of Spain (Baena and La Chinata). The relationship between Mn and alkaline earth metals and the soil has been proven and used to differentiate between foodstuffs of different geographical origin. It is suggested that a future study focus on whether genetics has an influence on the Al concentration by analyzing different types of olives grown in the same soil.

Na, Ca, and Mg make it possible to distinguish between oils from the south of Spain (Baena and La Chinata) and oils from the north (Bajo Aragón, Campo de Borja, and Catalonia) but provide no information concerning the other oils. A more sensitive determination technique would be required for Na, Ca, and Mg since most of the samples available for this study were below detection limits when FAAS or FAES was used.

ACKNOWLEDGMENTS

This work was sponsored by project DGICYT BQU 2000-0992 and project COMSID-DGA PO76/2001. R. Velarte would like to thank COMSID-DGA for the research grant.

Received November 25, 2003.

REFERENCES

1. W.W. Lundberg, Autooxidation and Antioxidant, Vol II, Wiley Interscience Publishers, New York (1966).
2. M. Murillo, Z. Benzo, E. Marcano, C. Gomez, A. Garaboto, and C. Marín, J. Anal. At. Spectrom. 14, 815 (1999).
3. J.R. Castillo, M.S. Jimenez, and L. Ebdon, J. Anal. At. Spectrom.14, 1515 (1999).
4. J.R. Castillo, M.S. Jimenez, and L. Ebdon, J. Anal. At. Spectrom. 18, 1154 (2003).
5. F. Wahdat, S. Hinkel, and R. Neeb, Fresenius' Z. Anal. Chem. 352 (3-4), 393 (1995).
6. A. Guadarrama, M.L. Rodríguez-Méndez, C.Sanz, J.L. Ríos, and J.A. de Saja, Anal. Chim. Acta 432, 283 (2001).
7. Y. Gonzalez, M.C. Cerrato, J.L. Pérez, C. Garcia, and B. Moreno, Anal. Chem. 449, 69 (2001).
8. E. Stefanoudaki, F. Kotsifaki, and A. Koutsaftakis, Food Chemistry 60 (3), 425 (1997).
9. D-S. Lee, E-S. Lee, H-J. Kim, and S-O. Kim K. Kim, Anal. Chem. 429, 321 (2001).
10. G. Alberghina, L. Caruso, S. Fisichella, and G. Musumarra, J. Sci. Food Agric. 56, 445 (2001).
11. D-S. Lee, B-S. Noh, and S-Y. Bae, K. Kim, Anal. Chem. 358, 163 (1998).
12. L. Wbster, P. Simpson, A.M. Shanks, and C.F. Moffat, Analyst 125, 97 (2000).
13. F. Angerosa, O. Breas, S. Contento, C. Guillou, F. Reniero, and E. Sada, J. Agric. Food Chem. 47, 1013 (1999).
14. P.M. Padín, R.M. Peña, S. García, R. Iglesias, S.Barro, and C. Herrero, Analyst 126, 97 (2001).
15. M.J. Latorre, R. Peñañ, C. Pita, A. Botana, S. García, and C. Herrero, Food Chemistry 66, 263 (1999).
16. S. J. Haswell and A.D. Walmsley, J. Anal. At. Spectrom. 13, 131 (1998).
17. M.J. Benito, M.C. Ortiz, M.S. Sánchez, L.A.Sarabia, and M.Iñiguez, Analyst 124, 547 (1999).
18. M.I. Guerrero, C. Herce-Pagliai, A.M. Cameán, A.M. Troncoso, and A.G. González, Talanta 45, 379 (1997).
19. M.D. Garrido, I. Frias, C. Diaz, and A. Hardisson, Food Chemistry 50, 237 (1994).
20. M. Martin-Polvillo, T. Albi, and A. Guinda, JAOCS 71 (4) 347 (1994).
21. I. Karadjova, G. Zachariadis, G. Boskou, and J. Stratis, J. Anal. At. Spectrom. 13, 201 (1998).
22. G. Ramis Ramos, and Mª C. García Álvarez-Coque, Quimiometría, ed Síntesis, Madrid (2001).
23. N.J. Millar and J.C. Miller, Statistics and Chemometrics for Analytical Chemistry, fourth edition, Prentice Hall, Pearson Education, New Jersey, U.S.A
24. D.L. Massart, B.G.M. Vandeginste, L.M.C. Buydens, S.De Jong, P.J. Lewi, and J. Smeyers-Verbeke, Data Handling in Science and Technology 20A, Handbook of Chemometrics and Qualimetrics: Part A, Elsevier, Amsterdam, The Netherlands.

Development and Validation Method for the Determination of Rare Earth Impurities in High Purity Neodymium Oxide by ICP-MS

Man He, *Bin Hu, Zucheng Jiang, and Yan Zeng
Department of Chemistry, Wuhan University, Wuhan 430072, P.R. China

ABSTRACT

The analytical procedure for the determination of trace rare earth impurities in high purity neodymium oxide (Nd_2O_3) by ICP-MS is described. The effect of ICP-MS operating parameters on the $REO(H)^+/RE^+$ production ratio was studied in detail, and the optimal ICP operating conditions were established. In this context, the relationship between $REO(H)^+/RE^+$ production ratio and the bond strength of the rare earth oxides is also discussed briefly. For the correction of the spectral interference induced by the matrix (neodymium), a simple correction equation was used for correcting the interferences of the polyatomic ions NdO^+ and $NdOH^+$ with ^{159}Tb and $_{165}Ho$. The proposed method was applied to the determination of trace rare earth impurities in high purity Nd_2O_3, and the analytical results were in good agreement with the recommended reference values.

INTRODUCTION

Trace rare earth element (REE) determination is always an important field of study in analytical chemistry. As one of the major REE analytical methods, ICP-OES (inductively coupled plasma optical emission spectrometry) has been widely applied to the determination of trace REEs in metallurgy, geology, biology, the environment, and high purity rare earth material. However, in some cases, the sensitivity of ICP-OES is not enough to satisfy the demand of high purity REE material (99.99 %) analysis.

It has been shown that ICP-MS is the most effective modern analytical tool for trace element determination and possesses several advantages (1,2): high sensitivity, broad linear range, capability of multi-element analysis, and determination of isotope ratio. Compared with ICP-OES, the most obvious merit of ICP-MS in REE determination is its excellent detection capability, in which pg mL^{-1} detection limit levels can be obtained for REEs. Also, the sensitivity for single REEs is very close, and their difference in detection limit is less than one order of magnitude (3). Presently, ICP-MS is more widely applied for the analysis of high purity rare earth compounds (4,5).

However, it should be pointed out that interferences can be divided into spectral and non-spectral interferences (matrix interference), a ubiquitous problem in ICP-MS. In order to determine trace REE impurities in high purity rare earth oxides, some effective measures can be taken to overcome the non-spectral interferences such as (a) matrix matching (6), (b) internal standard addition (7), and (c) sample dilution. For spectral interferences, however, the production ratio of REO^+/RE^+ is generally at the X‰ (thousandths) level or much lower, and the contribution of this kind of interference is quite low, just around ng/g. Even though the production ratio of $REOH^+/RE^+$ is much less, its contribution is negligible and spectral interferences between trace REE impurities can be ignored. However, in the determination of trace heavy rare earth impurities in a light rare earth oxide matrix, the $REO(H)^+$ interference induced by the matrix (light REEs) has been reported and should be carefully considered (3,8).

Research on polyatomic response (including oxide interference) has been reported during the initial development of ICP-MS instrumentation (9,10). The identification of $REO(H)^+$ and the effect of instrumental operating parameters on the production ratio have been discussed in ICP-MS studies (11–13), but this is still an interesting research topic (14). Quantification of oxide (MO^+) and hydroxide (MOH^+) ions is generally expressed as the oxide production ratio (MO^+/M^+) and hydroxide production ratio (MOH^+/M^+). It is documented that the metal oxide/hydroxide production ratio depends on operational parameters such as plasma power (15,16), carrier gas flow rate (11,15,17), sampling depth and the sampler and skimmer orifice sizes (11,15,17). High plasma power and a low nebulizer gas flow rate were used to reduce the oxide production ratio (<2 % CeO/Ce) (17,18).

Nevertheless, the reduction or elimination of spectral inter-ferences and the development of an effective method for ICP-MS determination of trace REE impurities in high pure RE oxides (especially trace heavy rare earth impurities in a light rare earth matrices) is still an unsolved problem which continues to puzzle analytical chemists. Various approaches have been reported to reduce or eliminate the spectral interference in ICP-MS determination of REEs in various matrices. Chemical separation based on the separation of the matrix, such as ion chromatography (19), ion

*Corresponding author.
e-mail: binhu@whu.edu.cn
Tel.:86-27-87218764

exchange chromatography (18), liquid chromatography (20), and solvent extraction (21), has proven to be efficient. However, chemical separations are time-consuming and laborious. Also, high concentrations of organic eluents and buffer reagents might lead to carbon deposition on the sampling orifice of ICP-MS systems or might cause clogging of the ICP torch, resulting in a drift in instrument sensitivity. High resolution ICP-MS (HR-ICP-MS) can, in some cases, separate analyte signals from the interfering oxides; its validity has been demonstrated for the determination of REEs in rocks (22). However, HR-ICP-MS is very expensive, and most ICP-MS users still work with quadrupole ICP-MS instruments. An alternative method to solve the above problems is to use a suitable mathematical method to correct the raw data. Zhu and co-workers (23) developed a PLSR (Partial Least Squares Regression) model to eliminate or correct the REO, REOH, and isotope interferences in the determination of REEs by ICP-MS. Likewise, Elokhin et al. (24) used a simplex approach for data processing and claimed that the main features of the simplex approach were adequate automatic correction for all possible spectral overlaps. A routine method for oxide and hydroxide interference correction was also proposed for ICP-MS determination of trace REEs in geological sample (25). However, it should be noted that most of this research involves the determination REEs in geological and environmental samples; only a few are reported for the determination of REE impurities in high purity rare earth oxides.

The purpose of the present study is to examine the effect of ICP operating parameters on the $REO(H)^+/RE^+$ production ratio, to explore the relationship between the $REO(H)^+/RE^+$ production ratio and the bond strength of corresponding rare earth oxide, and to develop a simple and effective method to determine trace rare earth impurities in high purity Nd_2O_3 by ICP-MS.

EXPERIMENTAL

Instrumentation

Rare earth element determination was performed by a quadrupole (Q) ICP-MS (Model Agilent 7500a, Hewlett-Packard, Yokogawa Analytical Systems, Tokyo, Japan) with a Babington nebulizer; the instrumental operating parameters are given in Table I.

Chemicals and Standard Solution

The rare earth element standard stock solutions were prepared by dissolving the appropriate amount of corresponding SpecPure (Shanghai No. 1 Reagent Factory, Shanghai, P.R. China) rare earth oxides. A standard solution of REEs was prepared by diluting the stock solution of each element in 2% (v/v) HNO_3. The high purity Nd_2O_3 reference material was provided by Jiahua Rare Earth Corporation of Jiangyin, P.R. China, and the high purity Nd_2O_3 sample was provided by Yuelong Rare Earth Research Institute of Shanghai, P.R. China. Other chemicals were of SupraPure grade. Double distilled water was used throughout the experiment.

Sample Preparation

50.00 mg Nd_2O_3 powdered sample was weighed into a 50-mL beaker and 5 mL (1+1) (v/v) HNO_3 was added, then heated on a graphite plate. After cooling, it was diluted to 50 mL in a flask to obtain a 1.0 g L^{-1} Nd_2O_3 concentration. Then, 100 mg L^{-1} and 10 mg L^{-1} Nd_2O_3 samples were obtained by diluting the 1.0 g L^{-1} Nd_2O_3 sample concentration.

TABLE I
ICP-MS Operating Parameters

Plasma		Ion Lenses	
Incident Power	1300 W	Extract 1	–143.5 V
RF Natching	1.6 V	Extract 2	–67 V
Carrier Gas (Ar) Flow Rate	1.16 L min^{-1}	Einzel 1,3	–94 V
External Gas (Ar) Flow Rate	15 L min^{-1}	Einzel 2	0 V
Sampling Depth	7 mm	Plate Bias	0 V
Sample Uptake Rate	0.4 mL min^{-1}	Omega Bias	–27 V
Q-Pole		Omega (+)	2.7 V
AMU Gain	126	Omega (–)	–0.1 V
AMU Offset	126	QP Focus	7.3 V
Axis Gain	0.9998		
Axis Offset	0.02	Integration Time	0.1 s
QP Bias	1.2 V	Nebulizer	Babington
Detector		Torch	Fassel (quartz)
Discriminator	8.7 mV		
Analog	1460 V	Sampler	Ni, 1.0 mm diameter orifice
Pulse HV	900 V	Skimmer	Ni, 0.4 mm diameter orifice

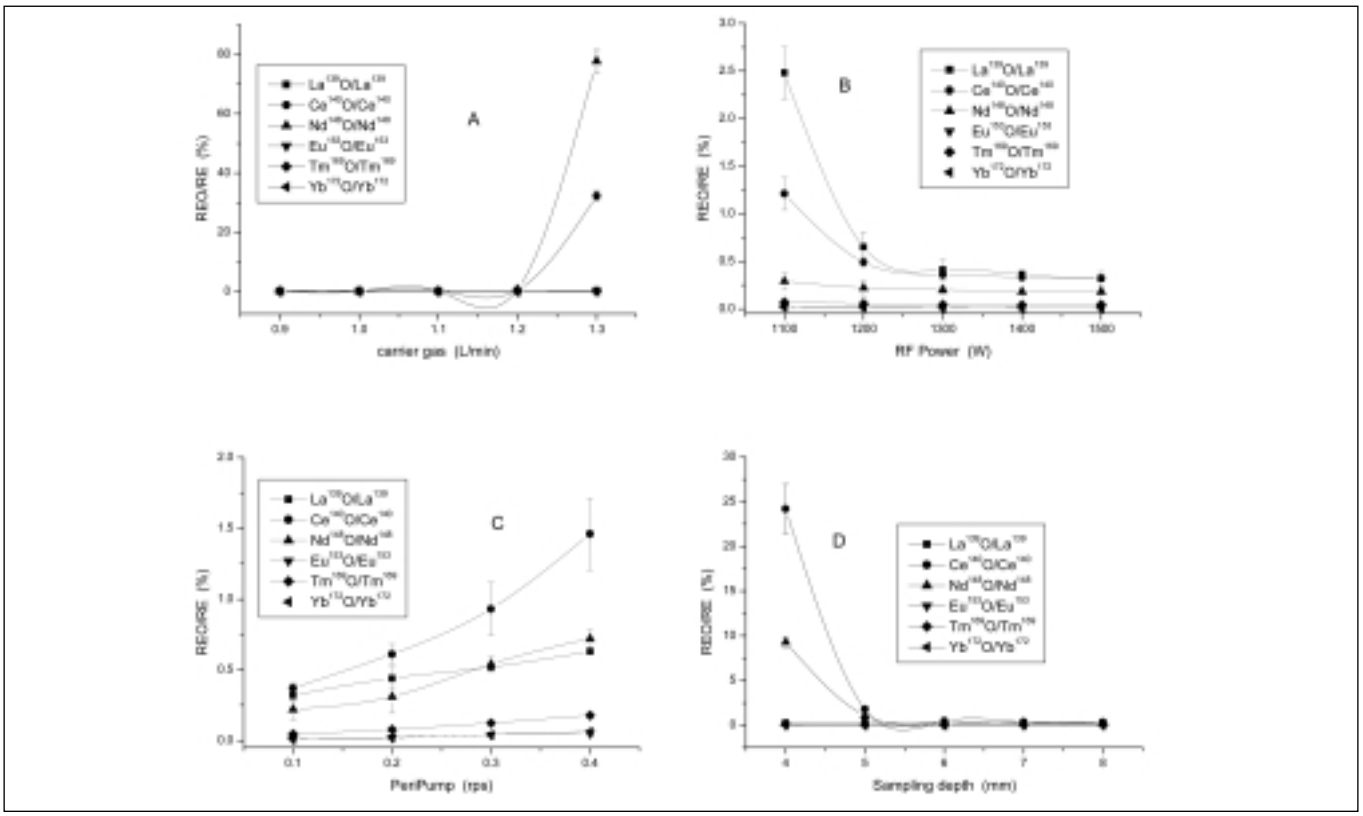

Fig. 1 (A–D). Factors affecting the production ratio of REO^+/RE^+. Error bar indicates two times the standard deviation (n=3). A=Carrier gas flow rate. B=RF power. C=Sample solution uptake rate. D=Sampling depth.

RESULTS AND DISCUSSION

Factors Affecting the Production Ratio of REO^+/RE^+

Carrier Gas

The carrier gas flow rate plays an important role in the formation quality of the analyte aerosol and its transport. Figure 1A shows the effects of carrier gas flow rate on the ratio of REO^+/RE^+. As can be seen, no obvious variation of the REO^+/RE^+ ratios was found in a flow rate range of 0.9 L min^{-1} ~1.2 L min^{-1}; the ratios were very low. However, when the flow rate exceeds 1.2 L min^{-1}, the ratio of LaO^+/La^+, CeO^+/Ce^+, and NdO^+/Nd^+ increases sharply, while no large ratio change was observed for Eu, Tm, and Yb. These experimental results demonstrate that a low carrier gas flow rate is beneficial for a low and stable production ratio of REO^+/RE^+. The reason for this may be that the amount of the aerosol transported into the ICP source in a unit of time would increase rapidly when a much higher carrier gas flow rate is used. As a result, this would cause an overload of the ICP and lead to the rapid increase of the REO^+/RE^+ ratio (3). This situation is much worse for some RE oxides (LaO, CeO, NdO) with higher dissociation energies. In contrast, the permissible variation range for the carrier gas flow rate is much broader for the REO (EuO, TmO, YbO) with a lower dissociation energy.

RF Power

Generally, higher RF power benefits the dissociation of REO and results in a decrease of the REO^+/RE^+ ratio. The influence of RF power on the REO^+/RE^+ ratio was studied, and the results are shown in Figure 1B. For some REO (EuO, TmO, YbO) with a low dissociation energy, the production ratio of REO+ is low and little REO^+/RE^+ ratio change can be found when the RF power is varied from 1.1 kW to 1.5 kW. Thus, a low RF power can be chosen for the determination of these REEs. But for REO (LaO, CeO) with a higher dissociation energy, a higher RF power is necessary for their determination. The mid-RF power is required for the determination of Nd.

Sample Solution Uptake Rate

The sample solution uptake rate indicates the amount of analyte that is transferred into the nebulizer per unit time, and is determined by the rotation rate of the pump. Figure 1C

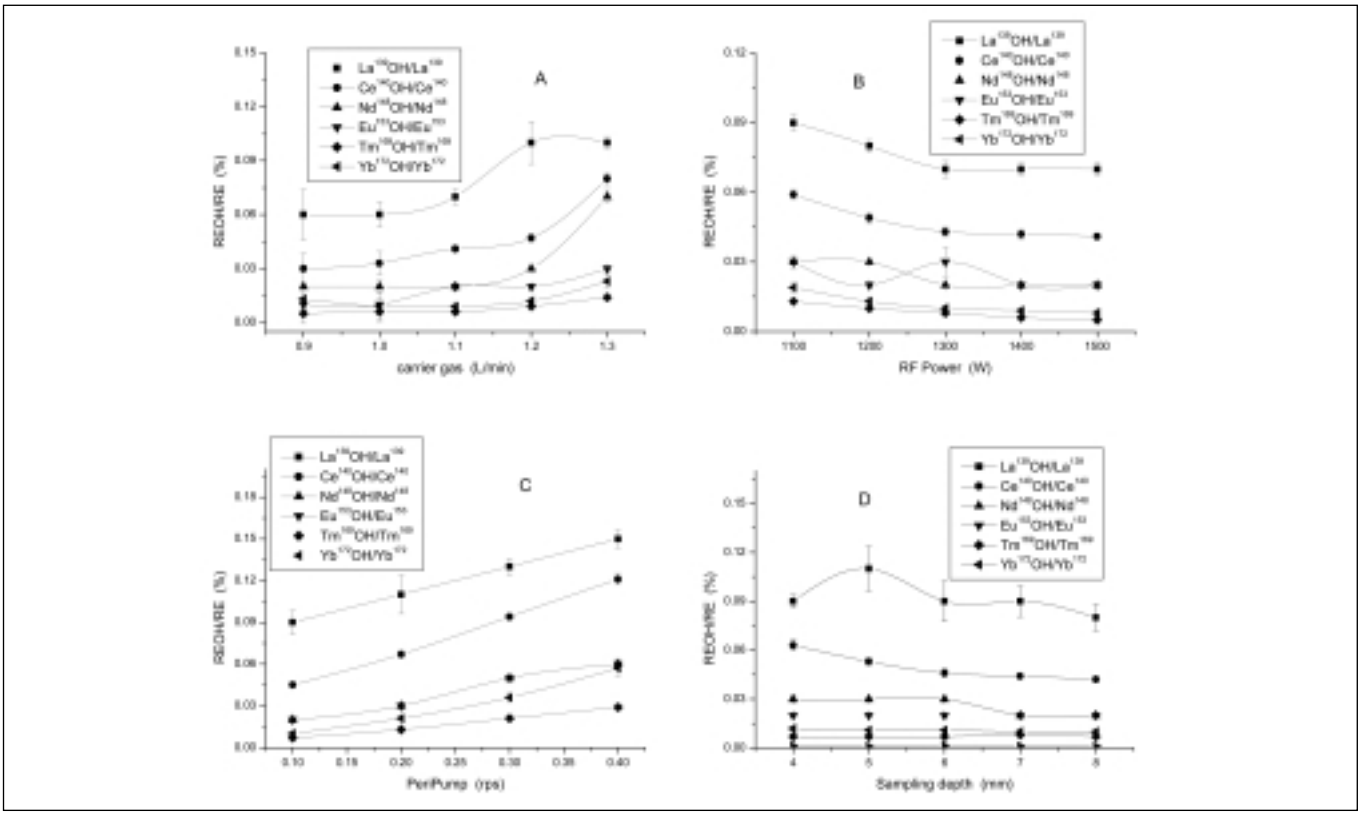

Fig. 2 (A–D). Factors affecting the production ratio of $REOH^+/RE^+$. Error bar indicates two times the standard deviation (n=3). A=Carrier gas flow rate. B=RF power. C=Sample solution uptake rate. D=Sampling depth.

shows the dependence of REO^+/RE^+ ratio on the sample solution uptake rate. The results indicate that the REO^+/RE^+ ratio increased with the increase of the sample solution uptake rate, but this increase is different for different rare earth oxides owing to their different bond strength of REO. In other words, the maximum allowable amount of REEs to produce a consistently low level of oxide in the ICP source varies by element; REOs with high dissociation energy have much lower allowable amounts than those with lower dissociation energy.

Sampling Depth

The effect of sampling depth on REO^+/RE^+ production ratio is shown in Figure 1D. As can be seen, in a broad range of the sampling depth, no obvious REO^+/RE^+ ratio variation appears for rare earth oxides with low dissociation energy. However, for those REO with higher dissociation energy, the REO^+/RE^+ ratio decreases with the increase of the sampling depth. Therefore, a compromise sampling depth should be selected for the determination of light/heavy REEs simultaneously.

Factors Affecting Production Ratio of $REOH^+/RE^+$

Figure 2 shows the effects of the above parameters (carrier gas flow rate, RF power, sample consumption, and sampling depth) on the production ratio of $REOH^+/RE^+$. It was found that these parameters have a similar influence on REOH with the only difference being that the production ratio of REOH+/RE+ is much lower than that of REO+/RE+.

Relationship Between REO(H)+/RE+ Production Ratio and REE Concentration

The variation of $REO(H)^+/RE^+$ production ratio with the change of REE concentration was investigated; the results are given in Table II. It can be seen that the $REO(H)^+/RE^+$ production ratio is stable roughly with REE concentrations varying from 1~100 mg L^{-1}. This indicates that the variation of $REO(H)^+/RE^+$ production ratio depends only on the ICP operating parameters instead of the REE concentration in solution.

Stability of $REO(H)^+/RE^+$ Production Ratio

As mentioned above, low $REO(H)^+/RE^+$ production ratio can be achieved by optimizing the ICP operating parameters. It is also very

TABLE II
Relationship Between $REO(H)^+/RE^+$ Production Ratio (%) and REE Concentration

Ratio	REE Concentration (μg mL^{-1})				Ratio	REE Concentration (μg mL^{-1})			
(%)	1	10	20	100	(%)	1	10	20	100
LaO^+/La^+	0.37	0.37	0.37	0.38	$LaOH^+/La^+$	0.06	0.06	0.06	0.06
CeO^+/Ce^+	0.45	0.46	0.45	0.45	$CeOH^+/Ce^+$	0.08	0.09	0.09	0.09
NdO^+/Nd^+	0.20	0.21	0.21	0.21	$NdOH^+/Nd^+$	0.03	0.03	0.03	0.03
EuO^+/Eu^+	0.03	0.02	0.02	0.02	$EuOH^+/Eu^+$	0.02	0.02	0.02	0.02
TmO^+/Tm^+	0.04	0.04	0.05	0.06	$TmOH^+/Tm^+$	0.01	0.01	0.01	0.01
YbO^+/Yb^+	0.01	0.01	0.01	0.01	$YbOH^+/Yb^+$	0.01	0.01	0.01	0.01

TABLE III
Stability of the REO(H)+/RE+ Production Ratio (%RSD, n=11)

	LaO+/La+	CeO+/Ce+	NdO+/Nd+	EuO+/Eu+	TmO+/Tm+	YbO+/Yb+
RSD(%)	4.2	3.8	7.1	2.8	2.1	7.6
	LaOH+/La+	CeOH+/Ce+	NdOH+/Nd+	EuOH+/Eu+	TmOH+/Tm+	YbOH+/Yb+
RSD(%)	5.0	1.5	1.5	3.1	5.2	5.4

TABLE IV
Bond Strength of REO (KJ mol^{-1})

Element	Bond Strength	Element	Bond Strength
Y - O	715	Tb - O	707
La - O	799	Dy - O	711
Ce - O	795	Ho - O	619
Pr - O	753	Er - O	611
Nd - O	703	Tm - O	557
Sm - O	573	Yb - O	418
Eu - O	470	Lu - O	695
Gd - O	716		

important to keep the production ratio stable. For this reason, under the compromise conditions, stability of the $REO(H)^+/RE^+$ production ratios of most rare earth elements were observed for eleven times sequentially (one determination for every 30 min, total of 330 min); the results are shown in Table III. It can be concluded that the $REO(H)^+/RE^+$ production ratio remains stable as long as the experimental conditions remain stable.

Relationship Between REO^+/RE^+ Production Ratio and Bond Strength of REO

The bond strength of rare earth oxides (26) is listed in Table IV. Under the compromise conditions, the relationship between the REO^+/RE^+ production ratio and the bond strength of their corresponding REO was plotted in Figure 3. It can be seen that the REO^+/RE^+ production ratio is low when the bond strength of the corresponding REO is low. In contrast, the greater the bond strength of rare earth

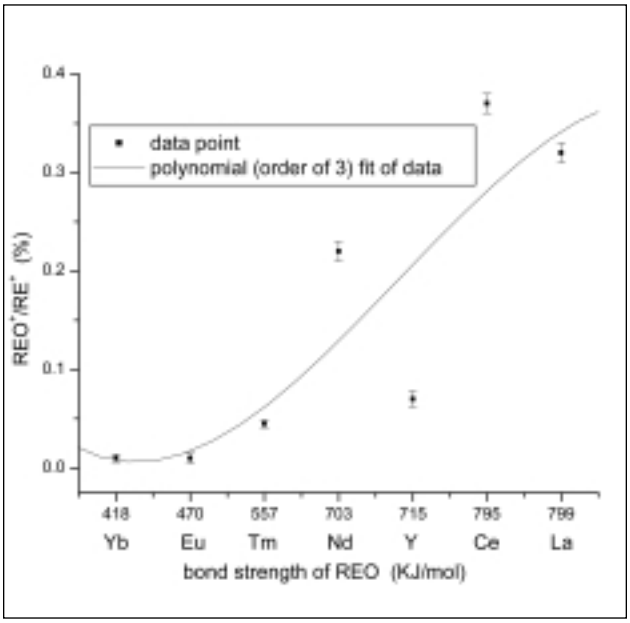

Fig. 3. Relationship between the REO^+/RE^+ production ratio and the bond strength of REO.
Error bar indicates two times the standard deviation (n=11).

oxide, the higher the REO^+/RE^+ production ratio. The reason for this is that the higher the bond strength/dissociation energy of rare earth oxides, the higher the thermal stability of the rare earth oxides, and the more difficult it is for the rare earth oxides to dissociate. Thus, compromise ICP operating parameters are required to obtain a low and stable REO^+/RE^+ production ratio.

Determination of RE Impurities in High Purity Nd_2O_3

As is well known, there is much less research on the determination of REE impurities in light rare earth matrices than in heavy rare earth matrices. One of the most important reasons for this is that the spectral interferences (REO^+, $REOH^+$, in particular) produced by the light REE matrix are much more severe than those produced by heavy REE matrices. Also, the interferences of light REEs with multiple isotopes are more complicated. Nd is a such an element, and has seven isotopes. Table V lists the possible spectral interferences produced by the matrix (Nd) on the other REEs. As can be seen, ^{159}Tb is interfered by both $^{142}NdOH$ and ^{143}NdO, while ^{165}Ho is interfered by ^{148}NdO. Therefore, it is impossible to accurately determine trace Ho and Tb in high purity Nd_2O_3, and an effective spectral interference correction should be performed. For the correction of these interferences, the following correction equations were adopted:

$$S_{Tb159} = S_{159} - S_{142} \times {}^{142}NdOH^+/Nd^+ - S_{143} \times {}^{143}NdO^+/Nd^+$$

$$S_{Ho165} = S_{165} - S148 \times {}^{148}NdOH^+/Nd^+$$

Where S_{Tb159} and S_{Ho165} are the net signal intensity of ^{159}Tb and ^{165}Ho, respectively; S_{159}, S_{142}, S_{165} and S_{148} are the total signal intensity of ^{159}Tb, ^{142}Nd, ^{165}Ho, and ^{148}Nd, respectively.

These correction equations were used to correct the interferences induced by the Nd matrix in the determination of Tb and Ho in Nd_2O_3. The analytical results for a reference material with and without corrections are shown in Table VI. The results obtained indicate that the spectral interferences induced by the Nd matrix are very serious for Tb and Ho, but they can be corrected by the correction equations described above. It should be noted that a low and stable $REO(H)^+/RE^+$ production ratio is a prerequisite for these corrections.

In order to demonstrate the validity of the analytical procedure, both reference and real samples of high purity Nd_2O_3 were analyzed; the analytical results, together with reference values and recoveries, are given in Tables VII and VIII, respectively. As can be seen, good agreement between the determined values and the reference values was obtained. For the real sample analysis, the recovery ranged from 93–115% for all RE impurities except that the recovery of Tb was 65–117%.

CONCLUSION

In this paper, the $REO(H)^+/RE^+$ production ratio of six REEs (La, Ce, Nd, Eu, Tm, Yb) and their effects on the ICP-MS determination of REEs were studied in detail. A simple, rapid, and effective ICP-MS method was developed for the determination of trace rare earth impurities in high purity Nd_2O_3. Based on the research results, the

TABLE V
Possible Spectral Interferences Induced by the Matrix (Nd)

Isotope of Nd	Abundance (%)[a]	Interference of NdO	Interference of NdOH
142	27.2	^{158}Gd (25%), ^{158}Dy (0.1%)	^{159}Tb (100%)
143	12.2	^{159}Tb (100%)	^{160}Gd (22%), ^{160}Dy (2.3%)
144	23.8	^{160}Gd (22%), ^{160}Dy (2.3%)	^{161}Dy (19%)
145	8.3	^{161}Dy (19%)	^{162}Dy (26%), ^{162}Er (0.14%)
146	17.2	^{162}Dy (26%), ^{162}Er (0.14%)	^{163}Dy (25%)
148	5.7	^{164}Dy (28%), ^{164}Er (1.6%)	^{165}Ho (100%)
150	5.6	^{166}Er (34%)	^{167}Er (23%)

[a] (%) Indicates isotope abundance of the element.

TABLE VI
Determination Results (μg g^{-1}) of Tb and Ho in High Purity Nd_2O_3 Reference Sample With and Without Correction

Element	Spiked Amount (μg L^{-1})	Without Correction (μg g^{-1})	With Correction (μg g^{-1})	Reference Value (μg g^{-1})	Recovery (%)
Tb	0	169	5.12	–[a]	
Ho	0	4.6	<0.8	<1.7	
Tb	1.0	178	14.6		95
Ho	1.0	22.1	11.0		110
Tb	2.0	191	26.5		107
Ho	2.0	30.8	20.3		102
Tb	5.0	219	55.0		100
Ho	5.0	59.8	49.8		100

Spiked amount indicates the concentration of REEs spiked into the matrix (100 μg L^{-1}).
[a] No reference value.

TABLE VII
Analytical Results of Trace REEs (μg g^{-1}) in High Purity Nd_2O_3 Reference Sample by ICP-MS (n = 3)

Element	Mass	External Standard	Standard Addition	Reference Values
Y	89	13.7 ± 0.3	13.5 ± 0.4	14.4
La	139	47.9 ± 0.9	50.6 ± 1.2	53.8
Ce	140	3.67 ± 0.07	3.56 ± 0.10	4.6
Pr	141	250 ± 5	237 ± 5	226
Sm	152	50.2 ± 1.1	51.4 ± 1.3	---[b]
Eu	153	0.60 ± 0.02	0.55 ± 0.02	0.4
Gd	157	2.06 ± 0.07	2.14 ± 0.07	1.7
Tb[a]	159	5.12 ± 0.21	5.05 ± 0.24	---[b]
Ho[a]	165	<0.8	<0.8	<1.7
Er	168	1.89 ± 0.09	1.91 ± 0.08	1.9
Tm	169	0.28 ± 0.02	0.26 ± 0.02	0.3
Yb	172	1.58 ± 0.04	1.55 ± 0.03	1.4
Lu	175	0.21 ± 0.01	0.21 ± 0.01	0.3

Note: Results are means of three measurements ± standard deviation.
[a] The result of this element has been corrected by the correction equation.
[b] No reference value.

TABLE VIII
Analytical Results of Trace REEs in High Purity Nd_2O_3 by ICP-MS and Recovery of Spiked Sample

Element	Mass	External Standard (μg g^{-1})	Standard Addition (μg g^{-1})	(%) Recovery		
				1.0[a]	2.0[a]	5.0[a]
Y	89	1.5	1.9	94	105	110
La	139	2.3	2.6	93	100	115
Ce	140	1.2	0.8	98	99	103
Pr	141	6.2	5.3	103	100	104
Sm	152	1.9	2.6	105	110	109
Eu	153	0.5	0.4	96	105	108
Gd	157	1.8	1.4	102	101	102
Tb[b]	159	<0.2	<0.2	65	80	117
Ho[b]	165	1.2	1.0	94	98	99
Er	168	0.7	0.9	101	102	106
Tm	169	0.3	0.3	100	100	101
Yb	172	0.3	0.3	100	103	104
Lu	175	0.6	0.6	100	102	102

[a] The spiked amount of RE (μg L^{-1}) into 100 μg L^{-1} Nd_2O_3 sample solution.
[b] The result of this element has been corrected by the correction equation.

following conclusions can be drawn:

The influence of ICP operating parameters on the production ratio of REO^+ is similar to that of $REOH^+$, but the production ratio of the latter is much lower than that of the former.

This influence is related to the bond strength of corresponding RE oxides, instead of the concentration of REEs in the solution.

Under optimal ICP operating conditions, the stability (%RSD) of the $REO(H)^+/RE^+$ production ratio can be maintained at 10% over 5-1/2 hours.

The proposed method is simple and accurate, and no matrix matching is required. It can be extended to the ICP-MS analysis of trace rare earth impurities in other high purity rare earth oxides.

ACKNOWLEDGMENTS

The authors express their thanks to the National Natural Science Foundation of China for financial support.

Received June 25, 2003.

REFERENCES

1. Jeffrey R. Bacon, Jeffrey S. Crain, Luc Van Vaeck, and John G. Williams, J. Anal. At. Spectrom. 17, 969 (2002).
2. Steve J. Hill, London: Sheffield Academic Press; Boca Raton, FL, USA, CRC Press (1999).
3. Zucheng Jiang, Ruxiu Cai, and Huashan Zhang, Analytical Chemistry of Rare Earth Elements, Science Press, pg. 446 (in Chinese) (2002).
4. W.R. Pedreira, J.E.S. Sarkis, C. Rodrigues, I. A. Tomiyoshi, C.A. da Silva Queiroz, and A. Abrão, Journal of Alloys and Compounds, Vol. 323-324, 49-52 (2001).
5. R. Pedreira, J.E.S. Sarkis, C. Rodrigues, I.A. Tomiyoshi, C.A. de Silva Queiroz, and Brão, Journal of Alloys and Compounds 344, 17-20 (2002).
6. Soulin Lin, Man He, Shenghong Hu, Honglin Yuan, and Shan Gao, Anal. Sci.16, 1291-1295 (2000).
7. Claudio N. Ferrarello, Maria Montes Bayon, J. Ignacio Garcia Alonso, and Alfredo Sanz-Medel, Anal. Chim. Acta 429, 227-235 (2001).
8. Xinde Cao, Ming Yin, and Xiaorong Wang, Spectrochim. Acta Part B, Vol. 56, 431-441 (2001).
9. Alan R. Date, Yuk Ying Cheung, and Marianne E. Stuart, Spectrochim. Acta Part B, Vol. 42, 3-19 (1987).
10. Alan L. Gray and John G. Williams, J. Anal. At. Spectrom. 2, 599-606 (1987).
11. H.P. Longerich, B.J. Fryer, D.F. Strong, and C.J. Kantipuly, Spectrochim. Acta. Part B, 42B, 75 (1987).
12. Frederick E. Lichte, Allen L. Meier, and James G. Crock, Anal. Chem. 59, 1150 (1987).
13. Peter Dulski, Fresenius' J. Anal. Chem. 350, 194-203 (1994).
14. M.G. Minnich and R.S. Houk, J. Anal. At. Spectrom. 13, 167 (1998).
15. J.A. Olivares and R.S. Houk, Anal. Chem. 58, 175 (1986).
16. M.A. Vaughan and G. Horlick, Appl. Spectrosc. 40, 434 (1986).
17. E. Poussel, J. -M. Mermet, and D. Deruaz, J. Anal. At. Spectrom. 9, 61 (1994).
18. X. Romero, E. Poussel, and J. –M. Mermet, Spectrochim. Acta. Part B, 52B, 487 (1997).
19. Shu-Xiu Zhang, Shinichiro Murachi, Totaro Imasaka, and Midori Watanabe, Anal. Chim. Acta 314, 193-201 (1995).
20. Qin Shuai, Zucheng Jiang, Bin Hu, Yongchao Qin, and Shenghong Hu, Fresenius' J. Anal. Chem. 367, 250-253 (2000).
21. Bing Li, Yan Zhang, and Ming Yin, Analyst 122, 543-547 (1997).
22. Philip Robinson, Ashley T. Townsend, Zongshou Yu, and Carsten Münker, Geostd. Newsl. 23, 31-46 (1999).
23. W. Zhu, E. W. B. Deleer, M. Kennedy, P. Kelderman, and G.J.F.R. Alaerts, J. Anal. At. Spectrom. 12, 661-665 (1997).
24. V.A. Elokhin, S.V. Protopopov, S.N. Retivykh, and S.M. Chernetskii, J. Anal. Chem.(Transl. From Zh. Anal. Khim.) 52(11), 1030 (1997).
25. Sébastien Aries, Michel Valladon, Mireille Polvé, and Bernard Dupré, Geostd. Newsl. 24, 19-31 (2000).
26. D.M. Golty, D.C. Gregoire, and C.L. Chakrabarti, Spectrochim. Acta. Part B, 50B, 1365-1382 (1995).

Evaluation of Matrix Effects and Mathematical Correction for the Accurate Determination of Potassium in Environmental Water Samples by Axially Viewed ICP-OES*

**Yanhong Li and Harold VanSickle
Water Services Laboratory, City of Phoenix
2474 S. 22nd Avenue, Phoenix, AZ 85009 USA

*Presented at the Fourth International Conference on Monitoring and Measurement of the Environment, Toronto, Canada, May 27-30, 2002.

ABSTRACT

The severe matrix enhancement effects for potassium determination in environmental water samples using axially viewed inductively coupled plasma optical emission spectrometry (ICP-OES) was investigated in this study. The severe enhancement caused by matrix interference components, such as Li, Na, Mg, and Ca, was demonstrated thoroughly, and the correlation between the enhanced K results and the interference concentrations was investigated. The results showed that both individual and combined interference elements contributed to this kind of enhancement effect. The enhancement ratios (enhanced K/expected K) range from 101%-212% due to the presence of Li, Na, Mg, and Ca, either presented individually or combined in the solution, in the concentration of 10–250 ppm of each interference element. In order to overcome matrix effects and to avoid the use of the time-consuming procedures (such as matrix matching, the method of standard addition, and gradual sample dilution), the approach of mathematical correction was implemented and adequate procedures were developed to handle this problem.

The analyses of Proficiency Testing and Quality Control Reference Standards and a series of test solutions evaluated the validity of this method. The accuracy of the reference standards was within 98.3–104.6%. The corrected spike recoveries from test solutions ranged between 90–110% (most of the recoveries were between 95–105%) and the precision (RSD%) was below 1%.

These preliminary experimental results suggested that this approach of mathematical correction provides a reliable and practical way to overcome the severe matrix enhancement effects for K determination by axially viewed ICP-OES. Precise and accurate K results were obtained by analyzing proficiency testing and quality control reference standards for environmental water samples and serial test solutions in the matrix concentration range of 10–250 ppm of each interference element.

INTRODUCTION

Potassium (K) is an important nutritional element for both plants and animals. Thus, K determination is essential in many different fields and applications, including agriculture, food and drug industries, clinical applications, and environmental monitoring. There are different instrumental techniques available for K determination. Traditionally, flame atomic absorption was used to determine K. But this single-element analysis capability limits productivity when multi-element analyses are required for the same sample. Alternatively, inductively coupled plasma optical emission spectrometry (ICP-OES) is the appropriate technique for the effective multi-element determination in the same sample, including K. Determination of Na, K, Mg, and Ca in urine and saline water and their relative matrix effects, using radial ICP-OES (1) and dual-viewed ICP-OES (2), respectively, are demonstrated and discussed.

Matrix interference effects in ICP-OES analysis have been of concern for application analysts and researchers. Numerous studies have demonstrated the trend of matrix effects under different operational conditions and different applications aspects. It is especially essential to investigate and understand the matrix effects for samples containing high concentrations of alkali and alkali earth elements when using axially viewed ICP-OES analysis since this method tends to present more matrix interferences in certain situations than radially viewed ICP-OES. An overall review of ICP-OES regarding both axially and radially viewed plasma, and the associated features and applications, has been presented and documented (3). The matrix effects of Na and Ca in multi-element analysis using axial and radial ICP-OES have been studied, and the degree of matrix interference and the impact on detection limit has been documented (4–6). Matrix effects in the

**Corresponding author.
e-mail: yanhong.li@phoenix.gov

presence of nitric acid, Ca, Na, K, and P have also been studied, and their impact on analyte transport rate, emission intensities, as well as correlation with excitation energy and plasma excitation conditions have been discussed (7). The study of matrix interferences in the trace element analysis of environmental samples addresses the concerns on changes that occur in the plasma or the nebulization device due to matrix differences between standards and samples (8). Meanwhile, the efficiency of using internal standardization in ICP-OES has been evaluated (9–11). In a more specific case, the matrix effect on dissolved phosphorus determination by axially viewed ICP-OES has been observed in the presence of Na and Ca (12). And the matrix effects under different ICP-OES operational conditions have also been described (13–15).

However, the severe enhancement effect in the determination of K using axially viewed ICP-OES has not been addressed specifically. Although the addition of an ionization buffer was considered and tested to overcome the matrix effect, a few problems emerged, for axially viewed ICP-OES, due to overloading the plasma. In order to compensate for this severe matrix effect sufficiently, introduction of a high concentration ionization buffer is required. This creates a dilemma itself over the potential benefit of compensating matrix effect, including instability of sample intensity, increased chance of system contamination, carryover while analyzing other trace level elements, increased instrument drift and gradual clogging of sample introduction components.

Therefore, there is a need to understand this matrix interference and, more importantly, to find an efficient and practical approach to deal with this problem. This study focuses on the demonstration of matrix enhancement effects for K determination using axially viewed ICP-OES in environmental water samples, with the objective of developing adequate and effective mathematical correction procedures to overcome matrix effects for routine analyses.

In general, practical solutions for overcoming matrix effects such as sample dilution, matrix matching and/or the method of standard addition can be regarded as costly and time-consuming procedures for various and unknown sample matrices. Therefore, mathematical correction, based on the interference concentration, becomes an alternative and effective approach.

This study developed a series of mathematical equations to correct matrix enhancement effects for K determination using the enhancement correction ratio (R). The validity of this approach has been verified in the matrix concentration range of 10–250 ppm for Na, Ca, and Mg.

EXPERIMENTAL

Instrumentation

This study was performed using an Optima™ 3300 XL axially viewed ICP-OES (PerkinElmer Life and Analytical Sciences, Shelton, CT, USA). The instrument was equipped with a GemCone™ nebulizer (Part No. N0690671), cyclonic spray chamber (Part No. N8122188), and 2-mm i.d. alumina injector (Part No. N0695442). The instrumental operating conditions are listed in Table I.

Reagents and Standards

Analytical grade nitric acid and deionized water (18.2 MΩ.cm, E-Pure, Barnstead, Dubuque, IA, USA) were used to prepare the standards and test solutions. Single-element stock standard solutions (K, Ca, Mg, Na, Li, Ba, Cs, Sr, and Y) were obtained from SpexCertiPrep (Metuchen, NJ, USA). Proficiency Testing and Quality Control Reference Standards, which are validated against NIST SRMs, were provided by NIST certified suppliers (AccuStandard, New Haven, CT, USA, and Resource Technology Corporation, Laramie, WY, USA). These reference standards were analyzed to validate the procedure and to verify the accuracy of this method.

Procedure

In order to investigate the matrix enhancement effects for K determination, serial test solutions were made to demonstrate the trend and level of enhancement from matrix interference elements. The test solutions were comprised of varying concentrations of individual and combined interference elements.

All test solutions were prepared to contain individual and/or combinations of elements at specific concentrations in 1% (v/v) HNO_3 by adequate dilution of the stock standards. For individual interference

TABLE I
Operating Conditions of the Optima 3300 XL for the Determination of K

RF Power	1350 W
Nebulizer Flow	0.55 L/min
Auxiliary Flow	0.5 L/min
Plasma Flow	15 L/min
Sample Pump Flow	1 mL/min
Plasma Viewing	Axial
Processing Mode	Area
Auto-integration (min – max)	5–20 s
Read Delay	60 s
Rinse	60 s
Replicates	3
Background Correction	Manual, 2 points
Nebulizer	GemCone
Nebulizer Chamber	Cyclonic
Injector	Alumina, 2 mm

element effects, Ca, Mg, Na, and Li were investigated in the concentration range of 10–250 ppm. To evaluate the combined matrix effects, solutions that contained Na+Ca, Na+Mg, Ca+Mg, and Na+Ca+Mg were also prepared in the concentration range of 10–250 ppm. The test solutions were spiked with 20 ppm K to assess the trend and level of enhancement effects from the matrix interference on K determination.

The wavelength for K at 766.49 nm was used with two points background correction for instrument calibration. Blank solutions of 1% (v/v) HNO_3 and 20 ppm K in 1% (v/v) HNO_3 were used to generate calibration curves with a K linearity of 70 ppm.

Other Group I and II elements, such as Ba, Sr, and Cs, were studied briefly in the concentrations of 10, 30, and 50 ppm. Since there is no significant enhancement effect at these matrix concentration levels, no further evaluation was carried out.

To demonstrate other potential interferences from different blanks, two blank solutions [1% (v/v) HNO_3 + 5% (v/v) HCl, 100 ppm Ca +100 ppm Mg +100 ppm Na in 1% (v/v) HNO_3] were also analyzed for K.

The on-line addition of internal standard (IS), Y at 371.029 nm, was used to monitor instrument stability and to compensate for variations of different matrices.

RESULTS AND DISCUSSION

Matrix Effect

This study has demonstrated that Li, Na, Ca, and Mg contribute severe matrix enhancement effects at various element concentrations when K is determined by axially viewed ICP-OES. A comparison of 20 ppm K peak intensities in different matrices is given in Figure 1.

The enhancement effects of individual interference elements are shown in Figure 2 for 10–250 ppm of Ca, Mg, Na, and Li. As the curves demonstrates, the enhancement effects on K determination tend to increase in proportion to interference element concentrations. Twenty ppm K would be enhanced to have false reading of 25.8 ppm in the presence of 10 ppm Li. 250 ppm Li would enhance 20 ppm K to read as 42.4 ppm, which illustrated an enhancement ratio (enhanced K/expected K) of 212%. Similar enhancement trends occur on K determination caused by co-existence of single Na, Mg, and Ca with K. A series of test results indicated that the enhancement ratios of individual interference elements can range from 101–212% in the presence of 10–250 ppm of Li, Na, Mg, and Ca, and can reach as high as 134%, 147%, 174%, and 212% for Ca, Mg, Na, and Li matrices up to 250 ppm, respectively.

The mixed element enhancement effects for the combined solutions of Na+Ca, Na+Mg, Ca+Mg, and Na+Ca+Mg, all in the concentration range of 10–250 ppm,

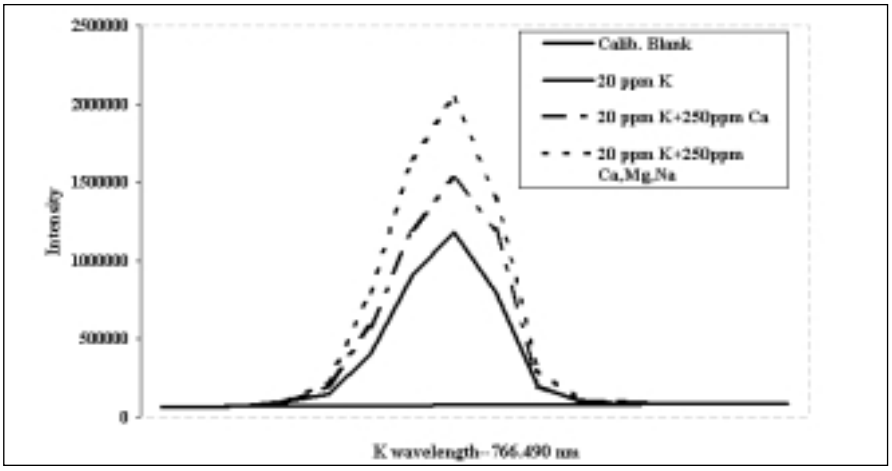

Fig. 1. Spectrum peak comparisons of enhanced K intensity in different matrices.

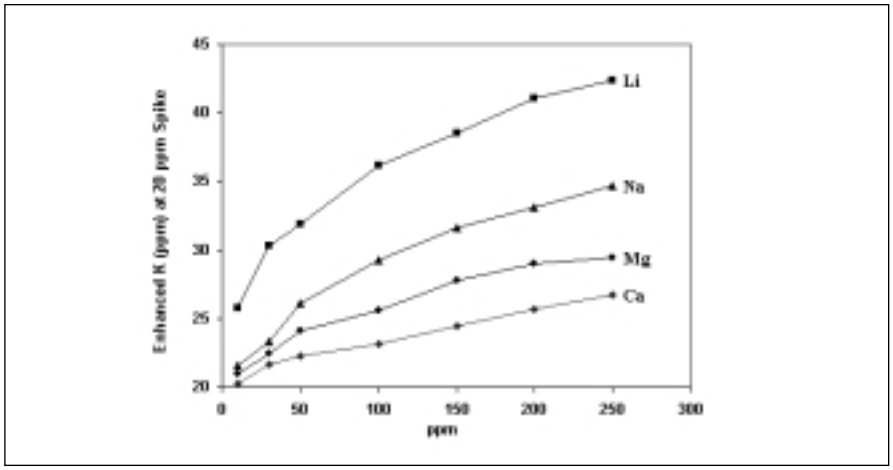

Fig. 2. Individual enhancement effect of Ca, Mg, Na, and Li on K determination.

are shown in Figure 3. For the mixed composition, the combined enhancement impacts are higher than the individual element matrix, but they are not simply additive. In general, the enhancement ratios of the combined matrices are as high as 153%, 182%, 184%, and 188% for Ca+Mg, Na+Ca, Na+Mg, and Na+Ca+Mg up to 250 ppm of each element, respectively. It is worth noting that Na contributed more impact on the combined enhancement (excluded Li). The results in Figure 3 show that there are no significant differences of enhancement ratios when Na was mixed with Ca or Mg only, compared with Na, Ca, and Mg mixed together.

The experimental results also show that Li has the strongest enhancement impact of the elements studied (Li, Na, Ca, Mg, Ba, Cs, and Sr). In general, the individual element enhancement presents the strength in the order of Li>Na>Mg>Ca in the same concentration ranges. Although Li demonstrated the strongest enhancement effect for K determination, it is less likely to find Li at concentrations of high ppm levels for general aqueous environmental samples, such as drinking water, surface water, and wastewater (excluding extreme cases). Meanwhile, Na, Ca, and Mg, which are commonly present in ppm levels in environmental samples, warrant further investigation to handle this matrix effect.

A brief study was conducted to verify the impact from Ba, Cs, and Sr on K determination. The results showed that matrices of 10, 30, and 50 ppm of each Ba, Cs, and Sr did not significantly enhance K determination with axially viewed ICP-OES.

Additionally, in order to demonstrate the impact from different acids and/or similar matrices without the presence of K, two blank solutions [1% (v/v) HNO_3 + 5% (v/v) HCl, 100 ppm Ca +100 ppm Mg +100 ppm Na in 1% (v/v) HNO_3] were analyzed for K, and no bias K intensity was observed. The blank tests suggested that the interference element alone does not elevate the K intensity without the presence of K in the solution. The K intensity will be enhanced only when K co-exists with the matrix-interfering elements.

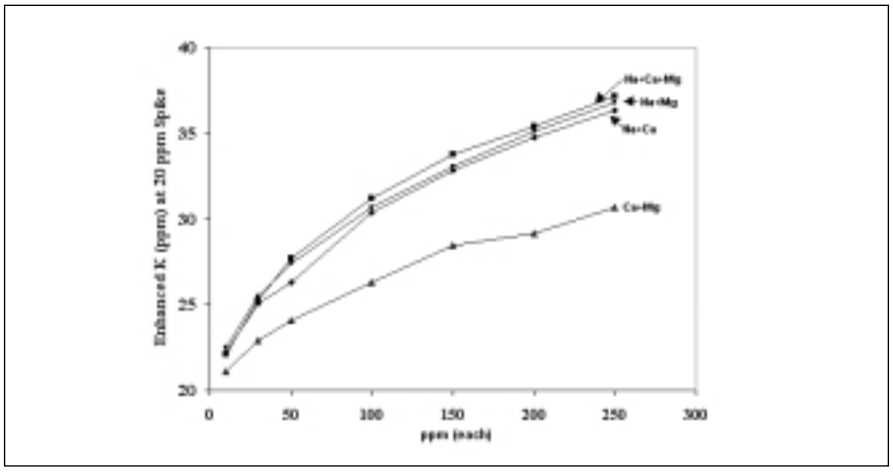

Fig. 3. Combined enhancement effect of Na+Ca, Na+Mg, Ca+Mg, and Na+Ca+Mg on K determination.

Further evaluation of the experimental results suggested that even though different elements and different combinations of elements in the matrices demonstrated various levels of enhancement effects, the enhancement ratio is related to the concentration of the interference elements. This trend describes the relationship between the matrix concentrations and the enhancement ratio. This approach was used for this study in order to develop a practical method for overcoming matrix effects for K determination by axially viewed ICP-OES.

Mathematical Correction – Overcoming Matrix Effects

Since the enhancement effects for K determination correlate to the concentration of a certain matrix composition, it is possible to generate mathematical equations to convert the enhanced K signals to the corrected K results by applying the enhancement correction ratio (R) based on matrix concentrations. Because this work focused on environmental application for general aqueous environmental samples, such as drinking water, surface water, and wastewater (excluding extreme cases), Na, Ca, and Mg enhancement impacts for K determination were studied thoroughly.

In order to develop the enhancement correction ratio (R), eight series of test solutions were prepared. Each series contained individual or combined matrix elements of Ca, Mg, Na, and Li with seven gradually increasing concentration levels -- ranging from 10 ppm to 250 ppm. Each test solution was spiked with 20 ppm K. All test solutions and K calibration standards were acidified to 1% (v/v) HNO_3.

The following mathematical equations were obtained through experimental data. The equations were applied for correction later by method validation, and the corrected results of Proficiency Testing and Quality Control Reference Standards were evaluated.

Kc = Ke / R

Kc---corrected K result (ppm)

Ke---enhanced K reading (ppm)

R---enhancement correction ratio

Since different matrix compositions contribute to different levels of enhancement, each situation was evaluated separately. The equations were obtained by finding the most suitable mathematical equations in order to illustrate the actual enhancement based on the experimental data. The developed equations are shown below:

1. Ca
$R = \{[(2\sqrt{Ca} - 4) / 100] + 1\} \times 100\%$

2. Mg
$R = \{[(2\sqrt{Mg} + 5) / 100] + 1\} \times 100\%$

3. Na
$R = \{[(4\sqrt{Na} + 2) / 100] + 1\} \times 100\%$

4. Na+Ca
$R = \{[(3\sqrt{Na} + 2\sqrt{Ca}) / 100] + 1\} \times 100\%$

5. Na+Mg
$R = \{[(3\sqrt{Na} + 2\sqrt{Mg}) / 100] + 1\} \times 100\%$

6. Ca+Mg
$R = \{[(\sqrt{Ca} + 2\sqrt{Mg}) / 100] + 1\} \times 100\%$

7. Na+Ca+Mg
$R = \{[(3\sqrt{Na} + \sqrt{Ca} + \sqrt{Mg}) / 100] + 1\} \times 100\%$

8. Li
$R = \{[(8\sqrt{Li}) / 100] + 1\} \times 100\%$

Note: √Ca, √Mg, √Na, and √Li represents the square root of concentrations in ppm for Ca, Mg, Na, and Li, respectively.

As the experimental data show, each individual element contributes to different levels of enhancement (see Figure 2). At the same time, the increased enhancements of the combination of these individual elements were not simply additive (see Figure 3). It becomes necessary to evaluate each individual element and each combination of matrices in order to obtain a more accurate mathematical equation to represent the actual enhancement for each situation, as shown in equations 1 through 8. Thus, it seems difficult to try to use one general equation to simplify the complex situations when multiple variables could impact the outcome of enhancement.

The results also showed that Na strongly impacts the enhancement when Na is mixed with Ca or Mg only, or mixed with Ca and Mg together. As Figure 3 shows, there are similar degrees of enhancement found when Na is present in the mixed solutions of Ca and/or Mg. Meanwhile, Ca and Mg show a similar degree of enhancement in mixed solutions in the presence of a significant quantity of Na (i.e., Na 10 ppm or more). Therefore, equation 7 for Na+Ca+Mg was almost converted to equation 5 for Na+Mg and to equation 4 for Na+Ca (i.e., $3\sqrt{Na} + \sqrt{Ca} + \sqrt{Mg} \approx 3\sqrt{Na} + 2\sqrt{Mg} \approx 3\sqrt{Na} + 2\sqrt{Ca}$). Thus, when samples contain Na, Mg, and Ca (excluding extreme or specific cases), it is recommended that equation 7 be used as the general solution to correct matrix effects in the concentration ranges specified for this study. In the cases of only individual interference element in the solution, the corresponding equation for the element should be applied for enhancement correction.

Impact of Internal Standard

All tests were analyzed with an added internal standard (Y 371.029 nm) to monitor instrument stability and to compensate for variations of different matrices. The results show that the absolute intensities of internal standard do not change significantly while matrix components and/or matrix concentrations vary. The relative percent differences (RPD %) of Y intensities compared to initial intensity of Y were less than 5% over four hours of continuous analyses (see Figure 4). On the other hand, the enhanced absolute K intensities responded directly to the changes of matrix components and/or matrix concentrations. As the interference concentrations increased, K intensities increased proportionally while no significant intensity changes were observed for the internal standard. Since the internal standard has less measurable impact over the severe enhancement of K caused by matrix effects, there are no significant differences between the absolute K intensities and the converted K intensities by the internal standard (see Figure 5). Therefore, neither the internal standard Y can

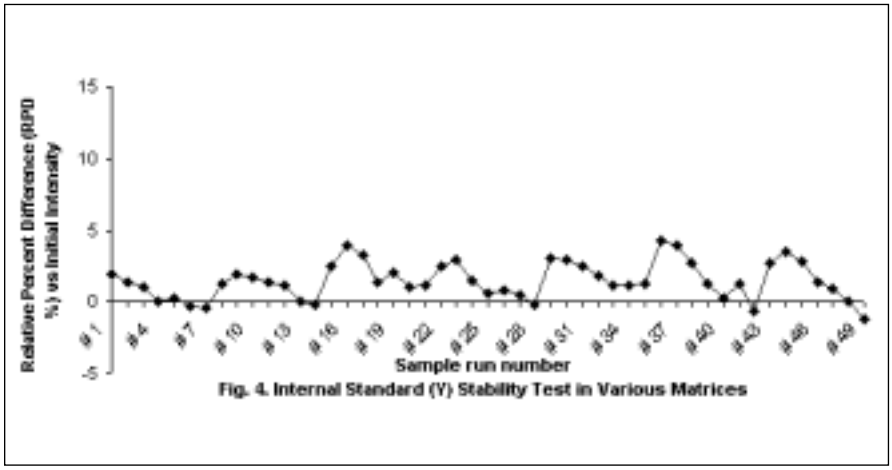

Fig. 4. Internal standard (Y) stability test in various matrices.

be used effectively to compensate for this matrix effect on K, nor does the internal standard Y itself show significant enhancement or suppression caused by these matrices.

Method Validation

When the developed equations were applied to the eight series of test solutions with various matrix concentrations, the corrected K results were agreeable with the expected K value (20 ppm). All recoveries ranged between 90-110% (most of the recoveries between 95-105%) in the interference concentration range of 10–250 ppm (see Tables II and III).

To further validate the applicable accuracy of this approach, several Proficiency Testing and Quality Control Reference Standards provided by NIST certified suppliers, which are validated against NIST SRMs, were analyzed in this study. These reference standards contain various concentration levels of interference elements (Ca, Mg, Na) along with K (see Table IV). The analyses of these standards are suitable to verify the mathematical correction of this method. All corrected results were found to be within the acceptance limits of the certified values, with recoveries between 98.3–104.6% (see Table IV and Figure 6), thus confirming the validity of this method.

Discussion

As a single interference element, Li generates the strongest enhancement on K determination, and we briefly studied the effect of Li on K. The results showed that 1 ppm Li tends to enhance K at approximately 5% or less. Most environmental water samples have Li levels significantly less than 1 ppm Li.

To seek a similar matrix enhancement among other elements, a brief investigation was also performed to evaluate matrix effects

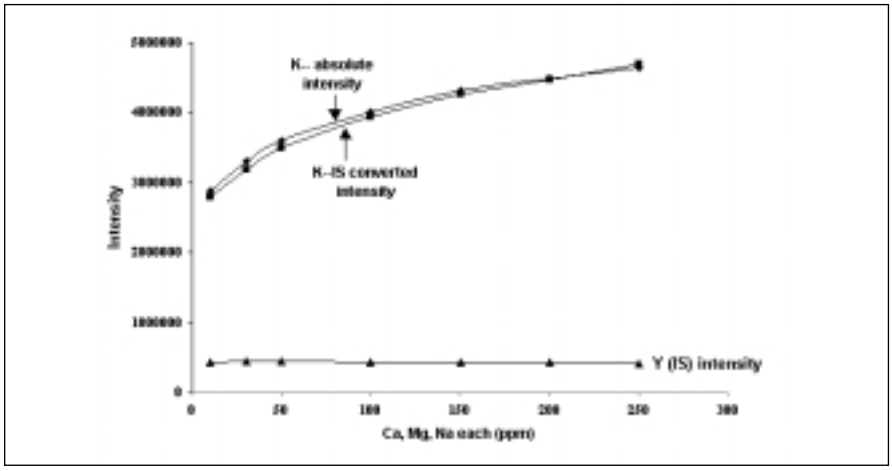

Fig. 5. Enhanced absolute K intensity vs. converted intensity by internal standard (Y). Matrices: Ca+Mg+Na.

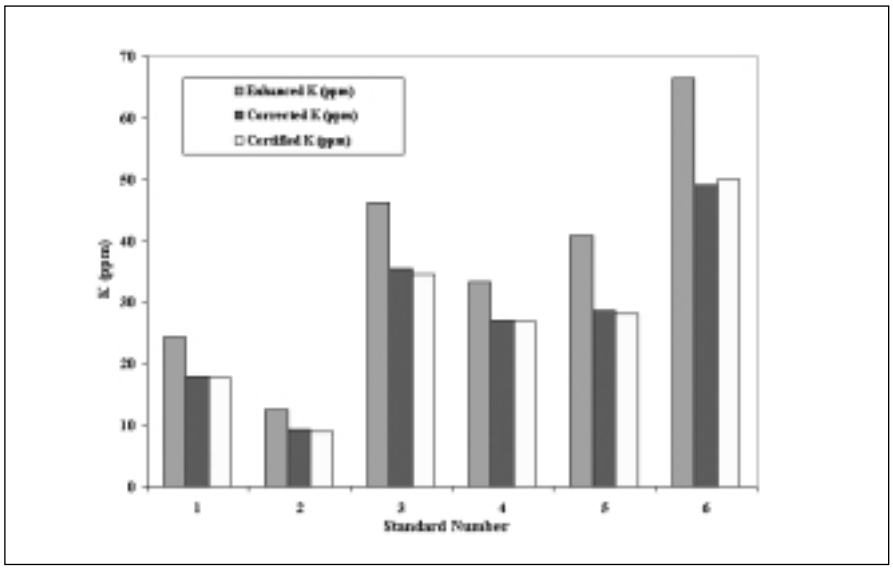

Fig. 6. Proficiency testing and quality control reference standards verification.

of Li, K, Mg, and Be on the determination of Na by axially viewed ICP-OES. The results showed that 20 ppm Li will enhance approximately 10% on the determination of 20 ppm Na, 60 ppm Li will enhance approximate 20% on the determination of 20 ppm Na. No enhancement effects were observed from single 20 ppm of K, Mg, and Be, respectively, on the determination of 20 ppm Na.

The advantages of using mathematical correction for the determination of K by axially viewed ICP-OES include (a) eliminating the time-consuming sample dilution process to overcome matrix effects, (b) better approach to understand the matrix effects of unknown and various sample matrices, (c) providing an alternate and effective method instead of using the costly method of standard addition, (d) avoiding the procedure of overloading the plasma with the addition of an ionization buffer, thus reducing the chance of sample contamination and the need of instrument maintenance.

TABLE II
Individual Element Enhancement Effect of Ca, Mg, Na, and Li on K Determination (20 ppm Spike)

Ca (ppm)	Enhanced K (ppm)	SD (ppm)	RSD (%)	Enhancement Ratio (%)[a]	Enhancement Correction Ratio (%)[b]	Corrected K (ppm)	Recovery (%)
10	20.26	0.069	0.34	101.3	102.3	19.80	99.0
30	21.62	0.022	0.10	108.1	107.0	20.21	101.1
50	22.27	0.044	0.20	111.4	110.1	20.22	101.1
100	23.18	0.006	0.03	115.9	116.0	19.98	99.9
150	24.42	0.048	0.19	122.1	120.5	20.27	101.3
200	25.68	0.031	0.12	128.4	124.3	20.66	103.3
250	26.74	0.013	0.05	133.7	127.6	20.95	104.8

Mg (ppm)	Enhanced K (ppm)	SD (ppm)	RSD (%)	Enhancement Ratio (%)[a]	Enhancement Correction Ratio (%)[b]	Corrected K (ppm)	Recovery (%)
10	21.00	0.030	0.15	105.0	111.3	18.86	94.3
30	22.45	0.100	0.44	112.3	116.0	19.36	96.8
50	24.10	0.170	0.72	120.5	119.1	20.23	101.1
100	25.57	0.080	0.33	127.9	125.0	20.46	102.3
150	27.79	0.080	0.29	139.0	129.5	21.46	107.3
200	29.03	0.060	0.22	145.2	133.3	21.78	108.9
250	29.46	0.100	0.33	147.3	136.6	21.56	107.8

Na (ppm)	Enhanced K (ppm)	SD (ppm)	RSD (%)	Enhancement Ratio (%)[a]	Enhancement Correction Ratio (%)[b]	Corrected K (ppm)	Recovery (%)
10	21.59	0.056	0.26	108.0	114.6	18.83	94.2
30	23.33	0.045	0.19	116.7	123.9	18.83	94.1
50	26.11	0.085	0.32	130.6	130.3	20.04	100.2
100	29.25	0.095	0.32	146.3	142.0	20.60	103.0
150	31.63	0.008	0.03	158.2	151.0	20.95	104.7
200	33.12	0.110	0.33	165.6	158.6	20.89	104.4
250	34.71	0.066	0.19	173.6	165.2	21.01	105.0

Li (ppm)	Enhanced K (ppm)	SD (ppm)	RSD (%)	Enhancement Ratio (%)[a]	Enhancement Correction Ratio (%)[b]	Corrected K (ppm)	Recovery (%)
10	25.76	0.078	0.30	128.8	125.3	20.56	102.8
30	30.28	0.088	0.29	151.4	143.8	21.05	105.3
50	31.92	0.061	0.19	159.6	156.6	20.39	101.9
100	36.15	0.046	0.13	180.8	180.0	20.08	100.4
150	38.49	0.122	0.32	192.5	198.0	19.44	97.2
200	41.05	0.070	0.17	205.3	213.1	19.26	96.3
250	42.41	0.039	0.09	212.1	226.5	18.72	93.6

[a] Enhanced K/20 ppm.
[b]Calculated using equations.

TABLE III
Combined Enhancement Effect of Na+Ca, Na+Mg, Ca+Mg, and Na+Ca+Mg on K Determination (20 ppm Spike)

Na (ppm)	Ca (ppm)	Enhanced K (ppm)	SD (ppm)	RSD (%)	Enhancement Ratio (%)[a]	Enhancement Correction Ratio (%)[b]	Corrected K (ppm)	Recovery (%)
10	10	22.22	0.07	0.31	111.1	115.8	19.19	95.9
30	30	25.08	0.02	0.01	125.4	127.4	19.69	98.4
50	50	26.32	0.07	0.27	131.6	135.4	19.45	97.2
100	100	30.39	0.04	0.14	152.0	150.0	20.26	101.3
150	150	32.83	0.08	0.23	164.2	161.2	20.36	101.8
200	200	34.75	0.07	0.19	173.8	170.7	20.36	101.8
250	250	36.35	0.07	0.18	181.8	179.1	20.30	101.5

Na (ppm)	Mg (ppm)	Enhanced K (ppm)	SD ppm)	RSD (%)	Enhancement Ratio (%)[a]	Enhancement Correction Ratio (%)[b]	Corrected K (ppm)	Recovery (%)
10	10	22.49	0.09	0.40	112.5	115.8	19.42	97.1
30	30	25.48	0.05	0.21	127.4	127.4	20.00	100.0
50	50	27.39	0.06	0.20	137.0	135.4	20.24	101.2
100	100	30.68	0.07	0.23	153.4	150.0	20.45	102.3
150	150	33.04	0.05	0.16	165.2	161.2	20.49	102.5
200	200	35.09	0.01	0.02	175.5	170.7	20.56	102.8
250	250	36.80	0.02	0.05	184.0	179.1	0.55	102.8

Ca (ppm)	Mg (ppm)	Enhanced K (ppm)	SD (ppm)	RSD (%)	Enhancement Ratio (%)[a]	Enhancement Correction Ratio (%)[b]	Corrected K (ppm)	Recovery (%)
10	10	21.12	0.03	0.16	105.6	109.5	19.29	96.4
30	30	22.93	0.04	0.17	114.7	116.4	19.69	98.5
50	50	24.08	0.06	0.26	120.4	121.2	19.87	99.3
100	100	26.27	0.06	0.24	131.4	130.0	20.21	101.0
150	150	28.45	0.03	0.10	142.3	136.7	20.81	104.0
200	200	29.17	0.01	0.03	145.9	142.4	20.48	102.4
250	250	30.65	0.01	0.03	153.3	147.4	20.79	103.9

Na (ppm)	Ca (ppm)	Mg (ppm)	Enhanced K (ppm)	SD (ppm)	RSD (%)	Enhancement Ratio (%)[a]	Enhancement Correction Ratio (%)[b]	Corrected K (ppm)	Recovery (%)
10	10	10	22.12	0.02	0.10	110.6	115.8	19.10	95.5
30	30	30	25.23	0.16	0.65	126.2	127.4	19.81	99.0
50	50	50	27.69	0.05	0.19	138.5	135.4	20.46	102.3
100	100	100	31.22	0.03	0.09	156.1	150.0	20.81	104.1
150	150	150	33.74	0.08	0.02	168.7	161.2	20.93	104.6
200	200	200	35.37	0.03	0.08	176.9	170.7	20.72	103.6
250	250	250	37.16	0.02	0.04	185.8	179.1	20.75	103.8

[a] Enhanced K/20 ppm.
[b] Calculated using equations.

TABLE IV
Proficiency Testing and Quality Control Reference Standards Verification

Standards	Na (ppm)	Ca (ppm)	Mg (ppm)	Enhanced K (ppm)	SD (ppm)	RSD (%)	Enhancement Correction Ratio (%)[a]	Corrected K (ppm)	Certified K (ppm)	Accuracy (%)	Acceptance Limits
1	53	71.6	33.8	24.39	0.032	0.13	136.1	17.92	17.7	101.2	15.1–20.3
2	72.5	26.2	11.8	12.58	0.011	0.09	134.1	9.38	8.97	104.6	7.53–10.5
3	62.9	28.1	1.05	46.14	0.16	0.35	130.1	35.46	34.5	102.8	29.9–39.3
4.	27.8	None	None	33.28	0.028	0.09	123.1	27.04	26.9	100.5	23.2–30.7
5	104	57.3	17.9	40.86	0.396	0.97	142.4	28.7	28.1	102.1	24.2–32.1
6	50	50	50	66.5	0.19	0.29	135.4	49.13	50	98.3	N/A

Standard 1: RTC PEI-027-12, Laramie, WY, USA
Standard 2: AccuStandard IPE-MET-005, lot #186493-68-01, New Haven, CT, USA
Standard 3: RTC QCI-027, lot #9, Laramie, WY, USA
Standard 4: AccuStandard IPE-MET-005, lot #186494-01-01, New Haven, CT, USA
Standard 5: AccuStandard IPE-MET-005, lot #156829-06-01, New Haven, CT, USA
Standard 6: SpexCertiPrep ICAL-1, Metuchen, NJ, USA

[a] Use equation 7 for standards 1, 2, 3, 5, and 6; use equation 3 for standard 4.

CONCLUSION

The severe magnitude of matrix effects was observed while using axially viewed ICP-OES for the determination of K. The group I elements (Li, Na) and group II elements (Mg, Ca) contribute to this matrix effect. The matrix effect varied depending on the concentration of the different interference elements and/or different combinations of interference elements. The level of enhancement ratio can range from 101–212% in the presence of 10–250 ppm of Li, Na, Ca, and Mg. The strength of enhancement is in the order of Li>Na>Mg>Ca.

To overcome the matrix effects in the determination of K in unknown and various aqueous environmental samples, a practical and effective approach is needed to handle this problem for the accurate determination of K. In this preliminary study, we developed a successful mathematical correction method using the enhancement correction ratio (R), which is based on the interference concentration in the sample matrix. Evaluation and accuracy of this method was validated by the analysis of several Proficiency Testing and Quality Control Reference Standards. The results of these reference standards are within acceptable limits and are quite satisfactory. This has proven that the suggested approach of mathematical correction provides a reliable and practical way to overcome the severe matrix effects for K determination by axially viewed ICP-OES in the matrix concentration range of 10–250 ppm for Na, Ca, and Mg.

ACKNOWLEDGMENTS

The authors acknowledge the cooperation of the co-workers and the support of Randy Gottler and Jennifer Calles of the City of Phoenix Water Services Laboratory.

Received May 19, 2003.

REFERENCES

1. A. Krejcova, T. Cernohorsky, and E. Curdova, J. Anal. At. Spectrom. 16, 1002 (2001).
2. K. Mitko and M. Bebek, At. Spectrosc. 21(3), 77 (2000).
3. I.B. Brenner and A.T. Zander, Spectrochim. Acta, Part B, 55, 1195 (2000).
4. I.B. Brenner, A.T. Zander, M. Cole, and A. Wiseman, J. Anal. At. Spectrom. 12, 897 (1997).
5. I.B. Brenner, M. Zischka, B. Maichin, and G. Knapp, J. Anal. At. Spectrom. 13, 1257 (1998).
6. I.B. Brenner, A. Le Marchand, C. Daraed, and L. Chauvet, Microchem. J. 63 344 (1999).
7. B. Budic, J. Anal. At. Spectrom. 13, 869 (1998).
8. M. Hoenig, H. Docekalova, and H. Bacten, J. Anal. At. Spectrom. 13, 195 (1998).
9, R.M. Belchamber and G. Horlick, Spectrochim. Acta, Part B, 37, 1037 (1982).
10. J.C. Ivaldi and J.F. Tyson, Spectrochim. Acta, Part B, 51, 1443 (1996).
11. X. Romero, E. Poussel, and J.M. Mermet, Spectrochim. Acta, Part B, 52, 487 (1997).
12.J. L. M. de Boer, U. Kohlmeyer, P.M. Breugem, and T. Van der Velde-Koerts, Fresenius' J. Anal. Chem. 360, 132 (1998).
13. J.M. Mermet, J. Anal. At. Spectrom. 13, 419 (1998).
14. M. Stepan, P. Musil, E. Poussel, and J.M. Mermet, Spectrochim. Acta, Part B, 56, 443 (2001).
15. C. Dubuisson, E. Poussel, J.L. Todoli, and J.M. Mermet, Spectrochim. Acta, Part B, 53, 593 (1998).

Multielement ICP-OES Analysis of Mineral Premixes Used to Fortify Foods

***Daniel Hammer, Marija Basic-Dvorzak, and Loïc Perring**
Department of Quality and Safety Assurance, Nestlé Research Center
P.O. Box 44, Vers chez-les-Blanc, CH-1000, Lausanne 26, Switzerland

ABSTRACT

A method for the multielement analysis of mineral premixes using inductively coupled plasma optical emission spectrometry (ICP-OES) was developed and validated. Due to the lack of certified premix samples, the validation was performed on five different purchased premixes.

A microwave-assisted acid hydrolysis was used to bring the elemental composition into solution.

A standardized dilution scheme permitted the determination of different ranges of elemental concentrations found in premixes. Calcium, chromium, copper, iron, magnesium, manganese, molybdenum, selenium, and zinc were determined simultaneously by ICP-OES. Robust repeatability and intermediate reproducibility were estimated and found to be sufficient for three out of five premixes. The same was true for accuracy which had been estimated by the determination of recovery from spiked premixes. Insufficient repeatability and accuracy for two pet food premixes was due to their heterogeneity. Using a larger sample size for these premixes significantly improved the repeatability and intermediate reproducibility for several elements.

The developed multielement method performed well on homogeneous mineral premixes, but high repeatability data are to be expected from pet food premixes due to their high heterogeneity.

INTRODUCTION

The fortification of foods with vitamins and minerals is one of the most effective methods to improve health and prevent nutritional deficiencies. This method has helped to eliminate diseases such as goitre, rickets, and beriberi in many countries. Examples of early fortified foods are iodized salt in the 1920s, milk with vitamin D in the 1930s, and flour and bread enriched with vitamins B1, B2 and Fe in the 1940s. Nowadays, fortification allows the standardization of nutrient content in foods that show natural variable concentrations (1).

It is obvious that the concentrations of vitamins and minerals in premixes have to be exact in order to ensure the quality of the finished products. In the case of Se, this is not only a quality issue but also a safety concern because the concentration range between beneficial and adverse health effects is narrow (2).

Analytical methods for minerals in foodstuff range from colorimetric methods to inductively coupled plasma mass spectrometry (ICP-MS). However, only a few methods report on the analysis of fortified foods or food supplements. A rapid method for iron determination in such foods has been described recently using spectrophotometry (3). The selenium concentration in dietary supplements is mainly checked by ICP-MS or hydride generation atomic absorption spectroscopy (HG-AAS) (4,5). In fact, atomic absorption spectroscopy (AAS) is one of the most commonly used tools for mineral determination in foods or animal feed and some methods have been reported in the literature (6–9). The major drawback of AAS, however, is that not all important elements can be measured with one system and that analysis is not simultaneous. Inductively coupled plasma optical emission spectrometry (ICP-OES) features multielement capability, wide linear dynamic range, high analytical sensitivity, and high sample throughput. Multielement analysis by ICP-OES has become routine and accuracy is better or at least comparable to AAS (10). No ICP-OES multielement analysis with regard to the problem of mineral premixes has been found in a recent literature survey. However, the simultaneous determination of minerals in multivitamin and salinated water samples has been reported (11,12). These studies address similar problems such as high salt concentrations and a high concentration range of minerals which have to be taken into account by appropriate dilutions. Table I lists the concentration range encountered in the investigated premixes.

It was the aim of this study to develop and validate a method using ICP-OES for the determination of Ca, Cu, Cr, Fe, Mg, Mn, Mo, Se, and Zn in mineral premixes. Acid microwave digestion was used for sample preparation, a widely used method in food sample digestion (13-16). Several emission lines were tested for interferences and correction by internal standards was applied for all elements in order to compensate for adverse effects of high salt charges. Limits of quantitation, robust repeatability, intermediate reproducibility, and accuracy (recovery of minerals from spiked premixes) were estimated.

**Corresponding author.*
e-mail: daniel.hammer@rdls.nestle.com

TABLE I
Expected Concentration Range of Minerals in Most Premixes Used for Food Fortification

	Ca	Cr	Cu	Fe	Mg	Mn	Mo	Se	Zn
Min ($mg \cdot kg^{-1}$)	8000	20	50	500	25000	1	15	10	500
Max ($mg \cdot kg^{-1}$)	80000	1000	40000	100000	40000	90000	15000	7000	90000

EXPERIMENTAL

Instrumentation

A CEM (MDS 2000, max. 630 W at 100% of Power) microwave digestion system with glass volumetric flasks was used for sample preparation.

For the nine element measurements, a Varian Vista-Pro Axial ICP-OES (Varian, Mulgrave, Victoria, Australia) was used. A cyclonic spray chamber (thermostated at 15°C) coupled with a Micromist nebulizer (Glass Expansion, West Melbourne, Victoria, Australia) was used as the injection device. The operating conditions are shown in Table II.

A solution containing internal standards (strontium and indium) was mixed on-line with analytical solutions using a mixing manifold (2 ways in and 1 way out) linked between the peristaltic pump and the nebulizer.

Reagents and Standard Solutions

High-purity water (18.2 MΩ) using a Milli-Q™ Plus system (Millipore, Bedford, MA, USA).

Nitric acid freshly sub-distilled from conc. nitric acid (analytical grade, 65% p.a.). Suprapur® hydrochloric acid (30%) (Merck, Darmstadt, Germany). Suprapur hydrogen peroxide (30% v/v) (Merck).

Nine element standards were prepared by dilution of a 1000-mg L^{-1} single-element stock solution (Merck) in a 5% HNO_3 matrix.

TABLE II
Axial ICP-OES Operating Conditions

Power	1300 W	
Plasma gas-flow	18 L min^{-1}	
Auxiliary flow	2.25 L min^{-1}	
Spray chamber	Cyclonic, internal volume = 100 mL	
	Argon flow 0.90 L min^{-1}	
Nebulizer	Micromist, Micro-concentric nebulizer	
	1 mL min^{-1}	
Replicate read time	5 s	
Replicates	5	
Main emission lines (nm)	Ca 422.673	Cr 283.563
	Cu 324.754	Fe 259.940
	Mg 279.553	Mn 257.610
	Mo 202.032	Se 196.026
	Zn 213.857	
	In 303.936 (internal standard, 40 mg L^{-1})	
	Sr 338.071 (internal standard, 10 mg L^{-1})	
Alternatively studied emission lines (nm)	Cr 205.560	Cr 267.716
	Mo 204.598	Mg 280.270
	Mg 285.213	

Strontium was prepared by dilution of a 1000-mg L^{-1} Sr stock solution (Fluka, Buchs, Switzerland)

Indium was prepared by dilution of a 1000-mg L^{-1} In stock solution (Merck).

Sample Preparation

Microwave Digestion

One g of sample was weighed into 100-mL glass volumetric flasks. Five mL of 65% HNO_3 was added and left to react for half an hour at ambient temperature; then the volumetric flask was heated on a hot plate (150°C) until the acid digestion started (yellow fume production). Then 5 mL of 30% H_2O_2 was slowly added to prevent a fast reaction. After predigesting the samples, the flasks were put into the microwave oven and an appropriate power program was used, depending on the number of samples to be digested (see Table III). The first step required 20 min heating time. After this step, the flasks were carefully taken out of the microwave oven and 5 mL 30% HCl was added. The flasks were reheated for 10 min using the same program. After removing the flasks from the oven, they were left standing to cool, then each flask was brought to volume with high purity water. A preparation blank was included in each series of digestions.

TABLE III
Microwave System: Digestion Program

No. of Vessels	Power (%)
5	23
6	27
7	31
8	35
9	39
10	43
11	47
12	51

Dilutions

Each digested sample was analyzed undiluted, 20 times diluted, and 200 times diluted. The dilutions were produced using a 5% HNO_3 solution.

RESULTS AND DISCUSSION

Calibration and Linearity

Calibration was performed using six standards with 0.2, 0.5, 1.0, 1.5, 2.0, and 5.0 mg L^{-1} concentrations for Ca, Cu, Fe, Mg, Mn, Mo, and Zn and 0.1, 0.2, 0.4, 0.6, 0.8, and 1.0 mg L^{-1} for Se and Cr. On our apparatus, the calibration type was a linear fit for all elements, with the exception of Mg, which followed a quadratic calibration model. All calibration curves had a $R^2 > 0.99$.

Ruggedness-Study of Interferences

Wavelengths were chosen according to their least probability of interferences with other elements. Recoveries were determined from low concentration spikes of analytes (0.1 mg L^{-1}) in matrices with a high concentration of the other eight elements (25 mg L^{-1}). Recoveries were calculated using the following equation:

$$\%\text{Recovery} = \frac{[\text{Analyte} + 8\ \text{Elements}]}{\text{Analyte}} \cdot 100\%$$

[Analyte + 8 Elements] = Concentration of analyte found in the sample with the analyte and the 8 other elements

Analyte = Concentration of analyte in the sample without other elements

The recoveries were found to be between 95–110% for all elements, except for Zn (see Table IV). Zinc was strongly influenced by signals from Cu 213.854 nm and Fe 213.859 nm (Figure 1a and Table V). This was only true when Zn was present in low concentration compared to the interfering element. Zinc was not influenced when Fe and Cu were present at the same concentration (2.5 mg L^{-1}) (see Figure 1b and Table V) and therefore the Zn line at 213.851 nm was chosen for our method. Two alternative wavelengths for Cr were tested and resulted in good recoveries; but in order to obtain maximal sensitivity, the Cr 283.563 nm was chosen.

Limits of Quantitation

Microwave digests of premix matrices (free of analyte) were spiked with low concentrations of the nine elements. The concentration of the lowest standard was chosen for these spikes. Limits of quantitation were calculated using the following equation and are listed in Table VI:

$$\text{LOQ} = \frac{[\text{Spike}]}{(A_{spike} - A_{matrix})} \cdot SD_{matrix} \cdot 10$$

[Spike] = Spike concentration in mg L^{-1}

$\mathbf{A}_{spike}$ = Peak height measured for the spike in the digested matrix.

$\mathbf{A}_{matrix}$ = Peak height measured for digested matrix expected free of analyte. In general this value was negligible compared with the peak height of the spiked sample.

$\mathbf{SD}_{matrix}$ = Standard deviation of peak height for digested matrix expected free of analyte.

TABLE IV
Recovery From Interference Study of Nine Elements
The underlined wavelengths were used for the final method; recoveries in bold were accepted. All measurements were carried out in duplicate.

Analyte and Wavelength (nm)	Concentration	Depending on Internal Std In	Sr
Ca 422.673	0.1 mg L^{-1} + 25 mg L^{-1}all	**113**	116
Cr 283.563	0.1 mg L^{-1} + 25 mg L^{-1} all	**106**	110
Cr 205.560	0.1 mg L^{-1} + 25 mg L^{-1} all	101	105
Cr 267.716	0.1 mg L^{-1} + 25 mg L^{-1} all	97	101
Cu 324.754	0.1 mg L^{-1} + 25 mg L^{-1}all	**101**	105
Fe 259.940	0.1 mg L^{-1} + 25 mg L^{-1} all	**98**	102
Mg 279.553	0.1 mg L^{-1} + 25 mg L^{-1} all	**109**	113
Mg 280.270	0.1 mg L^{-1} + 25 mg L^{-1} all	108	113
Mg 285.213	0.1 mg L^{-1} + 25 mg L^{-1} all	110	114
Mn 257.610	0.1 mg L^{-1} + 25 mg L^{-1} all	**101**	98
Mo 202.032	0.1 mg L^{-1} + 25 mg L^{-1} all	94	**99**
Mo 204.598	0.1 mg L^{-1} + 25 mg L^{-1} all	98	103
Se 196.026	0.1 mg L^{-1} + 25 mg L^{-1} all	**98**	106
Zn 213.857	0.1 mg L^{-1} + 25 mg L^{-1} all	179	170

Repeatability and Intermediate Reproducibility

Five premixes (A–E) were used for repeatability and intermediate reproducibility studies (see Table VII). Samples A–C were standard trace element premixes and D–E were pet food premixes (see Table VII). Robust relative repeatability limits (r%) (at 95% confidence interval) were calculated from 14 replicates per premix measured by the same operator at the same day; and the results are given in Table VII. The robust intermediate reproducibility limits (iR%) were calculated from duplicate analyses on six different days (carried out in the same laboratory and by the same operator) and are listed in Table VIII.

TABLE V
Recoveries From Interference Study with Zn
(The underlined wavelengths were used for the final method; recoveries in bold were accepted. All measurements were carried out in duplicates. See text for details.)

Analyte and Wavelength (nm)	Concentration	%Rec Depending on Internal Std	
		In	Sr
Zn 213.857	0.1 mg L^{-1} + 25 mg L^{-1} all	179	170
Zn 213.857	0.1 mg L^{-1} + 25 mg L^{-1} Cu	153	152
Zn 213.857	0.1 mg L^{-1} + 25 mg L^{-1} Fe	124	120
Zn 213.857	2.5 mg L^{-1}+ 2.5 mg L^{-1} Cu	100	**100**
Zn 213.857	2.5 mg L^{-1} + 2.5 mg L^{-1} Fe	101	**101**

TABLE VI
Limits of Quantitation Determined on a Digested Premix Matrix
(Concentrations are given in mg kg^{-1})

Ca	Cr	Cu	Fe	Mg	Mn	Mo	Se	Zn
1.0	1.0	1.0	2.0	0.1	0.1	1.5	20	0.5

The elemental composition of the premixes is given in the next paragraph (Accuracy, Table IX). Only those elements were evaluated that had been declared by the manufacturer of the premix. Others were not measured and their cells in Tables VII–X were left empty (–).

Tables VII and VIII show that the robust relative repeatabilities and intermediate reproducibilities were found to be < 5% and < 16%, respectively, for premixes A–C. Premixes D and E had high robust relative repeatability and intermediate reproducibility, and were reanalyzed using 2.5 g as the sample size. The digestion method was adapted using 10 mL of HNO_3 and 10 mL of H_2O_2 for the first step in the microwave digestion. Microwave conditions and the added volume of HCl remained the same as in the above-described sample preparation. The samples were diluted twice with water in order to obtain the same HNO_3 concentration as present in the standards. Further dilutions were carried out based on these twice-diluted samples. The high repeatability and reproducibility data decreased through this adaptation of the method.

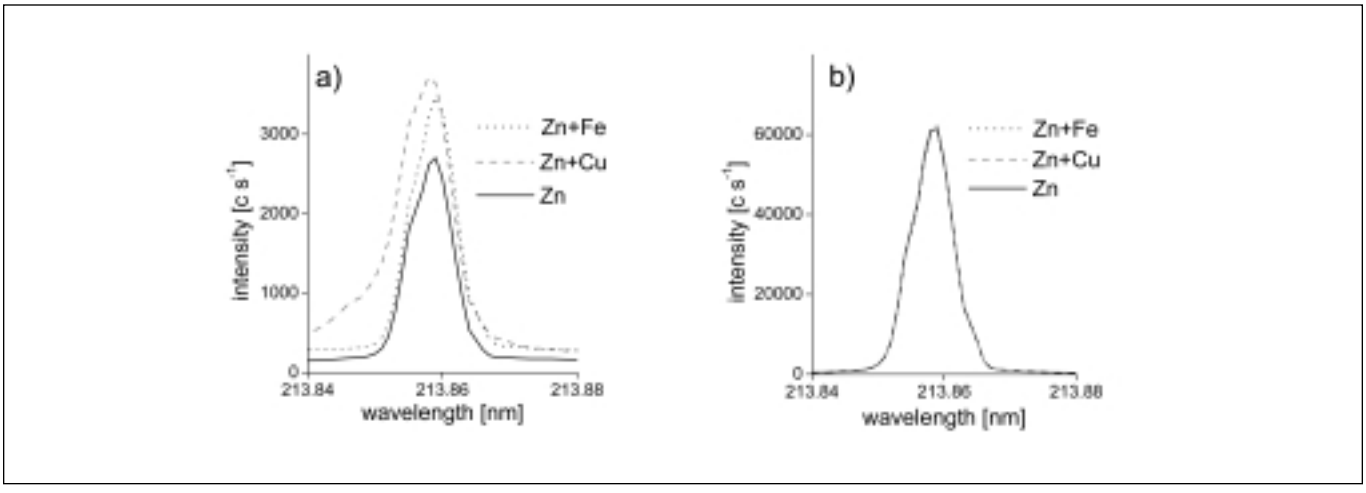

Fig. 1 (a + b). Zinc signals with and without interference.
Figure 1a was measured with an interferent to Zn ratio of 250 (25 mg L^{-1} to 0.1 mg L^{-1}).
Figure 1b was measured with an interferent to Zn ratio of 1 (2.5 mg L^{-1} to 2.5 mg L^{-1}).

TABLE VII
Limits of Robust Relative Repeatability of Nine Elements Determined From Five Premixes

	1-g Samples (r%)					2.5-g Samples (r%)	
	A	B	C	D	E	D	E
Ca	-	-	2	-	-	-	-
Cr	-	4	-	-	-	-	-
Cu	4	3	5	11	37	13	6
Fe	4	4	5	9	20	13	23
Mg	-	-	-	-	17	-	9
Mn	5	3	-	10	39	12	16
Mo	-	5	-	-	-	-	-
Se	-	4	-	84	-	34	-
Zn	5	4	4	10	37	9	16

TABLE VIII
Limits of Robust (Relative) Intermediate Reproducibility of Nine Elements Determined From Five Premixes

	1-g Samples (iR%)					2.5-g Samples (iR%)	
	A	B	C	D	E	D	E
Ca	-	-	4	-	-	-	-
Cr	-	16	-	-	-	-	-
Cu	5	12	5	13	59	7	44
Fe	5	8	9	26	36	14	15
Mg	-	-	-	-	19	-	22
Mn	6	8	-	14	38	9	31
Mo	-	8	-	-	-	-	-
Se	-	5	-	73	-	33	-
Zn	3	4	6	12	63	9	48

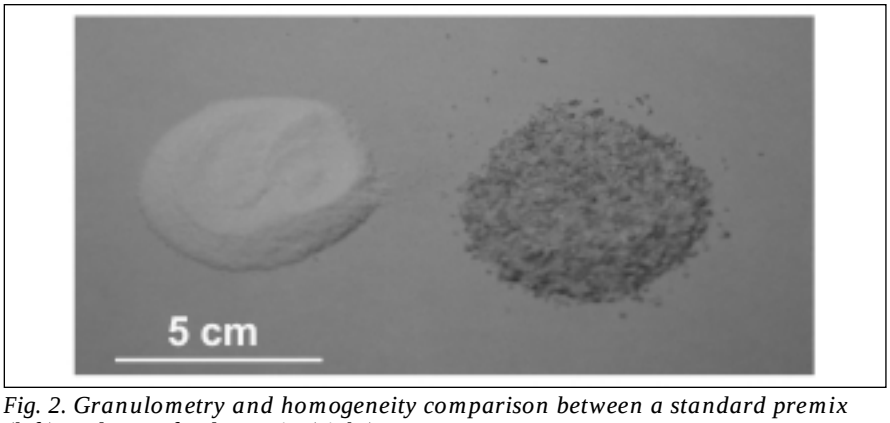

Fig. 2. Granulometry and homogeneity comparison between a standard premix (left) and a pet food premix (right).

The reason for the high repeatability limits of premixes D and E is explained by the heterogeneity of the materials as shown in Figure 2 [photograph of a standard premix (left) and a pet food premix (right)]. It is recommended to use 2.5 g as the sample size for pet food premixes. A homogenization of the pet food premixes by grinding a larger sample amount (>50 g) would certainly improve the repeatability of the method for the premix samples. However, two points have to be considered when applying grinding as a sample pretreatment:

(a) The gained homogeneity of the sample does not reflect the actual heterogeneity of the premix (loss of information about the quality of the premix).

(b) Homogeneity is harder to achieve for pet food premixes (based on salts as the major constituent) than for standard premixes (based on maltodextrine).

Accuracy

Due to a lack of certified reference materials for premix analysis, accuracy of the method was determined by the following steps:

(a) Comparison between the manufacturer's declared values and measured values, and

(b) By spiking recoveries.

(a) The first approach can only account for a qualitative estimation of accuracy of the method as the manufacturer's declared values are only based on the weights of different salts mixed together during the premix production. Heterogeneity of a production lot cannot be estimated without exactly knowing the production process (quantity and grain size of the different components). The manufacturer's declared and measured concentrations are listed in Table IX. The medians of the measured concentrations were obtained from the

TABLE IX. Manufacturer's Declared (Given) and Actually Measured Concentrations in Five Premixes

(Measured concentrations are medians of 14 replicates. Values in bold letters are measured concentrations of the given concentration range.)

		Concentration (mg kg^{-1}) Premix				
		A	B	C	D	E
Ca	Given	-	-	62500-76400	-	-
	Measured			**67650**		
Cr	Given	-	77-85	-	-	-
	Measured		**85**			
Cu	Given	460-531	3600-3960	51-59	3750-4500	433-520
	Measured	**502**	**3790**	**55**	**4208**	**459**
Fe	Given	9420-10870	27500-29700	510-590	25100-30200	3460-4100
	Measured	**9980**	**28380**	**488**	**25400**	**3615**
Mg	Given	-	-	-	-	25000-30000
	Measured					23900
Mn	Given	34-38	6540-13080	-	2050-2500	660-790
	Measured	43	**7300**		3688	840
Mo	Given	-	214-235	-	-	-
	Measured		208			
Se	Given	-	69-77	-	44-54	-
	Measured		**71**		41	
Zn	Given	5320-6140	32000-35200	670-780	49600-59500	3430-4100
	Measured	**5640**	**32700**	**736**	47601	4140

TABLE X. Recoveries Obtained From Spikes at Two Levels for Premixes A–C and One Level for Premixes D–E

(Recoveries of premixes A–C and of D–E were obtained from 1-g and 2.5-g sample sizes, respectively. Values are means of duplicates ± half the range between duplicates.)

Premix	A		B		C		D	E
Spike Conc	100%	20%	100%	20%	100%	20%	100%	100%
Analyte	Spike Recovery (%)							
Ca	-	-	-	-	95 ± 1	90 ± 7	-	-
Cr	-	-	93 ± 1	94 ± 4	-	-	-	-
Cu	103 ± 3	87 ± 1	100 ± 2	120 ± 25	94 ± 1	88 ± 6	96 ± 2	101 ± 1
Fe	98 ± 1	89 ± 4	96 ± 1	80 ± 5	96 ± 1	89 ± 7	88 ± 6	104 ± 1
Mg	-	-	-	-	-	-	-	91 ± 8
Mn	93 ± 2	81 ± 5	97 ± 1	113 ± 16	-	-	92 ± 4	96 ± 2
Mo	-	-	99 ± 1	103 ± 3	-	-	-	-
Se	-	-	100 ± 2	100 ± 2	-	-	124 ± 12	-
Zn	104 ± 2	93 ± 6	95 ± 1	81 ± 2	97 ± 1	84 ± 8	94 ± 2	102 ± 1

repeatability determinations (1-g sample size and 14 replicates for each premix). Sixteen of the 25 measured concentrations (values given in bold letters in Table IX) were in the range of the manufacturer's declaration. The values found out of the declaration range were not very far from the supplier's indications, which could be due to an inaccurate sampling procedure.

(b) Premixes A–E were spiked before digestion by pipetting 1 mL and 2.5 mL of concentrated solutions into premixes A–C (1-g samples) and D–E (2.5-g samples), respectively (see Table X). By applying small volumes of concentrated solutions, it was intended to minimize the dilution of the added acid and its digestion efficiency. Two levels of spiking were applied, corresponding to 20 and 100% of the concentrations of the analyte obtained from the sample. Only elements with claimed concentrations were taken into account.

For most of the 100% level spikes, the recoveries for the five investigated premixes (except Se in D) were satisfactory. For the 20% spikes (premixes A–C), the recoveries ranged from 80–120%, which can be considered satisfactory because good recoveries in low spikes are more difficult to achieve. For premixes D–E, the results for the 20% spikes were disregarded because of the heterogeneity of the original sample. Considering a variability of ±10% for the original sample concentration and the same variability for the spiked sample, the worst case recoveries could be estimated to be between 0 and 200%.

CONCLUSION

A method for the simultaneous determination of Ca, Cr, Cu, Fe, Mg, Mn, Mo, Se, and Zn in mineral premixes using ICP-OES has been evaluated. These food additives feature high concentration ranges of minerals and therefore demand high sensitivity and low interference for low mineral content and high dilution factors for high mineral content in premixes. The linearity of calibration was good for eight elements, only Mg had a quadratic calibration curve. Commonly used wavelengths for the nine elements were checked for interferences, but none was found significant when measured under premix conditions. The limits of quantitation were below the concentrations expected for the studied premixes, except for Se, where the lowest required concentration was half the limit of quantitation.

Robust relative repeatability and robust intermediate reproducibility were < 5% and < 16%, respectively, for three premixes out of five. Two other premixes were found to be very heterogeneous and were analyzed using a larger sample size. The robust relative repeatability for these samples was between 6% and 34% and the intermediate reproducibility was between 7% and 48% depending on the elements and their concentration levels. The recoveries of spikes on the homogeneous samples were relatively good when high spikes were applied (93–104%); the recoveries on the heterogeneous samples were poor (88–124%). The developed multielement method performed well on homogeneous premixes; however, high repeatability data are to be expected from pet food premixes due to their high heterogeneity.

Received May 16, 2003.

REFERENCES

1. L.A. Mejia, Food and Nutrition Bulletin 19, 278 (1995).
2. C. Reilly, Trends in Food Science and Technology 9, 114 (1998).
3. J.S. Kosse, A.C. Yeung, A.I. Gil, and D.D. Miller, Food Chemistry 75, 371 (2001).
4. C.P. Hanna, G.R. Carnrick, S.A. MacIntosh, L.C. Guyette, and D.E. Bergemann, At. Spectrosc. 16, 82 (1995).
5. L. Valiente, M. Piccinna, E.R. Ale, A. Grillo, and P. Smichowski, At. Spectrosc. 23, 129 (2002).
6. C.P. Bosnak and K.W. Barnes, At. Spectrosc. 19(2), 40 (1998).
7. International Organization for Standardization, International Standard ISO 6869:1 (2000).
8. L. Jorhem, Journal of AOAC International 83, 1204 (2000).
9. L. Jorhem and J. Engman, Journal of AOAC International 83, 1189 (2000).
10. N.J. Miller-Ihli, J. Agric. Food Chem. 44, 2675 (1996).
11. P.D. Krampitz and K.W. Barnes, At. Spectrosc. 19, 43 (1998).
12. K. Mitko and M. Bebek, At. Spectrosc. 20, 217 (1999).
13. S.P. Dolan and S.G. Capar, Journal of Food Composition and Analysis 15, 593 (2002).
14. A. Moeller, R.F. Ambrose, and S.S. Que Hee, Food Additives and Contaminants 18, 19 (2001).
15. D-H. Sun, J.K. Waters, and T.P. Mawhinney, Journal of AOAC International 83, 1218 (2000).
16. L. Perring and M. Basic-Dvorzak, Anal. and Bioanal. Chem. 374, 235 (2002).

Blending Procedure for the Cytosolic Preparation of Mussel Samples for AAS Determination of Cd, Cr, Cu, Pb, and Zn Bound to Low Molecular Weight Compounds

Rebeca Santamaría-Fernández[b], Sandra Santiago-Rivas[a], Antonio Moreda-Piñeiro[a], Adela Bermejo-Barrera[a] , *Pilar Bermejo-Barrera[a], and Steve. J. Hill[b]

[a] Department of Analytical Chemistry, Nutrition and Bromatology, Faculty of Chemistry, University of Santiago de Compostela, Avenida das Ciencias s/n, 15782 - Santiago de Compostela, Spain

[b] Department of Environmental Sciences, Plymouth Environmental Research Centre, University of Plymouth, Drake Circus, PL4 8AA Plymouth, Devon, U.K.

ABSTRACT

Simple methods for the determination of Cd, Cr, Cu, Pb, and Zn fractions bound to low molecular weight compounds (presumably metallothionein-like proteins) in mussels (Mytilus edulis) have been developed. The methods involve the novel application of using a blending (Stomacher) rather than a cutting mixer device to perform the homogenization between the fresh mussel tissue and the extractant solution [10 mM TRIS–HCl buffer at pH 7.4 with 5 mM 2–mercaptoethanol (2–MCE), 0.01 mM phenylmethylsulfonyl fluoride (PMSF), and 25 mM sodium chloride]. Optimum conditions for the cytosolic preparation (after an experimental design approach) were a ratio of sample weight : extracting volume of 0.2 g/mL and a blending time of 5 min. The Cu and Zn concentrations bound to low molecular weight compounds (LMW proteins) were measured by flame atomic absorption spectrometry using a high performance nebulizer, while Cd, Cr, and Pb levels in the cytosolic solutions were assessed by electrothermal atomic absorption spectrometry. A microwave-assisted acid digestion procedure was also applied to determine the total metal concentration. The limits of detection (LOD) for Cd, Cr, and Pb were 0.7, 3.0, and 6.6 ng g^{-1}, respectively, and for Cu and Zn they were 0.05 and 0.01 µg g^{-1}, respectively. The methods were applied to 16 mussel samples from the Ría de Arousa estuary.

INTRODUCTION

Metallothionein-like proteins (MT-like proteins) are low molecular weight proteins that have a high cystein content (around ±30% of the residues) and a strong affinity for heavy metals (1). These proteins play an important role in the metabolism and kinetics of Cd and Cu, and regulate the toxicity of various metals and trace elements. Metallothioneins (MTs) and MT-like proteins have been described for various foodstuffs, mainly fish and mollusks (1). It appears that in fish, MTs should be considered as a kind of stress protein that is particularly responsive to heavy metals. In mollusks, MTs seem more involved in responses to heavy metals and they can be considered as biomarkers of exposure to heavy metal contamination (2).

From the studies performed on MTs in mollusks and the results available in the literature (3), it can be said that several physiological and biochemical parameters might affect the concentration and isolation of MTs from mollusk tissue. Significant variations in isolation and quantification of MTs might depend on the purification and storage protocol and, as described by Isani et al. (4), the development of a standard protocol for MT isolation and quantification is still an important goal to be achieved. Although there is no standard method, it is well known that denaturation of the samples at low temperatures, instead of the solvent precipitation process, allows the isolation of MTs from other high molecular weight proteins without MT alteration (5,6). However, some works have reported important changes on metal distribution in MT-like protein isoforms due to heating treatments (7). Regarding the cytosol isolation process, Wolf et al. (8) have compared several homogenization procedures (cutting mixers, rotating pestles, and sonication devices) in terms of functionality. These authors concluded that sonication in comparison to pestles and cutting devices [Ultra–Turrax (9,10)] offers the best performance because there is no risk of contamination or formation of foam.

As recently reported by Prange and Schaumlöffel (3), several speciation studies have been performed to determine trace elements in MTs from rabbit (11,12), rat (13), and human (7) livers, as well as from mollusks (9,10,13,14,15). Hyphenated techniques with inductively coupled plasma mass spectrometry (ICP–MS) as a multi-element detector are used throughout these studies. Therefore, different modalities of high performance chromatography (HPLC), such as size exclusion chromatography (SEC) and capillary electrophoresis (3) were used to isolate different MTs and even different MT isoforms. These hyphenated techniques are, most of the time, expensive and not available in many laboratories.

*Corresponding author.
e-mail: pbermejo@usc.es

Therefore, the aim of this work was to develop simple atomic absorption spectrometric methods to determine the fraction of metals (Cd, Cr, Cu, Pb, and Zn) bound to MT–like proteins in mussels (*Mytilus Edulis*). Since a prior chromatographic stage is omitted, the term low molecular weight (LMW) compounds will be used rather than MT-like proteins. Additionally, a novel procedure for the homogenization of the mussel samples has been optimized by the use of a blending system (Stomacher) where the samples are contained within sterile metal-free disposable bags, thus eliminating instrument contamination, and achieving homogenization by blending.

EXPERIMENTAL

Instrumentation

A PerkinElmer Model 1100B atomic absorption spectrometer (PerkinElmer Life and Analytical Sciences, Shelton, CT, USA), equipped with an HGA®-400 graphite furnace and an AS-40 autosampler. Deuterium lamp background correction was used for Cd, Cr, and Pb measurements. A PerkinElmer Model 3100 atomic absorption/emission spectrometer with a high-performance nebulizer equipped with ceramic impact beads (PerkinElmer) was used for the Cu and Zn determinations. Background correction was found unnecessary for FAAS determinations.

Cd and Zn (PerkinElmer) and Cr and Cu (Cathadeon, Cambridge, U.K.) hollow cathode lamps, and a Pb electrodeless discharge lamp (PerkinElmer) connected to a power supply (PerkinElmer) were used as the radiation sources. The lamps were operated at the lamp currents/lamp voltages and with slit widths and wavelengths as recommended by the manufacturer. A Stomacher Lab Blender 400 (Seward Med. Ltd., London, UK) was used to blend and homogenize the fresh mussel samples using Stomacher sample bags (Part No. 6041/CLR). Centrifuge Centromix (Selecta, Barcelona, Spain), refrigerated centrifuge Laborzentrifugen 2K15 (SIGMA, Osterode, Germany), and ORION 720A plus pH meter with a glass calomel electrode (ORION, Cambridge, UK) were also used. A Samsung domestic microwave oven (Seoul, Korea), programmable for time and microwave power, was used for total sample digestion. The poly(tetra–fluoroethylene) (PTFE) bombs were laboratory-made with hermetic seals (suitable for work at low pressures). The chemometrics packages used were UNSCRAMBLER, 1998 (CAMO ASA, Trondheim, Norway) and Statgraphics Plus V 5.0 for Windows® OS, 1994-1999 (Manugistics Inc., Rockville, MD, USA).

Reagents and Standards

The chemicals were of ultrapure grade, using ultrapure water, resistance 18 MΩ cm (Millipore Co., Bedford, MA, USA). Stock standard solutions (1000 g L^{-1}) were obtained from Merck, Poole, Dorset, UK. Palladium nitrate stock standard solution, 10,000 g L^{-1} (from PerkinElmer). Magnesium nitrate stock standard solution was prepared from magnesium nitrate (from BDH, Poole, Dorset, UK). Hydrogen peroxide 33% (from Panreac, Barcelona, Spain). Nitric acid 70.0% and hydrochloric acid 37% (from J.T. Baker B.V., Deventer, Holland). The extracting solution was prepared with TRIS–hydroxymethyl–aminomethane (Riedel de Haën, Sigma-Aldrich, Stemheim, Switzerland), 2–mercaptoethanol (2–MCE) (Fluka, Sigma-Aldrich), phenylmethylsulfonyl fluoride (PMSF) (Fluka, Sigma-Aldrich), and sodium chloride (Merck, Darmstadt, Germany).

Mussel Samples

Fresh mussel samples were collected from mussel farms at Ría de Arousa estuary (Galicia, Northwest Spain). The mussels were analyzed as wet samples for total metal and fractions bound to low molecular weight compounds. All studies were performed using all mussel tissue (muscle and gill) by preparing a mussel pool mixture with all the mussels from each mussel farm.

Methods

Procedure for Cytosol Preparation

Cytosolic extracts were obtained based on a modified protocol of the methods reported by Roesijadi and Fowler (10) and Lobinski et al. (14). The extracting solution was prepared with TRIS-HCl at 10 mM (pH 7.4), 0.01 mM phenylmethylsulfonyl fluoride (PMSF), 5 mM 2–mercaptoethanol (2–MEC), and 25 mM NaCl. The homogenization and blending procedure was as follows: fresh mussel samples were accurately weighed (~5 g) into the Stomacher bag and 25 mL of extracting solution was added. The mixture was subjected to blending at high speed for 5 min, and was then transferred to a centrifuge tube and centrifuged at 3500 rpm for 30 min. The solid precipitated was separated by decantation and the liquid extract was transferred into a second centrifuge tube and warmed in a water bath at 60°C for 15 min. Posterior centrifugation at 4°C and at 19,890 g (15,300 rpm) for 30 min was carried out to separate the tertiary structure proteins which suffered denaturization at high temperature. Cytosols, obtained by decantation, were diluted to 25 mL with ultrapure water.

Microwave Acid Digestion

Acid digestion was carried out in a domestic microwave oven with laboratory-made low pressure PTFE bombs. The optimum conditions for the digestion of wet mussel

samples were based on a modified method for dry mussels (16), and it can be summarized as follows: Approximately 0.7 g of fresh mussel sample was weighed into the PTFE bombs and 2 mL of concentrated HNO_3 was added. The samples were subjected to two microwave heatings (100 W) for 2 min with a cooling stage (ice–bath for 10 min) in between. The low microwave power was required to avoid losses because low pressure PTFE bombs were used. Then, 1 mL of 33% (m/v) H_2O_2 was added and the samples were again subjected twice to microwave irradiation at 200 W for 2 min, also inserting a cooling stage. Finally, the acid digests were made up to 10 mL with ultrapure water and stored in polyethylene bottles at 4°C. This methodology was validated after analyzing different certified reference materials (DORM–1, DOLT–1 and TORT–1) as reported in References 16–18.

ETAAS and FAAS Measurements

Cu and Zn were determined by FAAS (oxidizing air/acetylene flame) while Cd, Cr, and Pb determinations were carried out by electrothermal atomic absorption spectrometry (ETAAS) under optimum conditions (see Table I). Chemical modification was necessary for Cd and Pb determinations and magnesium nitrate / palladium nitrate of 0.6/0.6 µg and 0.9/2.2 µg were found to be optimum for Cd and Pb, respectively. These chemical reagents were previously mixed with the samples and standard solutions before ETAAS measurements. Aqueous calibration was possible only for Cr determination by ETAAS. The use of the standard addition technique was required for Cu and Zn measurements by FAAS and for Cd and Pb determination by ETAAS.

TABLE I
Operating Conditions and Graphite Furnace Temperature Programs[a] for the ETAAS Determination of Cd, Cr, and Pb Bound to LMW Proteins

	Cd	Cr	Pb
Wavelength (nm)	228.8	357.9	283.3
Slit width (nm)	0.7	0.7	0.7
Lamp current (mA)	5	12	10[b]
Injection volume (µL)	20	20	20

	Step	Temp. (°C)	Ramp (s)	Hold (s)	Ar Flow Rrate (mL min^{-1})
Cd[c]	Drying	150	20	20	300
	Pyrolysis	500	15	25	300
	Atomization	1600	0	4	0 (Read)
	Cleaning	2200	1	3	300
Cr	Drying	150	20	20	300
	Pyrolysis	1400	10	15	300
	Atomization	2400	0	5	0 (Read)
	Cleaning	2650	1	2	300
Pb[c]	Drying	150	15	20	300
	Pyrolysis	800	20	10	300
	Atomization	1400	0	3	0 (Read)
	Cleaning	2200	2	3	300

[a] Pyrolytically coated graphite tubes with L'vov platforms, injection volume of 20 µL, integrated absorbance measurement.
[b] Power supply, 10 W.
[c] $Mg(NO_3)_2$ / $Pd(NO_3)_2$ as chemical modifier (0.6/0.6 µg for Cd and 0.9/2.2 µg for Pb).

RESULTS AND DISCUSSION

Optimization of the Cytosol Preparation

Optimization of the LMW protein extraction from mussel samples using the Stomacher blending device was carried out by using an experimental design approach. Variables such as pH and 2–mercaptoethanol (MEC) and phenylmethylsulfonyl fluoride (PMSF) concentrations were not considered in the study. A pH of 7.4 was required to extract MT-like proteins and 2-MEC and PMSF were used only to prevent MT-like protein degradation. Therefore, the variables under study were blending (extracting) time (T) and the ratio of sample weight : extracting volume (w/v). Optimization of these two variables results in reduced time and sample weight required for the analysis. A central composite design, 2^2 + star, involving 18 experiments was used for optimization. Blending time ranged from 7.5 to 25 min and the ratio of sample weight : extracting volume varied from 0.5 to 2.0. The response variables were the metal concentrations (Cd, Cr, Cu, Pb, and Zn) in each extract, determined by using an aqueous calibration or a standard addition graph and under optimum conditions. Details of the central composite design matrix (cube and star experiments) are given in Table II, as well as the response variables (concentrations of metal associated to MTs) for

TABLE II. 2^2 + Star Central Composite Design Matrix

Run	Time (min)	W/V (g mL^{-1})	Response Variables Cd (µg g^{-1})	Cr (µg g^{-1})	Cu (µg g^{-1})	Pb (µg g^{-1})	Zn (µg g^{-1})
1	3.88	1.25	0.029	0.031	0.171	0.009	1.69
2	3.88	1.25	0.023	0.029	0.173	0.010	2.27
3	28.62	1.25	0.031	0.027	0.143	0.010	5.64
4	28.62	1.25	0.033	0.029	0.117	0.009	2.87
5	16.25	0.19	0.057	0.035	0.348	0.047	3.99
6	16.25	0.19	0.069	0.035	0.348	0.044	2.86
7	16.25	2.31	0.015	0.015	0.086	0.007	1.27
8	16.25	2.31	0.014	0.022	0.085	0.009	0.83
9	7.50	0.50	0.035	0.031	0.289	0.023	6.25
10	7.50	0.50	0.037	0.034	0.258	0.018	2.96
11	25.00	0.50	0.031	0.028	0.200	0.007	2.66
12	25.00	0.50	0.030	0.034	0.200	0.008	3.24
13	7.50	2.00	0.024	0.028	0.114	0.004	2.39
14	7.50	2.00	0.017	0.019	0.086	0.006	1.55
15	25.00	2.00	0.030	0.018	0.087	0.006	2.00
16	25.00	2.00	0.032	0.017	0.087	0.006	1.85
17	16.25	1.25	0.031	0.020	0.115	0.006	2.83
18	16.25	1.25	0.036	0.018	0.116	0.006	2.15

TABLE III. Typical ANOVA Table for Cr Obtained by Response Surface Analysis

	Sum of Squares	Degree of Freedom	Main Squares	F–Ratio	p–Value
Summary					
Model	0.667	5	0.134	15.86	0.0001 [a]
Error	0.101	12	0.008		
Adjusted total	0.768	17	0.0452		
Variables					
Intercept	0.739	1	0.739	87.78	0.000 [a]
Time (A)	0.0203	1	0.0203	2.41	0.146
W/V (B)	0.522	1	0.522	61.98	0.000 [a]
AB	0.009	1	0.009	1.076	0.320
AA	0.114	1	0.114	13.51	0.003 [a]
BB	0.065	1	0.065	7.671	0.017 [a]
Model Check					
Main	0.542	2	0.271		
Interaction	0.009	1	0.009	1.076	0.302
Interaction + squares	0.116	2	0.058	6.908	0.010 [a]
Squares	0.116	2	0.058	6.098	0.010 [a]
Error	0.101	12	0.008		
Lack of Fit					
Lack of fit	0.0124	3	0.004	0.421	0.743
Pure error	0.089	9	0.010		
Total error	0.101	12	0.008		

Multiple correlation: 0.932 R–square: 0.869

[a] Statistically significant at a confidence level of 95.0%.

each experiment. It must be noted that after each experiment, the same procedure described before was performed (two centrifugation steps and a heating period in between).

After studying the ANOVA tables for each response variable (i.e., Table III for Cr), both variables (blending time and ratio of sample weight : extracting volume) were found to be independent and the effect of one does not produce variations in the other. In addition, it can be seen that the variable blending time is not statistically significant. Figure 1 shows the response surfaces achieved for each metal. It can be seen that blending time was found to be insignificant as long as it was kept between approximately 4 to 10 min for all elements; 5 min was chosen for further analysis. On the other hand, an optimum ratio of sample weight : extracting volume of 0.19 g mL^{-1} was found for Cd and Pb, and from 0.19 to 0.28 g mL^{-1} for Zn, and from 0.19 to 0.36 g mL^{-1} for Cu and Cr. In order to find compromise extracting conditions, a w/v ratio of 0.2 g mL^{-1} was chosen and was employed for further analysis. This w/v ratio means that 5 g of mussel sample and 25 mL of extracting solution was necessary. The optimum ratio obtained was quite different than previously reported by other authors (9,10,11,14), who used a ratio of 1 g mL^{-1} (10 g of mussel sample and 10 mL of extracting solution).

Comparison to Other Cytosol Preparations

The optimized blending procedure and the procedure described by Lobinski et al. (14), which uses a trituration device under recommended conditions, was applied three times to a mussel sample. Blank controls were performed for both cytosol preparation procedures and the Cd, Cu, Cr, and Zn concentrations were determined under optimum operating condi-

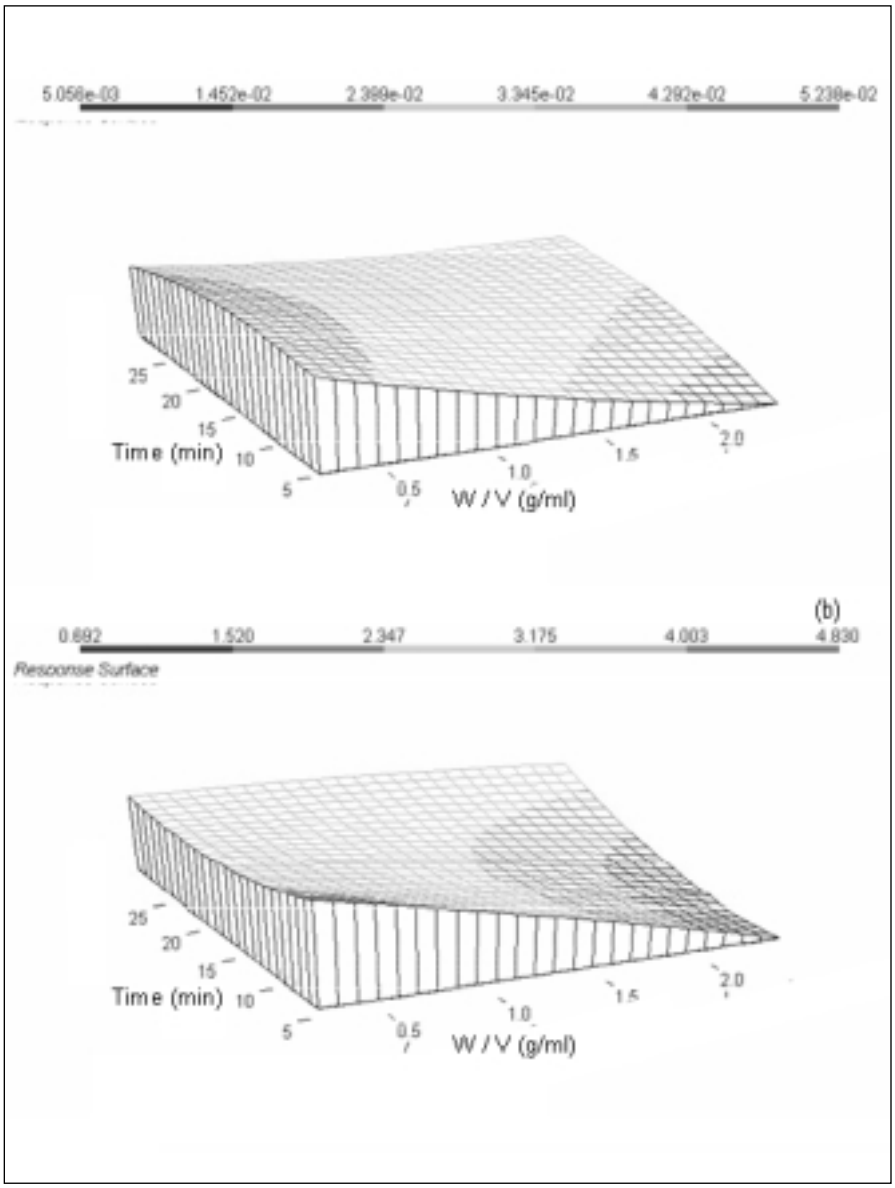

Fig. 1. Some estimated response surfaces from the central composite design in the extraction of LMW-compounds from mussels: (a) cadmium and (b) zinc.

TABLE IV
Results of Cd, Cu, Cr, and Zn Determination After Stomacher Blending and OMNI Mixer Trituration Cytosol Preparation Procedures (µg g^{-1})

Element	Stomacher		OMNI Mixer	
	Mussel	Blank[a]	Mussel	Blank[a]
Cd (µg g^{-1})	0.02 ± 0.01	0.0030 ± 0.0001	0.02 ± 0.01	0.0040 ± 0.0001
Cu (µg g^{-1})	0.10 ± 0.01	0.0010 ± 0.0001	0.12 ± 0.01	0.0010 ± 0.0001
Cr (µg g^{-1})	0.03 ± 0.01	0.0050 ± 0.0002	0.16 ± 0.01	0.071 ± 0.016
Zn (µg g^{-1})	2.73 ± 0.28	0.0080 ± 0.0002	2.58 ± 0.17	0.0070 ± 0.0003

[a] Absorbance units.

tions. Table IV lists the mean and standard deviations obtained for each case. It can be seen that the concentration of metals bound to LMW compounds reached by both procedures is similar, although random Cr contamination was found when using the OMNI Mixer trituration device. This contamination was also found after determining high Cr levels in the blank solutions. After applying an ANOVA test (95% confidence level), it can be concluded that the efficiency of the Stomacher blending procedure for mussel cytosol preparation is comparable to the efficiency obtained using the OMNI Mixer trituration procedure, with the additional advantage of avoiding Cr contamination.

Analytical Performance

A statistical comparison between the slopes of the aqueous calibration and the standard addition graphs was made. Both calibration techniques were performed seven times on different days, and the results are listed in Table V. The differences between the slopes was studied by employing the ANOVA test to assess whether there are statistically significant differences for the standard deviation of each group (aqueous calibration and standard addition graphs) according to the Barlett and Cochran tests (19). The results show that the slopes of the aqueous calibration and standard addition graphs are statistically different for Cd and Pb determination by ETAAS, and for Cu and Zn measurement by FAAS. There were no statistically significant differences in the ETAAS determination of Cr. Therefore, matrix effects are important for Cd, Cu, Pb, and Zn determination, and the standard addition technique was used for further experiments. The aqueous calibration technique will be used for Cr.

The limit of detection (LOD), limit of quantification (LOQ), and

the characteristic mass (20) were established. LOD values of 0.7, 3.0, and 6.6 ng g^{-1} were obtained for Cd, Cr, and Pb, respectively, with characteristic masses of 1.1 ± 0.2, 5.7 ± 0.2, and 34.1 ± 1.6 pg, respectively. The LOD values for Cu and Zn were 0.05 and 0.01 µg g^{-1}, respectively.

The within-run precision for 11 injections of LMW compound extracts and expressed as %RSD was 1.7, 3.1, and 1.5 % for Cd, Cr, and Pb, respectively. The values obtained for Cu and Zn by FAAS with regard to 11 subsequent measurements was 0.2% for both cases. In addition, the repeatability of the overall procedure was assessed by preparing a cytosolic extract seven times from the same mussel sample and analyzing each sample twice. The RSD values of 6.1, 7.0, 9.1, 7.8, and 6.3% were obtained for Cd, Cr, Cu, Pb, and Zn, respectively.

Application

Sixteen mussel samples from the Ría de Arousa estuary were analyzed for the elements Cd, Cr, Cu, Pb, and Zn bound to LMW compounds. A mixture was made with mussel samples selected from each sampling location. Five g of each mixture was subjected (in duplicate) to the LMW compound extraction procedure, and each cytosolic extract was measured by ETAAS or FAAS. Additionally, mussel mixture from each sampling location were subjected (in duplicate) to a microwave acid digestion procedure to assess the total metal concentrations. Table VI shows the (%) metal concentration ranges for total metal concentration and metals bound to the LMW compound in the 16 mussels. It can be seen that Cd, Cu, and Zn are the metals with high percentages bound to LMW compounds, slightly above 10%. The maximum yield was up to 56% for Cu and Pb, while values of 46%, 39%, and 24% were reached for Zn, Cd, and Cr, respectively. It should be noted that the highest percentages of Cr, Cu, Pb, and Zn bound to LMW compounds were found in mussel samples from sampling location 12, (while the highest Cd percentages of 39% and 3% were for mussel samples from locations 24 and 12, respectively. Supplementary studies about metal concentrations in seawater and marine sediments from each of the sampling locations would be of interest in order to confirm possible metal stress in those areas.

TABLE V
Aqueous Calibration and Standard Addition Slopes
(Expressed as mean ± standard deviation for n = 7)

	Slopes (µg L^{-1})	
	Standard Addition	Aqueous Calibration
Cd	0.053 ± 0.011	0.039 ± 0.001
Cr	0.0190 ± 0.004	0.0201 ± 0.003
Cu[a]	0.151 ± 0.008	0.199 ± 0.002
Pb	0.0043 ± 0.0003	0.0020 ± 0.0003
Zn[a]	0.472 ± 0.026	0.805 ± 0.024

[a] (mg L^{-1}).

TABLE VI
Total Metal and Metal-Bound LMW Compounds
(Concentration ranges in mussel samples.)

	Mussels (16 Samples)		
	Total Concentration Range (µg g^{-1}) Wet Weight of Tissue	Metal-bound LMW Compounds Range (µg g^{-1}) Wet Weight of Tissue	Metal-bound LMW Compounds Range (%)
Cd	0.069 – 0.122	0.010 – 0.036	10 – 39
Cr	0.075 – 0.294	0.010 – 0.029	8 – 24
Cu	0.507 – 0.940	0.179 – 0.370	24 – 56
Pb	0.034 – 0.730	0.020 – 0.075	4 – 56
Zn	7.0 – 15.7	1.5 – 3.4	15 – 46

CONCLUSION

The novel use of a blending system (Stomacher) to prepare cytosolic extracts from fresh mussel tissue offers important advantages over classical devices which are based on the cutting process. The proposed form of homogenization avoids metal contamination normally found to be significant with other homogenization systems. The proposed method also allows a fast LMW metal compound extraction from mussel tissue in which the homogenization process is complete within 5 min. The fractions of metals, such as Cd, Cu, Cr, Pb and Zn, associated to LMW compounds in mussels can be measured under the optimized ETAAS and FAAS, resulting in simpler and less expensive methods than those based on hyphenated techniques (such as HPLC-ICP-MS). The limits of detection (LOD) for Cd, Cr, and Pb were 0.7, 3.0, and 6.6 ng g^{-1}, respectively, and for Cu and Zn they were 0.05 and 0.01 µg g^{-1}, respectively. The proposed methods are sensitive and precise (RSDs lower than 10% for repeatability), and they can be applied as a first approach to measure the total concentration of metals bound to LMW compounds.

ACKNOWLEDGMENTS

The authors would like to thank the Secretaría Xeral de Investigación and Consellería de Medio Ambiente-Xunta de Galicia for financial support (research projects PGIDIT01MAM20902PR and PGIDIT02PXIB20901PR) and the Unidade de Control de Moluscos, Instituto de Acuicultura at the University of Santiago de Compostela for providing the mussel samples. R.S.-F. would like to acknowledge financial support from the British Geological Survey (BGS, Nottingham, UK). S.S.-R. would like to thank for the financial support from Consellería de Educación e Ordenación Universitaria–Xunta de Galicia.

Received July 31, 2003.

REFERENCES

1. M. Nordberg, Talanta 46, 243–254 (1998).
2. A. Viarengo, B. Burlando, F. Dondero, A. Marro, R. Fabbri, Biomarkers 4, 455–466 (1999).
3. A. Prange, D. Schaumlöffel, Anal. Bioanal. Chem. 373, 441–453 (2002).
4. G. Isani, G. Andreani, M. Kindt, and E. Carpene, Cell. Mol. Biol. 46, 311–330 (2000).
5. F. Geret, F. Rainglet, and R. P. Cosson, Mar. Environ. Res. 46, 545–550 (1998).
6. F. Geret, F. Rainglet, R. P. Cosson, and J. Rech. Oceanogr. 22, 151–156 (1997).
7. C. Wolf, U. Rösick, and P. Brätter, Fresenius' J. Anal. Chem. 368, 839–843 (2000).
8. C. Wolf, U. Rösick, and P. Brätter, Anal. Bional. Chem. 372, 491–494 (2002).
9. C. N. Ferrarello, M. R. Fernández de la Campa, J. F. Carrasco, and A. Sanz–Medel, Anal. Chem. 72, 5874–5880 (2000).
10. G. Roesijadi and B. A. Fowler, Methods Enzymol. 205, 263–273 (1991).
11. C. N. Ferrarello, M. R. Fernández de la Campa, H. Goenaga–Infante, M. L. Fernández–Sánchez, and A. Sanz–Medel, Analusis 28, 351–357 (2000).
12. K. Polec, J. Szpunar, O. Palacios, P. González–Duarte, S. Atrian, and R. Lobinski, J. Anal At. Spectrom. 16, 567–574 (2001).
13. J. P. Valles–Mota, A. R. Linde–Arias, M. R. Fernández de la Campa, J. I. García–Alonso, and A. Sanz–Medel, Anal. Biochem. 282, 194–199 (2000).
14. R. Lobinski, H. Chassaigne, and J. Szpunar, Talanta 46, 271–289 (1998).
15. C. N. Ferrarello, M. Montes–Bayón, M. R. Fernández de la Campa, and A. Sanz–Medel, J. Anal. At. Spectrom. 15, 1558–1563 (2000).
16. P. Bermejo–Barrera, S. Fernández–Nocelo, A. Moreda–Piñeiro, and A. Bermejo–Barrera, J. Anal. At. Spectrom. 14, 1893–1900 (1999).
17. P. Bermejo–Barrera, O. Muñiz–Naveiro, A. Moreda–Piñeiro, A. Bermejo–Barrera, Anal. Chim. Acta, 439 (2001) 211
18. P. Bermejo–Barrera, A. Moreda–Piñeiro, O. Muñiz–Naveiro, A. M. J. Gómez–Fernández, A. Bermejo–Barrera, Spectrochim. Acta Part B, 55 (2000) 1351.
19. Statgraphics Plus, V. 5.0, Reference Manual, Manugistics Inc., Rockville, MD, USA, Ch. 14, pp 14–1 to 14–19 (1992).
20. T. A. M. Ure, L. R. P. Butler, B. V. L'vov, Y. Rubenska, and R. Sturgeon, Pure Appl. Chem. 64, 253–259 (1992).

FAAS Determination of Metals in Complex Paint Driers Using Microwave Sample Mineralization

***A. Lopez-Molinero, M.A. Cebrian, and J.R. Castillo**
Department of Analytical Chemistry, Science Faculty, University of Zaragoza, 5009 Zaragoza, Spain

ABSTRACT

A new, simple, and fast procedure is proposed for the determination of metals in complex soap paint driers. The method has been developed for multi-metallic driers; it has high potential throughput and can be applied to different metals. The procedure involves the complete decomposition and mineralization of the organic matrix of paint driers using acid attack with microwave heating and direct metal determination in aqueous solutions by flame atomic spectrometry in either the absorption or emission mode depending on the sensitivity of the elements.

Eleven elements (barium, calcium, cerium, cobalt, iron, lithium, manganese, lead, strontium, zinc, and zirconium) were determined in single-metal and multi-metal paint driers and the results are compared with standard or alternative procedures. The method is evaluated in terms of accuracy and uncertainty of the sample preparation and instrumental measurement steps.

INTRODUCTION

Paint driers are catalysts used in paint and varnish formulations to help accelerate the drying effects and the formation of films. They are considered the most important additives in the production of coatings in general (1).

High quality paint driers are principally metallic salts of octoic acids, ethyl-hexanoic, and other branched acids in which the metallic elements most frequently include Ba, Ca, Co, Mn, Pb, and Zn. Today, there is considerable interest in finding less contaminating metals with a faster drying effect. Many other metals (rare earth and transition metals) have been tested with alternative organic acids and are included in the paint drier compositions.

There is evidence that the technical performance and quality of these preparations depends to a considerable degree on the selected metal. In addition, cost is a major factor in the selection of the metallic content of metal soap driers. Both considerations are important in the evaluation of the metallic content of paint driers in the manufacturing practice.

From an analytical chemistry point of view, quality control of the production processes of frequently used paint driers, based on alkaline-earth or transition metals [as single-metal soap preparations with a typical metallic content of around 10% (w/w) or more], is usually performed by titrimetric or gravimetric methods which are used as reference methods (2-4). These methods are very suitable for specific metal determinations, even without isolation of the metals. However, their application to complex paint driers without previous metal isolation can be difficult and may cause interferences. In addition, standard methods based on direct dry ashing gravimetry are only suitable for high purity single-metal paint driers. Consequently, multi-metallic determinations in actual complex or mixed paint driers, involving other non-common metals, require validated instrumental methods.

There are not many published articles dealing with the metal determination in paint driers. However, the use of differential-pulse polarography (5,6) or flame atomic absorption spectrometry (FAAS) for the determination of Co and Pb in emulsified solutions (7) has been reported. These instrumental methods were selected due to their speed and simplicity, low matrix effects, and high throughput but were only applied to single-metal driers and showed a bias of around 2% to nominal values with a reproducibility around 2% RSD. These methods have their advantages but also show the need for better instrumental alternatives particularly for other non-common metals and complex multi-metal formulations.

A new and more general procedure is reported in the present paper which can be applied not only to common metals but also to more current formulations with non-common metals including refractory elements. The procedure is based on sample mineralization of the organic matrix using acid attack and heating in a microwave oven, which leads to a relatively simple matrix solution with a low salt content. Finally, the metallic content of aqueous solutions is determined by standard FAAS or flame atomic emission spectrometry (FAES) with practically no interferences. The analytical performance of this method is evaluated and the results compared with standard reference methods in terms of accuracy and reproducibility.

EXPERIMENTAL

Instrumentation

A PerkinElmer® Model 2380 flame atomic absorption spectrometer was used for all measurements (PerkinElmer Life and Analytical Sciences, Shelton, CT, USA). When the determinations were measured using flame atomic absorption spectrometry (FAAS), the instrument was equipped with PerkinElmer hollow-cathode lamps.

**Corresponding author.*
e-mail: anlopez@unizar.es

The standard nebulization system was used with burners for air-acetylene (10-cm slot) and nitrous oxide-acetylene (5-cm slot). The instrumental conditions for measuring the atomic absorption (FAAS) of Ca, Co, Fe, Li, Mn, Pb, Sr, Zn, and Zr, and the emission intensity (FAES) of Ba and Ce are given in Table I.

A microwave muffle furnace Model MAS 7000 (CEM, Matthews, NC, USA) for dry ashing was used with a magnetron of 1400 W at 2455 MHz.

A Multiwave® microwave digestion system (Anton Paar, Graz, Austria) was used for the microwave-assisted acid mineralization of the paint driers (mono- and multi-metallic driers). It was equipped with PFA vessels which can withstand a maximum operating pressure up to 75 bar and a maximum temperature of 220ºC. Since the pressure was monitored for all vessels, it was possible to maintain the maximum operating conditions during the entire digestion process and thus ensure complete digestion of the samples.

Two different operating conditions, referred to as Program I and II, were applied to the decomposition and are listed in Table II.

TABLE I
Instrumental Operating Conditions for Flame Atomic Absorption or Emission Measurements

Element	Wavelength (nm)	Lamp Current (mA)	Flame	Technique	Working Range (µg mL^{-1})
Ba	553.6		N_2O-C_2H_2 Red, reducing	AES	0–20.0
Ca	422.7	5	Air-C_2H_2 Blue, oxidizing	AAS	0–5.0
Ce	269.9		N_2O-C_2H_2 Red, reducing	AES	0–500.0
Co	240.7	10	Air-C_2H_2 Blue, oxidizing	AAS	0–3.5
Fe	248.3	16	Air-C_2H_2 Blue, oxidizing	AAS	0–5.0
Li	670.8	5	Air-C_2H_2 Blue, oxidizing	AAS	0–3.0
Mn	279.5	7	Air-C_2H_2 Blue, oxidizing	AAS	0–2.0
Pb	283.3	5	Air-C_2H_2 Blue, oxidizing	AAS	0–20.0
Sr	460.7	15	N_2O-C_2H_2 Red, reducing	AAS	0–5.0
Zn	213.9	5	Air-C_2H_2 Blue, oxidizing	AAS	0–1.0
Zr	360.1	20	N_2O-C_2H_2 Red, reducing	AAS	0–600.0

TABLE II
Microwave Programs Used in the Mineralization of Paint Driers

Step	Initial Power (W)	Time (min)	Final Power (W)	Fan Speed (a.u.)
Program I				
1	100	5	600	1
2	600	5	600	1
3	1000	10	1000	1
4	0	15	0	3
Program II				
1	100	5	600	1
2	600	10	600	1
3	1000	15	1000	1
4	0	20	0	3

Reagents

Metallic standard stock solutions of 1000 mg L^{-1} were prepared for each element (Ba, Ca, Ce, Co, Fe, Li, Mn, Pb, Sr, Zn, and Zr) following the standard recommended procedures (8).

Additional dilute standard calibration solutions were prepared from the previous standard stock solutions immediately prior to use. In order to eliminate interferences (ionization, chemical), all metallic standard calibration solutions were prepared with 1% (v/v) HNO_3 to match the acid media of the sample mineralization procedure.

Other specific conditions considered for calibration or sample solutions containing certain metals were as follows: Barium solutions were made of 0.1% (w/v) potassium (as chloride), calcium solutions of 0.1% potassium and 0.1% Sr (as nitrate), cerium calibration standard solutions of 0.1% K, strontium solutions of 0.1% K, and zirconium solutions of 2125 mg L^{-1} Al and 0.4% (v/v) HF.

Deionized water of 18.2 MΩ.cm purity was obtained from a Milli-Q™ water system (Millipore, Bedford, MA, USA). Concentrated nitric acid [65% (w/w)] and all other chemicals used (Merck, Darmstadt, Germany; Fluka, Buchs, Switzerland and Aldrich, Milwaukee, WI, USA) were of P.A. grade.

Sample Preparation

The amount of the viscous driers ranged from 0.1 to 0.5 g according to their metallic content. In a typical case, 0.2 g of the paint drier was accurately weighed into PFA microwave digestion vessels and 5 mL of concentrated HNO_3 was added. The vessels were closed and placed into the microwave oven. Each sample was digested and analyzed with five replicates. After digestion and cooling, the attack solution was quantitatively transferred to 100-mL calibrated flasks and diluted to volume with deionized water.

Standard Reference Methods for Single-element Driers

Calcium

The sample (50–60 mg Ca) was dissolved with 10 mL of toluene, diluted with 2 mL of 2-propanol, and 3 mL of 4M HCl solution was added. Then, 10 mL of buffer solution (pH 10) was added to the solution and the mixture titrated using eriochrome black T. The color change was from violet-red to blue.

Cobalt

The sample (100–120 mg Co) was heated with 25 mL of 1M HCl, dissolved with 100 mL of 2-propanol. Then 15 mL of 40% hexamethylenetetramine was added and the mixture titrated using xylenol orange indictor. The color change was from violet to yellow.

Manganese

The sample (70–80 mg Mn) was dissolved in 10 mL of toluene and diluted with 50 mL of 2-propanol. Then about 0.1 g of ascorbic acid and 10 mL buffer solution (pH 10) was added and the mixture titrated with eriochrome black T. The color change was from violet-red to blue.

Lead

The sample (300–350 mg Pb) was dissolved in 10 mL of toluene and then diluted with 50 mL of 2-propanol. Then, 5 mL of 4M acetic acid (a few mg of tartaric acid can alternatively be used) and 25 mL of 0.1M EDTA were added. The EDTA excess was back-titrated with standard 0.05M Zn(II) (zinc sulphate) solution using eriochrome black T. The color change was from blue to violet-red.

Zinc

The sample (80–100 mg Zn) was dissolved in 10 mL of toluene and diluted with 50 mL of 2-propanol. Then, 10 mL of buffer solution (pH 10) was added and the mixture titrated using eriochrome black T. The color change was from violet-red to blue.

Zirconium

The sample (110–120 mg Zr) was dissolved with 40 mL of 2M sulphuric acid solution and heated to boiling for 5 min. After cooling, 25 mL of 0.1M EDTA solution was added. The solution was heated to boiling for 3 min, cooled and neutralized with ammonium hydroxide solution, then 25 mL of 30% (w/v) NaAc solution and 50 mL of acetone were added. The mixture was back-titrated with Zn sulphate using dithizone. The color change was from blue-green to red.

Iron

The sample (140–150 mg Fe) was dissolved with 15 mL of toluene, then 15 mL of ethanol and 25 mL of 2M sulphuric acid were added. The sample solution was boiled for 15 min and allowed to cool. Then 0.2 g of $NaHCO_3$, one drop of 0.01M ferroin solution (as redox indicator), and a few mL of 0.1M Ce(IV) standard solution were added until the color of the solution changed from red to green-yellow; then 0.2 g of $NaHCO_3$ and 4 g of KI were added. The mixture was left standing for 15 min in darkness and then titrated with 0.1M standard sodium thiosulphate solution using starch as the indicator. The color change was the disappearance of the blue starch-iodine color.

Barium

The sample (125–150 mg Ba) was mixed with 10 mL of concentrated sulphuric acid and a few mL of 30% (v/v) hydrogen peroxide. The solution was heated and diluted with deionized water and boiled. It was allowed to stand overnight to precipitate barium sulphate. The precipitate was filtered, dried, and heated in a microwave muffle at 800ºC and finally weighed as sulphate.

Cerium and Strontium by Dry Ashing Gravimetry

The sample (about 2 g) was placed into a quartz crucible and heated on a standard hot plate for about 1 h to eliminate the volatile content. It was then heated in a microwave muffle at 1000ºC for 10 min. After cooling, the ashes were weighed as oxides.

Lithium by Sulphate Dry Ashing Gravimetry

The sample (about 2 g) was placed into a quartz crucible with 2 mL of concentrated sulphuric acid, then heated on a standard hot

plate for about 1 h to eliminate the volatile content. Subsequently, the sample was heated in a microwave muffle at 1000ºC for 10 min. After cooling, the ashes were weighed as sulphates.

RESULTS AND DISCUSSION

Optimization of the Microwave Mineralization Program

A considerable number of articles deals with sample mineralization and preparation using microwaves. Generic and fundamental reviews can be found in the literature (9) as well as current trends and specific applications, i.e., for the determination of lead in paints related to driers (10–12).

In this work, three microwave digestion programs were tested to determine the one most suitable for the decomposition of organic driers. The microwave heating programs, the amount and type of acid as well as sample size used were initially in accordance with the manufacturer's recommendations (13).

Microwave programs I or II (listed in Table II) were applied to the digestion of reference drier samples and 5 mL of concentrated nitric acid was always used for the acid attack; flame atomic absorption spectrometry with air-acetylene flame (FAAS-Air) and nitrous oxide-acetylene (FAAS-NOX) or flame atomic emission spectrometry with nitrous oxide-acetylene flame (FAES-NOX) were used for the measurements. Single-metal driers containing Pb, Mn, Ce, and Zr were previously standardized by titrimetric or gravimetric methods. The results of the metal determinations are listed in Table III.

As can be seen, the results for Pb and Mn using Program I are in good agreement with those obtained using the reference methods. However, when applied to driers containing Ce or Zr (refractory elements), these elements were partially dissolved and the results obtained did not coincide with the reference results. Consequently, longer heating times were tested using Progam II. It was found that the difference between Programs I and II was the length of time for step 2 (at 600 W) and step 3 (at 1000 W). Program I required a total of 35 min compared with 50 min for Program II.

TABLE III
Metal Content Found by Reference Methods and the Alternative F-AS Method Using Microwave Programs I and II Acid Decomposition

Microwave Program	Drier Sample-Element Determined	Metallic Content[a] (g Metal/100 g Sample)		Type of Flame Method	Difference Between Means
		Reference Method	Flame Method		
I	M36-Pb	36.25±0.05	36.17±0.26	FAAS-Air	0.08
I	M6-Mn	6.30±0.10	6.12±0.03	FAAS-Air	0.18
II	M10-Ce	10.00±0.10	9.39±0.10	FAES-NOX	0.61
II	M12-Zr	12.03±0.01	12.10±0.41	FAAS-NOX	–0.07

[a] Means values ± s.d. from five independent determinations.

It can be seen that the Zr content found by the reference method is similar to that of the proposed method. However, the difference between the two methods is higher for Ce because the results obtained using the dry ashing gravimetry method are used as reference.

A third program, using shorter heating times and also requiring a smaller amount of nitric acid than for Program I, was devised in order to test the dissolution of common driers with transition metals. It was found that the results were not quantitatively comparable with the standard results. Consequently, programs using less heating time and less nitric acid than suggested in Program I are not recommended.

Program I was designed for and applied to the majority of common metals (alkaline earth and transition metals), whereas Program II was intended for refractory metals. Both programs are fast and reliable mineralization procedures that reduce the matrix content in the final sample solution and favor the implementation of instrumental measurements using simplified calibration.

Metal Determinations by Atomic Absorption or Atomic Emission and Influence of the Type of Flame

The performance of metal determinations (barium, calcium, cerium, cobalt, iron, lithium, manganese, lead, strontium, zinc, and zirconium) by FAAS or FAES and the use of air or nitrous oxide-acetylene flame were assessed.

FAAS measurements were carried out for Ca, Co, Fe, Li, Mn, Pb, Sr, Zn, and Zr. However, Ba and Ce were excluded on account of their low sensitivity. Standard air-acetylene flames were used in the determination of Ca, Co, Fe, Li, Mn, Pb, Sr, and Zn and a nitrous-acetylene flame was used for Sr (for comparison) and for Zr.

The results found with FAAS using air-acetylene flame (FAAS-Air), after drier mineralization by microwave heating and using Program I, are listed in Table IV. They are in good agreement with those found by the reference method, although Sr and to a lesser extent Zn show differences.

In the case of Sr, the difference could be due to the use of the less suitable air-acetylene flame for this metal (it does not impede chemical interferences) and the reference value obtained by dry ashing gravimetry does not discriminate possible interferences in the samples.

The difference with Zn is also appreciable. This metal was determined under different instrumental conditions using chemical standards of different quality, but the discrepancy always remained the same. The value of the difference was consistent with the magnitude of both methods, i.e., titrimetry used sample and reagents in 6-fold excess or more when compared to the instrumental method. Consequently and because this element is a well-known contaminant, the discrepancy was attributed to contamination.

A nitrous oxide-acetylene flame was also applied in the determination of Sr and Zr. This hotter flame is recommended as an alternative because it reduces chemical interferences during flame atomization. Mineralization using Program I or II for Sr and Zr, respectively, was used for their corresponding driers. The results of these determinations are also listed in Table IV (FAAS-NOX).

As can be seen, the bias for the Sr determination using the hotter flame has been reduced when compared to the air-acetylene flame. Although a discrepancy between the methods exists, it is less significant than in the results obtained for the "air" flame.

The Zr determination is in complete agreement with the reference value.

Ba, Ce, Li, Sr, and Zr were also determined by FAES using the hotter nitrous oxide-acetylene flame, which reduces chemical interferences. The results obtained after mineralization of the driers using the corresponding microwave Program I or II are listed in Table IV (FAES-NOX).

TABLE IV
Metals Determination in Drier samples by FAAS or FAES With Air-Acetylene or Nitrous Oxide-Acetylene Flame in Comparison to Reference Methods

Drier - Sample Element Determined	Metallic Content [a] (g Metal / 100 g Sample)		Type of Flame Method	Differene Between Means
	Reference Method	Flame Method		
M4-Ca	4.05±0.01	4.11±0.09	FAAS-Air	–0.06
M12-Co	12.19±0.01	12.10±0.23	FAAS-Air	0.09
M6-Fe	5.53±0.04	5.57±0.13	FAAS-Air	–0.04
M2-Li	1.70±0.11	1.85±0.03	FAAS-Air	–0.15
M6-Mn	6.30±0.01	6.12±0.03	FAAS-Air	0.18
M36-Pb	36.25±0.05	36.17±0.26	FAAS-Air	0.08
M18-Sr	17.06±0.38	16.41±0.18	FAAS-Air	0.65
M6-Zn	5.97±0.01	5.66±0.38	FAAS-Air	0.31
M18-Sr	17.06±0.38	16.67±0.26	FAAS-NOX	0.39
M12-Zr	12.03±0.03	12.10±0.41	FAAS-NOX	–0.07
M12.5-Ba	12.45±0.06	12.60±0.12	FAES-NOX	–0.15
M10-Ce	9.26±0.40	9.39±0.10	FAES-NOX	–0.13
M2-Li	1.70±0.11	1.84±0.03	FAES-NOX	–0.14
M18-Sr	17.06±0.38	16.57±0.29	FAES-NOX	0.49
M12-Zr	12.03±0.03	11.58±0.20	FAES-NOX	0.45

[a] Means values ± s.d. from five independent determinations.

The results for Ba and Ce are in very good agreement with the reference values and their biases are around 0.1 g per 100 g of sample. Lithium shows a similar bias to that found by FAAS-Air with high reproducibility (Std. Dev. 0.03). However, Sr has a higher bias than the bias found by FAAS-NOX. The results found for Zr are similar to Sr. Thus, it can be concluded that the metal determination by FAES-NOX is an improvement for the Ba and Ce paint driers.

Comparison of the Proposed FAAS Method With Reference Values

The accuracy of the results obtained in the determination of 11 metals in single-metal paint driers using the optimum mineralization and measurement conditions as listed in Table V was evaluated by comparing the reference values of standard methods using the straight line regression method.

In the linear comparison using the least squares method, the reference values were assigned to the x-axis and the best results of the proposed method to the y-axis. Figure 1 shows the linear graph, where each point represents the analysis of the same element in the same sample by two methods. The adjusted straight line gives the slope m = 0.9955 with a standard

deviation of sm = 0.0064, an intercept b = 0.0088 with a standard deviation of sb = 0.0920 and a regression coefficient r = 0.9998. The standard deviation of residuals was s y/x = 0.57. From these results and using the t-value (t = 2.26) for P = 0.05 and 9 degrees of freedom (11 points), the confidence limits for the slope and intercept are m = 0.9955 ± 0.0145 and b = 0.0088 ± 0.2079, respectively. These values confirm that the slope and the intercept do not differ significantly at P = 0.05 from the ideal values of 1 and 0, respectively. It can therefore be concluded that there is no significant difference between the new values and the reference values.

The residuals of the regression line listed in Table V show two important tendencies. The results obtained by FAAS using Program I and the air-acetylene flame are in close agreement with the reference values. When using Program II, the biggest differences are for elements with reference values obtained by the generic dry ashing gravimetry method (referred to as G-ashing in Table V).

Uncertainty of the Proposed FAAS Method

Uncertainty was considered an important factor in the analysis of real paint driers for quality control purposes, expressed as the standard deviation (s.d.) and variance. In order to evaluate the uncertainty, different sub-samples were taken and repeatedly measured so that the two sources of influence could be separated. The first source included sampling and sample preparation. The second source included measurements and interpolation in the calibration graphs, i.e., the influence of the preparation mode and the influence of the instrumental measurements. The results were

TABLE V
Comparison of Two Analytical Methods (Reference and Flame Methods) for Metals in Paint Driers by Linear Regression.
Differences Between Methods According to the Residuals of the Regression Line.

Element	Micro-wave Program	Reference Method	Flame Method	Residuals
Ba	I	G-ISO	FAES: N_2O-C_2H_2	0.1966
Ca	I	T-ISO	FAAS: Air- C_2H_2	0.0692
Ce	II	G-D-Ashing	FAES: N_2O-C_2H_2	0.1624
Co	I	T-ISO	FAAS: Air-C_2H_2	–0.0445
Fe	I	T-ISO	FAAS: Air-C_2H_2	0.0558
Li	I	G-D-Ashing	FAAS: Air-C_2H_2	0.1488
Mn	I	T-ISO	FAAS: Air-C_2H_2	–0.1607
Pb	I	T-ISO	FAAS: Air-C_2H_2	0.0726
Sr	I	G-D-Ashing	FAAS: N_2O-C_2H_2	–0.3228
Zn	I	T-ISO	FAAS: Air-C_2H_2	–0.2922
Zr	II	T-ISO	FAAS: N_2O-C_2H_2	0.1148

[a] G-ISO: Gravimetry by ISO 4619; T-ISO: Titrimetry by ISO 4619, G-D-Ashing: Gravimetry by dry ashing.

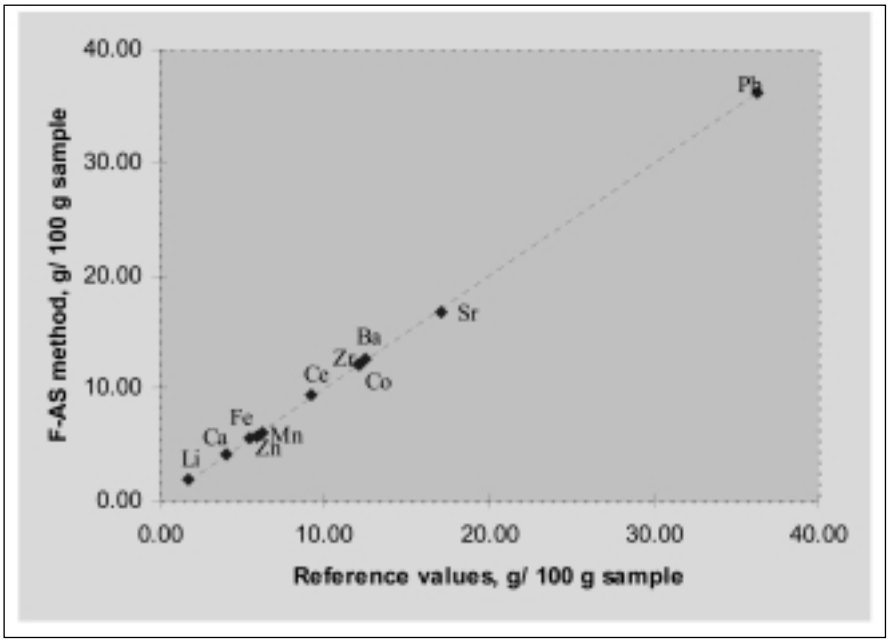

Fig. 1. Linear comparison of results by the proposed FAAS method with reference values of standard methods applied to the same elements in the same sample.

obtained by applying statistical ANOVA (14) and are listed in Table VI.

The results show that the total s.d. is affected mainly by the preparation step, whereas the measurement step is less significant for all of the metals.

The evaluation of the uncertainty ascribed to the individual steps shows that the sample preparation step has a s.d. of ≤0.1 g metal/100 g of sample for the majority of elements. Three elements have a s.d. of around 0.25, and only Zn and Zr display a value of around 0.4. The value for Zn is due to its contamination and the Zr value is due to its refractory behaviour. With regard to the uncertainty of the measurement step, it can be observed that all techniques show a low s.d. (s.d. of ≤0.1 g metal/100 g of sample) and this value is lower than 0.5 for the majority of the metals.

It should be noted that the sampling procedure is generally the major factor that influences the variance in the analysis. However, for these liquid samples, the homogeneity is good and, consequently, the variance of the first step (sampling and sample preparation) can be mainly identified with the variance in sample preparation.

TABLE VI
Uncertainty of Global Method, Preparation Step, and Measuring Step

Element-Flame Method	Standard Deviation		
	Total/(Metal Content) [a]	Preparation Step [b]	Measurement Step [c]
Ba-FAES: N_2O-C_2H_2	0.12/(12.60)	0.10	0.12
Ca-FAAS: Air- C_2H_2	0.09/(4.11)	0.09	0.02
Ce-FAES: N_2O-C_2H_2	0.10/(9.39)	0.10	0.03
Co-FAAS: Air-C_2H_2	0.23/(12.10)	0.23	0.04
Fe-FAAS: Air-C_2H_2	0.13/(5.57)	0.13	0.04
Li-FAAS: Air-C_2H_2	0.03/(1.84)	0.03	0.01
Mn-FAAS: Air-C_2H_2	0.03/(6.12)	0.025	0.015
Pb-FAAS: Air-C_2H_2	0.26/(36.17)	0.25	0.12
Sr-FAAS: N_2O-C_2H_2	0.26/(16.67)	0.25	0.09
Zn-FAAS: Air-C_2H_2	0.38/(5.66)	0.37	0.09
Zr-FAAS: N_2O-C_2H_2	0.41/(12.10)	0.41	0.04

[a] Total s.d. and metal content as g of metal per 100 g of sample.
[b] For 5 different sub-samples.
[c] For 3 replicates per sub-sample.

Multi-metal Determinations in Complex Driers

Since there were no certified reference multi-metal paint driers available and the reference method could not be applied to standard complex driers, the reliability of the proposed method was evaluated by analyzing real complex paint drier samples. The results obtained were compared with the alternative technique of inductively coupled plasma optical emission spectrometry (ICP-OES) using standard conditions (15).

The results obtained in the analysis of commercial paint driers containing nine metals (except for Ce and Fe which were not found in multi-metal commercial driers) using the proposed method with optimum microwave mineralization and flame atomic spectrometry are compared with the values obtained by ICP-OES (see Table VII).

The results are in good agreement for practically all of the metals, the differences being lower than 0.2 g metal/100 g of sample, except for Mn and Zr. A comparison of the means obtained with the two methods by linear regression showed that the confidence interval (at P = 0.05 and 7 degrees of freedom) for the slope was 0.9959 ± 0602, and the intercept was 0.1162 ± 0.3651. Consequently, both values include the reference data of 1 and 0, respectively. It can therefore be concluded that no systematic errors are introduced in the proposed method at the confidence level of P = 0.05.

CONCLUSION

The method proposed for the metals determination in single-metal and/or complex multi-metal paint driers is shown to be an alternative procedure to conventional methods and also overcomes some of their limitations.

The use of microwave digestion demonstrates that the samples were successfully mineralized (using 5 mL of nitric acid) with considerable speed, safety, and reduced sample preparation. The short Program I is recommended for Ba, Ca, Co, Fe, Li, Mn, Pb, Sr and Zn determination, while the long Program II is recommended for Ce and Zr determination. The metals Ca, Co, Fe, Li, Mn, Pb, and Zn were best measured by FAAS using air-acetylene flame; Sr and Zr by FAAS with nitrous oxide-acetylene flame; and Ba and Ce by FAES with nitrous oxide-acetylene flame.

TABLE VII
Determination of Metals in Complex Multi-metal Paint Driers by the Proposed Flame AS Method Compared with ICP-OES

Drier Metallic Composition	Determined Metal	Content by Flame AS[a]	Content by ICP-OES[a]	Difference of the Means
M 639-Ba,Co,Zn	Ba	7.45±0.12	7.60±0.23	–0.15
	Co	1.14±0.06	0.94±0.08	0.20
	Zn	3.70±0.03	3.86±0.06	–0.16
M 270-Ca,Co,Zr-	Zr	6.20±0.08	5.77±0.06	0.43
M745-Ca,Co,Li	Ca	4.23±0.20	4.31±0.01	–0.08
	Li	0.50±0.01	0.49±0.03	0.01
M 631-Ca,Co,Sr	Sr	4.43±0.09	4.38±0.09	0.05
M 26-Co,Mn	Mn	5.64±0.04	5.11±0.09	0.53
M 1012-Ca,Co,Pb	Pb	12.74±0.19	12.71±0.48	0.03

[a] Means of five independent determinations ± standard deviation; given as g metal/100 g sample.

The accuracy of the method shows a bias lower than 0.2 g/100 g of metal for the majority of metals, except for Sr and Zn. The uncertainty ascribed to the preparation step showed that it was the prevalent factor, whereas the flame atomic absorption spectrometric measurements always showed lower standard deviation values. This method can be adapted for other metals.

ACKNOWLEDGMENTS

The authors wish to thank Metalest (Zaragoza, Spain) for providing the paint drier samples and financial support.

Received July 3, 2003.

REFERENCES

1. J. Skalsky, Progress in Organic Coating 4, 137 (1976).
2. C.A. Luchesi and C.F. Hirn, Anal. Chem. 30, 1877 (1958).
3. International Organization for Standardization-ISO, Norm ISO 4619: Driers for paints and varnishes, Geneva, Switzerland (1998).
4. American Society for Testing and Materials-ASTM-, Standard D-564-47, Part 29, Vol. 20, p. 292, Philaphelphia, PA, USA (1980).
5. J. Garcia-Anton and J.L. Guiñon, Analyst 110, 1365 (1985).
6. J. Garcia-Anton and J.L. Guiñon, Analyst 111, 823 (1986).
7. J. Garcia-Anton and J.L. Guiñon, Analusius 14, 158 (1986).
8. Analytical methods for atomic absorption spectrophotometry. PerkinElmer Life and Analytical Instruments, Shelton, CT, USA (1982).
9. H.M. Kuss, Fresenius' J. Anal. Chem. 343, 788 (1992).
10. Microwave-enhanced chemistry. Fundamentals, sample preparation and applications. H.M. Kingston and S.H.J. Haswell, Eds.(American Chemical Society, Washington, D.C.,USA) (1997).
11. H.M.S. Kingston, At. Spectrosc. 19(2), 7 (1998).
12. D. Binstock, Anal.Lett. 33, 3397 (2000).
13. Microwave sample preparation system, Guide, Anton Paar GmbH, Graz, Austria (1998).
14. J.C. Miller and J. N. Miller, Statistics for analytical chemistry, Ellis Horwood, 2nd ed., New York (1988).
15. Plasma 40 Emission spectrometer, Guide, PerkinElmer Life and Analytical Instruments, Shelton, CT, USA (1987).

Atomic Spectroscopy
Vol. 25(1), Jan/Feb 2004

Printed in the United States and published six times a year by:

PerkinElmer Life and
Analytical Sciences
710 Bridgeport Avenue
Shelton, CT 06484-4794 USA
www.perkinelmer.com

SUBSCRIPTION INFORMATION

Atomic Spectroscopy
P.O. Box 3674
Barrington, IL 60011 USA
Fax: +1 (847) 304-6865

2004 Subscription Rates

- U.S. $60.00 includes third-class mail delivery worldwide; $20.00 extra for electronic file.
- U.S. $80.00 includes airmail delivery; $20 extra for electronic file.
- U.S. $60.00 for electronic file only.
- Payment by check (drawn on U.S. bank in U.S. funds) made out to: "*Atomic Spectroscopy*"

Electronic File

- For electronic file, send request via e-mail to: atsponline@yahoo.com

Back Issues/Claims

- Single back issues are available at $15.00 each.
- Subscriber claims for missing back issues will be honored at no charge within 90 days of issue mailing date.

Address Changes to:
Atomic Spectroscopy
P.O. Box 3674
Barrington, IL 60011 USA

Microfilm

Atomic Spectroscopy issues are available from:
University Microfilms International
300 N. Zeeb Road
Ann Arbor, MI 48106 USA
Tel: (800) 521-0600 (within the U.S.)
+1 (313) 761-4700 (internationally)

Guidelines for Authors

Atomic Spectroscopy serves as a medium for the dissemination of general information together with new applications and analytical data in atomic absorption spectrometry.

The pages of *Atomic Spectroscopy* are open to all workers in the field of atomic spectroscopy. There is no charge for publication of a manuscript.

The journal has around 1500 subscribers on a worldwide basis, and its success can be attributed to the excellent contributions of its authors as well as the technical guidance of its reviewers and the Technical Editors.

The original of the manuscript should be submitted to the editor by mail plus electronic file on disk or e-mail in the following manner:

1. Mail original of text, double-spaced, plus graphics in black/white.
2. Provide text and tables in .doc file and figures in doc or tif files.
3. Number the references in the order they are cited in the text.
4. Submit original drawings or glossy photographs and figure captions.
5. Consult a current copy of *Atomic Spectroscopy* for format.
6. Or simply e-mail text and tables in doc file and graphics in doc or tif files to the editor: anneliese.lust@perkinelmer.com or annelieselust@aol.com

All manuscripts are sent to two reviewers. If there is disagreement, a third reviewer is consulted.

Minor changes in style are made in-house and submitted to the author for approval.

A copyright transfer form is sent to the author for signature.

If a revision of the manuscript is required before publication can be considered, the paper is returned to the author(s) with the reviewers' comments.

In the interest of speed of publication, a pdf file of the type-set text is e-mailed to the corresponding author before publication for final approval.

Additional reprints can be purchased, but the request must be made at the time the manuscript is approved for publication.

Anneliese Lust
Editor, *Atomic Spectroscopy*
PerkinElmer
Life and Analytical Sciences
710 Bridgeport Avenue
Shelton, CT 06484-4794 USA

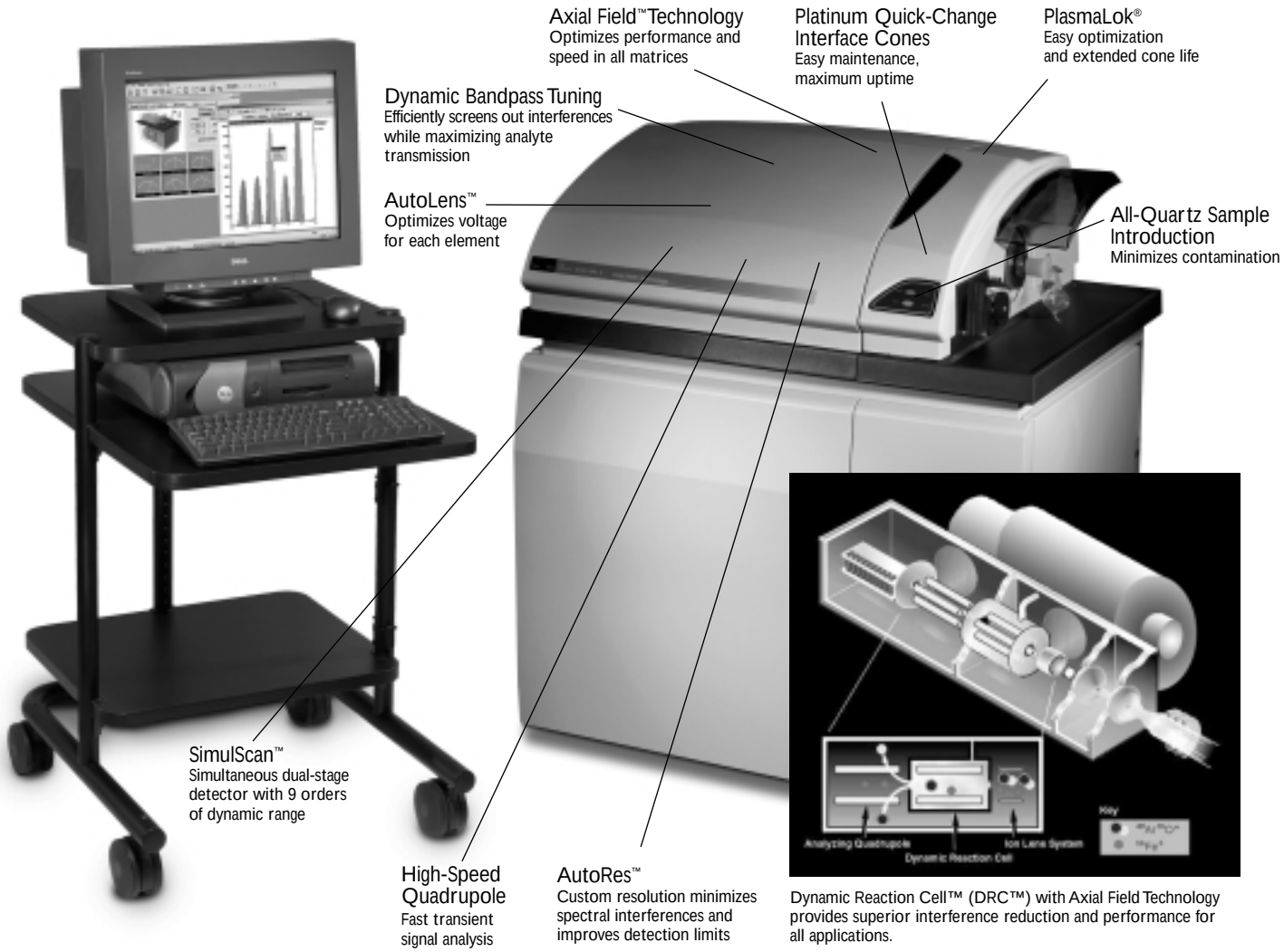

Dynamic Reaction Cell™ (DRC™) with Axial Field Technology provides superior interference reduction and performance for all applications.

Eliminates interferences **COMPLETELY**

When your applications extend beyond the capabilities of conventional ICP-MS, you need the power of the innovative ELAN® DRC II. The DRC II combines the power of patented Dynamic Reaction Cell (DRC) technology with performance-enhancing Axial Field Technology, providing uncompromised sensitivity and performance in all matrices for even the toughest applications. Unlike collision cell, high-resolution, or cold plasma systems, the DRC II completely eliminates polyatomic interferences providing ultratrace-level detection limits.

The DRC II uses chemical resolution to eliminate plasma-based polyatomic species before they reach the quadrupole mass spectrometer. This ion-molecule chemistry uses a gas to “chemically scrub” polyatomic or isobaric species from the ion beam before they enter the analyzer, resulting in improved detection limits for elements such as Fe, Ca, K, Mg, As, Se, Cr, and V.

Unlike more simplistic collision cells, patented DRC technology not only reduces the primary interference; it eliminates sequential side reactions that create new interferences. Unless kept in check by DRC technology, these uncontrolled reactions increase spectral complexity and create unexpected interferences.

PerkinElmer® precisely.